Exploring chemokine-mediated inflammatory responses in the testis and epididymis: insights into ectopic lymphoid organ formation

Inaugural Dissertation

submitted to the

Faculty of Medicine

in partial fulfilment of the requirements

for the PhD -Degree

of the Faculty of Medicine

of the Justus Liebig University Giessen

as part of the binational joint award PhD program of the Justus Liebig University Giessen and the Monash University Melbourne

by

Hiba Hasan

from

Abu Dhabi, United Arab Emirates

Giessen. 2024

From the Department of Anatomy and Cell Biology

Director/Chairman: Prof. Dr. Eveline Baumgart-Vogt

Of the Faculty of Medicine of Justus Liebig University of Giessen, Germany

Supervisor and first reviewer: Prof. Dr. Andreas Meinhardt/ Dr. Monika Fijak

Second reviewer: PD Dr. Joachim Weitzel

Vice-chair: Prof. Dr. Christine Wrenzycki

Chair: Prof. Dr. Klaus-Dieter Schlüter

Date of Doctoral Defense:

12/06/2024

MONASH University

Exploring chemokine-mediated inflammatory responses in the testis and epididymis: insights into ectopic lymphoid organ formation

Hiba Hasan

M.Sc.

A thesis submitted for the degree of Doctor of Philosophy at

Monash University in 2024

Faculty of Medicine, Nursing, and Health Sciences

as part of the binational joint award PhD program of the Justus Liebig University Giessen and the Monash University Melbourne

Copyright notice

© Hiba Hasan (2024).

I certify that I have made all reasonable efforts to secure copyright permissions for third-party content included in this thesis and have not knowingly added copyright content to my work without the owner's permission.

Abstract:

Infertility is regarded as a worldwide problem where male factors account for approximately 50% of infertility cases. To date, a plethora of causes have been identified that can contribute to male infertility. Among the identifiable and potentially curable causes, infection and inflammation of the genital tract are the most frequent.

Experimental autoimmune epididymo-orchitis (EAEO) is a mouse model of chronic testicular inflammation characterized by several symptoms reported also in cases of infertility in men. They include immune cell infiltration, elevation of pro-inflammatory and pro-fibrotic mediators (e.g. TNF, CCL2, activin A), impairment of spermatogenesis, destruction of the seminiferous tubule architecture as well as steroidogenic disturbances and fibrotic remodeling. CCL2 and its receptor CCR2 are well-characterized as a major chemokine signaling pathway involved in recruitment of monocytes and macrophages to sites of inflammation, where they contribute to tissue damage. Activin A, a pleiotropic factor whose production correlates with the severity of EAEO, has the capacity to modulate expression of chemokine receptors and ligands, specifically CCR2.

Consequently, this study aimed to investigate how the chemokine network is changing during testicular inflammation in C57BL/6J (WT) and CCR2 deficient (Ccr2-/-) mice and how activin A can influence the expression of chemokines and their receptors. EAEO was induced in *WT* and *Ccr2*$^{-/-}$ mice and the testes were collected 50 days from the first immunization. The mRNA expression results show that the key chemokines and their receptors essential for macrophage trafficking are increased in EAEO testis, while the deficiency of CCR2 attenuates these changes. The expression of chemokine/chemokine-receptor-encoding genes was examined in human testicular biopsies. Accordingly, an increase in macrophages expressing CCR2 was demonstrated in human testicular biopsies with impaired spermatogenesis and focal leukocytic infiltrates. Importantly, the biopsies showing impaired spermatogenesis and concomitant focal leukocytic infiltration exhibited higher expression of CCL2 and CCR2 than control biopsies with no signs of inflammation and intact spermatogenesis. Moreover, using an *in-vitro* setup where bone marrow derived macrophages were used as a surrogate

for testicular macrophages, it was revealed that activin A serves as an essential regulator of chemokine network expression. The inhibitor of activin A, follistatin, ameliorated the effects on the chemokine network. To add, macrophages were identified as the major cell population in EAEO testis expressing activin A. This implicates both CCR2 and activin A as potential therapeutical targets.

Alterations in chemokine expression can predispose the affected tissue to immune cell infiltration, which can in some instances organize into aggregates that resemble lymph nodes in their structure, composition, chemokine expression as well as their functionality. Tertiary lymphoid organs (TLO) develop as a consequence of inflammation, which can be driven by a myriad of causes, such as infection and autoimmunity. Therefore, in the second part of the study, the putative development of TLO in the testis and epididymis under inflammatory conditions was investigated using two mouse models, i.e., sterile EAEO and acute UPEC-infection. Acute epididymitis is commonly caused by bacteria, where UPEC is a predominant pathogen. In the UPEC-infection model, different parts of the epididymis respond differently to the infection, so that the cauda epididymidis is selectively severely damaged displaying interstitial fibrosis, loss of epithelial integrity, increase in luminal diameter, immune cell infiltration and abscess formation. The results revealed that elements of TLO formation were not found in the EAEO testis, but they were detected in the inflamed cauda epididymidis. The cauda from EAEO mice and especially from animals infected with UPEC exhibited multiple elements and immune cells associated with TLO formation. UPEC-infected cauda epididymides showed the presence of distinct B and T cell zones, with high endothelial venules (HEV) in the T cell region containing CXCL13 within their lumen. Importantly, the B cells were proliferating, highlighting their possible role in performing germinal center reaction activities. In addition, the clustered immune cells demonstrated a reticular network, which could provide structural support and influence migration of immune cells and formation of antibodies. The B and T cells clustered into separate zones and this was in accordance with the high expression of TLO-related chemokines (Cxcl13, Ccl19 and Ccl21). Moreover, the genes critical for HEV formation (Tnf, Ltα) and maturation (Ltβ, Tnfsf14) were elevated. The cauda of EAEO mice also developed TLO and HEV, but in a less organized manner. Based on these

results, it is speculated that the epididymis is susceptible to TLO formation under inflammatory conditions. Future studies investigating the impact of TLO development in the epididymis on male fertility are needed.

Declaration

This thesis is an original work of my research and contains no material which has been accepted for the award of any other degree or diploma at any university or equivalent institution and that, to the best of my knowledge and belief, this thesis contains no material previously published or written by another person, except where due reference is made in the text of the thesis.

Signature:

Print Name: Hiba Hasan

Date: 15.12.23

Table of contents

List of figures:

List of Tables

1. Introduction

1.1. Male reproductive tract

The mammalian male reproductive tract consists of one pair of testes, epididymides, vasa deferentia and ejaculatory ducts, as well as the accessory sex glands. The testes are the location where spermatogenesis and steroidogenesis take place. The epididymides are the paired tubes connected to the testes where spermatozoa mature to acquire their fertilization capacity and are stored. The accessory sex glands are responsible for production of the seminal plasma. After the spermatozoa have matured, they travel from the rete testis in the hilum of the testicle through the efferent ducts and along the length of the epididymides where they are stored prior to ejaculation. At the time of ejaculation, the sperm travel through the vas deferens. Production, maturation, and release of spermatozoa is mainly governed by particular functions of testicular somatic cells, as well as the epididymal epithelium (Haschek et al., 2010).

1.1.1. Testis

1.1.1.1. Testicular histology

The major functions of the testis are steroidogenesis and spermatogenesis, which each occur in distinct compartments. The adult testis is surrounded by a thick layer of connective tissue, called the tunica albuginea, which extends inwards into the testis separating it into multiple lobes of tightly packed tubules, called seminiferous tubules, embedded within a relatively sparse interstitial tissue. The tubules are surrounded by myoid peritubular cells (PTC), which provide structural and contractile elements to assist movement of the immotile spermatozoa into the lumen (Fijak & Meinhardt, 2006; Li et al., 2012; Zhao et al., 2014). The PTC form one cell layer in rodents, while in humans they form several layers (Mayerhofer, 2013). The seminiferous tubules are the site for spermatogenesis and are divided into a basal compartment, where precursors of spermatozoa, spermatogonia, solely reside, and an adluminal compartment, where haploid germ cells are produced.

Spermatogenesis is a complex process which involves mitotic divisions to produce type B spermatogonia from a self-renewing stem cell population, meiotic divisions by spermatocytes to produce haploid cells followed by maturation into elongated spermatids in a process called spermiogenesis. The process by which haploid spermatozoa develop, initiates during puberty and is regulated by an increase in testosterone. At this stage, spermatogonia enter meiosis for the first time to produce primary then secondary spermatocytes. This process begins at the base of the seminiferous tubule epithelium and maturing cells move progressively into the lumen where haploid stages are found **(Fig. 1)** (Gilbert, 2000).

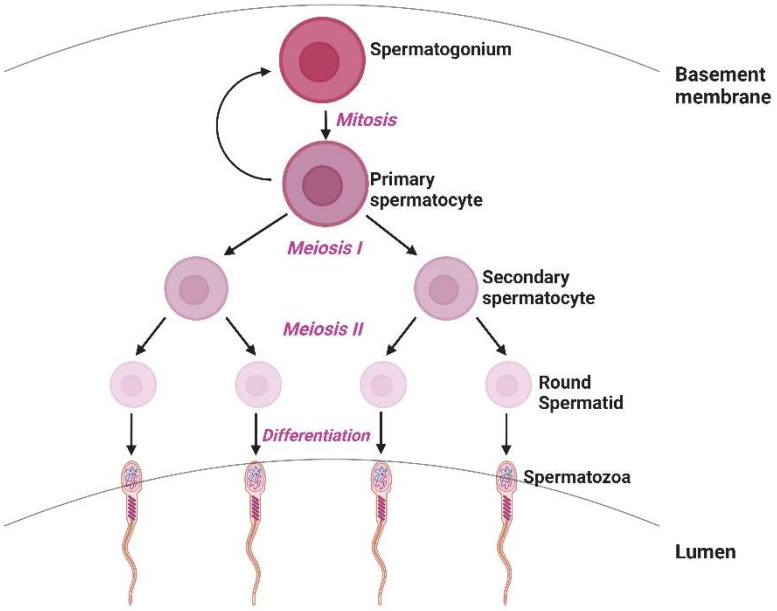

Figure 1. The process of spermatogenesis and spermiogenesis in the testis. Figure created with BioRender.

The compartmentalization of the seminiferous tubules is established by tight, adherens and gap junction between neighboring Sertoli cells (Bhushan et al., 2020) **(Fig. 2)**. The Sertoli cells provide structural and nutritional support for the developing germ cells and are regarded as “nurse cells” (Petersen & Söder, 2006). Steroidogenesis takes place in the interstitial space located between the seminiferous tubules. The pituitary gonadotropin, luteinizing hormone (LH), stimulates Leydig cells (LC) to synthesize and release the male sex steroid,

testosterone which acts as a paracrine factor diffusing into the seminiferous epithelium. Testosterone plays critical roles in maintaining the dynamics of blood-testis barrier while spermatocytes are transiting through from the basal to luminal compartment. It is involved in the formation of elongated spermatids by ensuring that adhesions between Sertoli cells and elongated spermatids are maintained. Testosterone is also essential for the completion of meiosis in spermatogenesis. Moreover, it allows for the release of mature spermatozoa which in its absence would be retained and phagocytized by Sertoli cells (Smith & Walker, 2014).

Testicular macrophages (TM), which are in close physical association with the Leydig cells, have been implicated in steroidogenesis, whereby they secrete steroid precursor, 25-hydroxycholesterol (Gu et al., 2022; Hutson, 2006; Nes et al., 2000). In addition, the Leydig cells do not develop normally in the absence of TM, and when TM are activated, steroidogenesis is inhibited (Hales, 2002). The TM are the major immune cell population present in the testis. Besides TM, dendritic cells, T cells and mast cells also are present in the interstitial space (Bhushan et al., 2020).

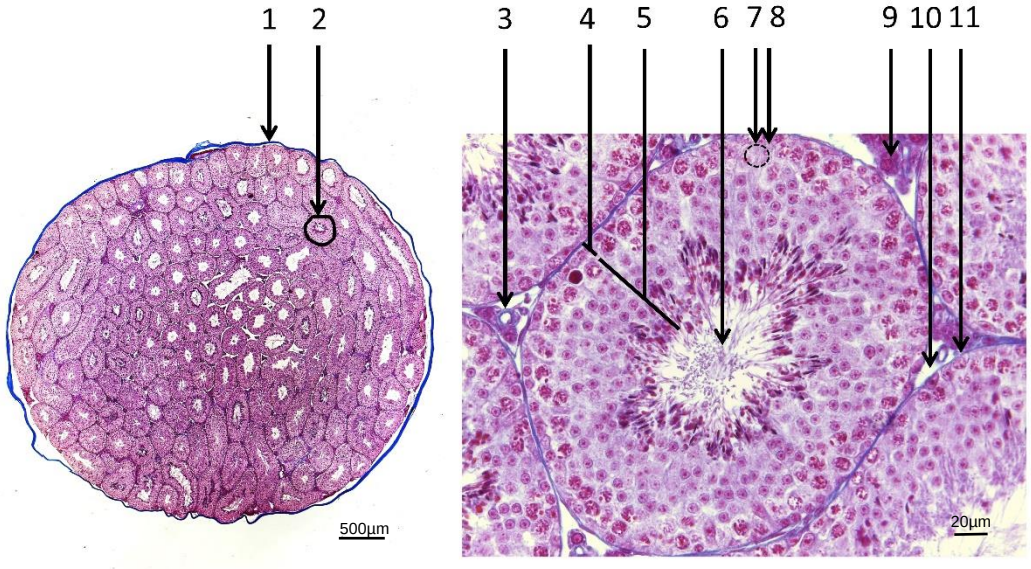

1 Tunica albuginea
2 Seminiferous tubule
3 Blood vessel
4 Basal compartment
5 Adluminal compartment
6 Lumen
7 Tight junctions
8 Sertoli cell
9 Leydig cell
10 Interstitial space
11 Peritubular cell

Figure 2. Histological structure of the mouse testis at low magnification (left) and high magnification (right). Azan staining of paraffin-embedded testicular sections from the adult C57BL6J mouse.

1.1.1.2. The immune system: the innate and adaptive immune systems

Beyond the structural and chemical barriers that protect from infections, the immune system is composed of two lines of cellular defense, the innate and the adaptive line, which work together to accomplish the task of fending against environment threats, such as pathogens. Macrophages and neutrophils are the two major cellular components of the innate immune system which provide the first defense in the face of pathogens. Other elements of the innate immune system include other cells such as mast cells and soluble factors such as the complement system. When a foreign antigen, such as ones derived from fungi or bacteria, is encountered, it is recognized via its pathogen-associated molecular patterns (PAMP). Examples of PAMP include lipopolysaccharides (LPS) from bacteria and double-stranded ribonucleic acid (RNA) produced during viral infection. Toll-like receptors (TLR) present on immune cells recognize PAMP which allows the innate immune cells to secrete a range of pro-inflammatory mediators such as cytokines like Interleukin (IL)-6 and TNF as well as reactive oxygen species (ROS). The binding also allows the activated immune cells to secrete chemokines which allows for rapid recruitment of mmune cells to the site of infection (Marshall et al., 2018).

The secreted cytokines lead to activation of immature dendritic cells which act as a bridge between the innate and adaptive immune responses. The adaptive immune response is essential when the innate immune response fails in containing the infection. Activated dendritic cells digest the antigen, then they become highly effective antigen presenting cells (APC) which then carry the antigens on their major histocompatibility (MHC) protein and travel to the nearest lymph node and have the capacity to prime and modulate T cell function. The peptide antigens presented by MHC trigger T-cell receptor (TCR) signaling. However, costimulatory and coinhibitory receptors present on T cells modulate T-cell function and determine the fate of the T cell. This antigen presentation combined with costimulatory signals can lead to T cell activation and

differentiation. The T cells differentiate primarily into cytotoxic or helper T cells. While cytotoxic T cells are activated by peptides present on MHC-I on infected cells, helper T cells are activated by peptides presented by MHC-II found on APC. B cells are activated when antigens bind to their B cell receptor (BCR), and this allows the B cells to differentiate and mature into antibody producing cells. Unlike the immune cells of the innate immune system, B and T cells exhibit immunologic memory whereby a secondary encounter with the same antigen allows for more rigorous and faster response (Alberts et al., 2008; Getz, 2005; Marshall et al., 2018).

1.1.1.3. Testicular immune privilege and role of immune cells

With the exception of the spermatogonia, most spermatogenic cells do not appear until puberty. The haploid germ cells possess surface antigens that are highly immunogenic, since they are first formed after the establishment of central immune tolerance in the body (Fijak & Meinhardt, 2006; Fisher & Hammarberg, 2017). Therefore, protective mechanisms exist to prevent the initiation of an aggressive immune response that would result in the destruction of these indispensable germ cells.

The testis, along with the eye, the brain and the placenta, are regarded as immune privileged sites. The term “immune privilege” was established when organs transplanted in certain locations were in fact found to be accepted rather than being rejected by the host (Barker & Billingham, 1978; Fijak & Meinhardt, 2006). When allografts or xenografts of skin and parathyroid glands were transplanted into the interstitial space of the rat testis, it was noticed that these grafts survived for a considerable amount of time. Parathyroid grafts placed in non-immune privileged sites, subdermally near the thoracic wall of under the renal capsule, were almost immediately rejected. On the other hand, the same grafts placed in intra-testicular regions survived significantly longer with some grafts functioning after 100 days of the transplantation (Head et al., 1983). It was first believed that the blood-testis barrier, formed by the junctions between the Sertoli cells, was the only player in shielding and protecting the developing germ cells from the immune system. Although the antigens in the adluminal

compartment are protected from the immune response, preleptotene spermatocytes and spermatogonia are not completely sequestered by the blood-testis barrier, and non-sequestered germ cell antigens can interact with antibodies outside of the blood-testis barrier (Yule et al., 1988). These egressed autoantigens promote regulatory T cell-dependent physiological, or peripheral tolerance. Transient depletion of regulatory T cells in mice during testicular inflammation results in an immune response against non-sequestered germ cell antigens, while sequestered antigens are non-tolerogenic (Tung et al., 2017). It is now well-established that, in addition to the blood-testis barrier, a physiological and immunological barrier involving active immunosuppressive and tolerogenic mechanisms maintains the testicular immune privileged status of the testis (Fijak et al., 2018; Li et al., 2012; Meinhardt & Hedger, 2011; Zhao et al., 2014).

Several cells and molecules are responsible for establishing this complementary immunological barrier. The TM are one population of testicular immune cells involved in maintaining immune privilege.

They are divided into two main subclasses: interstitial ($CD64^{hi}MHCII^{lo}$) and peritubular ($CD64^{lo}MHCII^{hi}$) macrophages (Mossadegh-Keller et al., 2017). Interstitial macrophages exhibit a close structural and functional association with LC. The ratio is 1 macrophage present for every 4 to 5 Leydig cells. These TM possess an anti-inflammatory and immunoregulatory phenotype and exhibit a reduced capacity to synthesize pro-inflammatory molecules, such as IL-1β, IL-6, CCL2 and TNF, compared with macrophages from other tissues. They also exhibit immunosuppressive characteristics, as evident by increased IL-10 and TGF-β secretion, which are known to prevent T cell activation (Fijak et al., 2018; Kern et al., 1995; Schuppe et al., 2008; Winnall et al., 2011). The peritubular TM, on the other hand, are in close association with the spermatogonial stem cells and can influence their differentiation. Given their high MHC II expression, these cells are speculated to play a role in tolerance by inducing regulatory T cells against germ cell auto-antigens (Mossadegh-Keller et al., 2017; Tung et al., 2017).

Dendritic cells present in the interstitial space are of immature phenotype, lacking costimulatory molecules CD80 and CD86, and they exhibit low T-cell stimulatory

activity under physiological conditions (Rival et al., 2007; Sainio-Pöllänen et al., 1996; Wang & Duan, 2016). Moreover, immunoregulatory T cells are present in the testis, including regulatory T cells and natural killer T cells (Fijak et al., 2018; Wheeler et al., 2011).

The Sertoli cells not only form the blood-testis barrier to protect auto-antigenic germ cells, but can also produce TGF-β, IL-10, FasL and indolamine 2,3-dioxygenase (IDO), that support the establishment of an immunosuppressive niche (Gualdoni et al., 2019; Kaur el al., 2014, Korbutt et al., 2000; Zhao et al., 2014). The Sertoli cells are also a source of activins, especially activin A, which inhibits the production of pro-inflammatory cytokines in response to an inflammatory stimulus (Phillips et al., 2009). Androgens, mainly testosterone produced by the LC, have immunomodulatory and -protective roles. A blockade of androgen production in the Leydig cells leads to rapid rejection of intratesticular allografts (Cutolo, 2009; Head & Billingham, 1985). Testosterone administration can prevent the accumulation of macrophages and significantly increase the number of regulatory T cells in mice during testicular inflammation (Fijak et al., 2011). Moreover, programmed death ligand -1, expressed in the testis, inhibits T cell activation via programmed death receptor -1 (Cheng et al., 2009). Therefore, several local mechanisms come together to ensure the maintenance of testicular immune privilege. However, if this immune tolerance profile is compromised, it can lead to the disruption of immune privilege in the testis (Fijak & Meinhardt, 2006; McLachlan, 2002; Naz, 2004).

1.1.2. Epididymis

1.1.2.1. Histology of the epididymis

The epididymis is a site for sperm transport, maturation, protection, and storage. It is a single, highly-convoluted duct, with a complex pseudostratified epithelium composed of several cell types that is surrounded by a basal lamina and smooth muscle cells. This thick muscular coat is essential for sperm movement through the epididymis. The epididymis connects the vas deferens with the efferent ducts. It is divided into four regions: initial segment, caput, corpus and cauda **(Fig. 3)** (De Grava Kempinas & Klinefelter, 2014; Pleuger et al., 2020). Septae present

between different regions of the epididymis divide it further into discrete segments, with 10 segments in mice and 19 in rats (Johnston et al., 2005), while in humans segmentation is less visible (Sullivan & Mieusset, 2016). The epithelium is lined by several different cell types: narrow, clear, principal, basal, apical and halo cells. Narrow cells are present only in the initial segment, while clear cells are also present in other regions of the epididymis. Narrow and clear cells are considered the major proton-secreting cells. Principal cells are the most prominent cell type throughout the epididymal duct, and they play a role in fluid and nutrient exchange and protein secretion. Basal cells are involved in regulating the microenvironment and ensuring proper communication between the epididymal lumen and the duct basal regions, while apical cells exert endocytic functions. Finally, halo cells (T cells) are a minor immune cell subset of the epididymis (Cornwall, 2009; Shum et al., 2011). Along the length of the epididymis, from the caput to the cauda, the epithelium decreases in height while the muscle layers and the lumen increase in size. During the transit through the epididymis, spermatozoa interact with contents of epididymal epithelium where they undergo biochemical and physiological modifications such as changes to their surface proteins as well as post-translational modifications of endogenous proteins which allows them to acquire progressive motility needed to undergo hyper activation as well as acquire fertilizing capacity. Once the sperm reach the cauda they have acquired almost all the necessary structural and functional alterations needed for fertilization (Cornwall, 2009; De Grava Kempinas & Klinefelter, 2014)

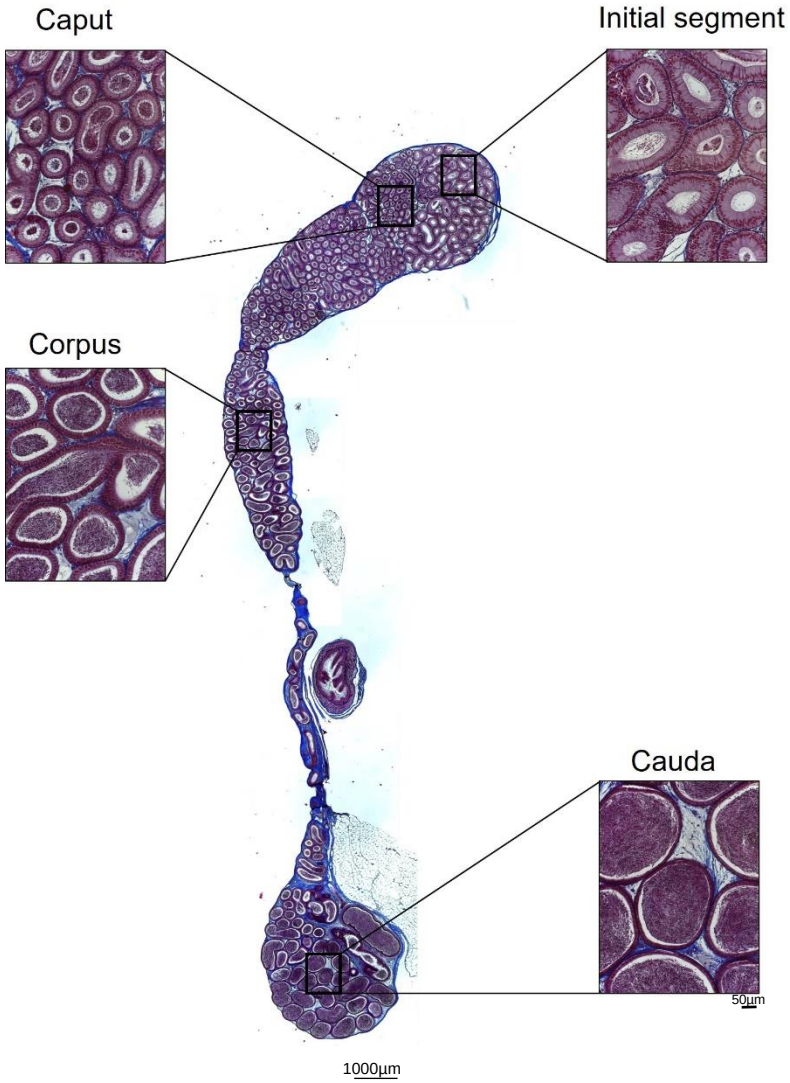

Figure 3. Histological structure of the mouse epididymis. Azan staining in paraffin-embedded epididymis sections.

1.1.2.2. Immune cells in the epididymis

The epididymis possesses a blood-epididymis barrier, composed of physiological, anatomical and immunological elements (Mita et al., 2011). There are remarkable differences in the immune cell populations, particularly the mononuclear phagocytes, throughout the epididymis consistent with the existence of immune tolerance in the proximal regions and immune defense at distal regions. In mouse models, it has been shown that immune cells are most prominent in the proximal regions with macrophages predominating and other

leukocytes accounting for <5%. The distal epididymis, on the other hand, has higher proportions of monocyte-derived cells as well as dendritic cells. It also contains more lymphocytes with innate immunity like-properties such as natural killer and γδ T cells. In particular, $CX3CR1^{+}$ macrophages, which possess homeostatic profiles are highly concentrated in the proximal regions, while the distal regions are heavily populated with pro-inflammatory monocyte-derived $CCR2^{+}MHCII^{+}$ cells (Pleuger et al., 2020, 2022). From the anatomical point of view, tight junctions between principal cells restrict movement of molecules and cells between the lumen and basal epithelium (Mita et al., 2011). The number and complexity of the tight junctions varies throughout the epididymis and is more extensive in the proximal regions (Friend & Gilula, 1972). The blood-epididymis barrier, compromised of the tight junctions along with other factors, seems to be less effective in preventing autoimmune responses compared to the blood-testis barrier. This was demonstrated when injection of spermatozoa or testicular germ cells led to formation of granulomas in the epididymis while no granulomas were detected in the testis (Itoh et al., 1999). Break down or breach of these two essential barriers can pave the way for altering the local microenvironment, eventually leading to infertility.

1.2. Male infertility

Infertility affects 1 out of every 6 couples worldwide (WHO, 2023). Infertility refers to failure to conceive after ≥12 months of regular unprotected sexual intercourse (Countries, 2004; Jequier, 2000). Male infertility can be the consequence of a myriad of causes, such as genetic mutations, trauma, infection, cancer as well as autoimmunity (Fijak et al., 2018; Schuppe et al., 2008). Of significant concern are infections and inflammation affecting the male genital tract, which are regarded as potentially curable entities and account for 13 - 15% of the cases of male infertility (Jequier, 2000; Weidner et al., 2013). This could present as urethritis, prostatitis, seminal vesiculitis, epididymitis, and orchitis, with the latter two causes being more likely to impair male reproductive function (Fijak et al., 2018; Haidl et al., 2008; Schuppe et al., 2008). Epididymo-orchitis and epididymitis arise as a result of infection, usually due to uropathogenic bacteria, or non-infectious

(sterile) inflammation. Isolated orchitis, most commonly caused by viral infections, is quite rare (Fijak et al., 2018; Schuppe et al., 2008). The majority of epididymitis cases most commonly stem from bacterial ascension from the urethra with *Escherchia coli* as the predominant pathogen followed by *Chlamydia trachomatis*, *Neisseria gonorrhoeae* and others (Fijak et al., 2018). Patients usually present with uni- or bilateral scrotal pain and swelling, with more than 40% of patients experiencing isolated pain in the cauda or in the entire epididymis. The pathological changes include interstitial edema, loss of epithelial integrity, leukocyte infiltration within the ducts and the interstitial space, along with fibrosis (Fijak et al., 2018; Pleuger et al., 2020). Severe forms of disease usually present with abscess formation commonly found in the cauda (Pilatz et al., 2015). These alterations can impair sperm maturation and secretory functions of the epididymis and can lead to duct obstruction and oligo- or azoospermia (Fijak et al., 2018; Pleuger et al., 2020). Given the fact that the testis is also affected in 60% of epididymitis cases, spermatogenesis is also affected (Fijak et al., 2018; Pilatz et al., 2013). Some patients with unilateral epididymitis exhibit testicular damage, presenting as destruction of seminiferous tubules, interstitial fibrosis and a thickened lamina propria that is accompanied by infertility (Osegbe, 1991). Even after successful antibiotic treatment, up to 40% of patients demonstrate long-term impaired fertility (Eickhoff et al., 1999; Rusz et al., 2012). After 3 months of antibiotics treatment, about 20% of the patients still exhibit an epididymal infiltrate, which can be detected via ultrasound or palpation (Fijak et al., 2018; Weidner et al., 1990).

In addition to infectious causes, non-infectious causes of inflammation of the testis and epididymis should be considered as causes of infertility. Patients with seminoma usually present with extensive inflammatory infiltrates (Xavier et al., 2021). Autoimmune diseases, such as vasculitis and lupus erythematosus, may affect blood vessels of the testis and epididymis leading to inflammatory diseases (Nistal & Paniagua, 2008). In addition, mutations of the AIRE gene, encoding a transcription factor (autoimmune regulator) essential for self-tolerance, can lead to production of anti-sperm antibodies in some patients (Zou et al., 2021). Moreover, in 50% of asymptomatic patients presenting with infertility, testicular leukocytic infiltration was reported. Leukocytic infiltrates were seen in the

interstitial, peritubular or perivascular compartment. Importantly, the infiltration was correlated with the destruction of seminiferous tubules, loss of spermatogenic cells, thickening of the lamina propria and fibrosis. Accurate diagnosis of sub-acute or chronic orchitis is usually hampered due to the lack of overt symptoms in most of the patients (Fijak et al., 2018; Schuppe et al., 2008; Schuppe & Bergmann, 2013). Considering access to tissues is usually hindered (Chakradhar, 2018), experimental models are indispensable for the comprehensive understanding of the cellular and molecular mechanisms involved in the initiation and progression of inflammation and its link to male infertility.

1.3. Experimental autoimmune epididymo-orchitis (EAEO)

Experimental autoimmune epididymo-orchitis (EAEO) serves as a model of autoimmune-based chronic testicular inflammation (Guazzone et al., 2011; Jacobo et al., 2015; Kohno et al., 1983; Nicolas et al., 2017a; Peng et al., 2022). The disease shares many features in common with some cases of male infertility. It is characterized by the production of auto-antibodies against testicular antigens accompanied by disruption of testicular immune privilege and aspermatogenesis (Kohno et al., 1983). EAEO can be induced in rodents by active immunization with testicular homogenate (TH) in complete Freund's adjuvant (CFA) followed by *Bordetella pertussis* toxin injection to boost the immune response (Guazzone et al., 2011; Jacobo et al., 2015; Kohno et al., 1983; Nicolas et al., 2017a; Peng et al., 2022). The inflammation mostly affects the seminiferous tubules (Kohno et al., 1983). The epididymis is also affected, showing atrophy along with remodeling of the epididymal duct with severe inflammatory and fibrotic changes reported in the cauda, but not in the caput (Wijayarathna et al., 2020). Interstitial lymphomononuclear and polymorphonuclear cell infiltrates are found around and in the seminiferous tubules, composed of macrophages, dendritic cells, lymphocytes, eosinophils, mast cells and neutrophils (Kohno et al., 1983; Nicolas et al., 2017a; Rival et al., 2006). This model is also characterized by reduced testosterone production (Fijak et al., 2011). Later stages of the disease are accompanied by disruption of the blood-testis barrier, leading to germ cell

sloughing, necrosis, fibrosis and granuloma-like changes (Kauerhof et al., 2019; Nicolas et al., 2017a; Pérez et al., 2012).

The critical role of testicular macrophages in EAEO development was demonstrated when the number of these cells was reduced, leading to significantly reduced EAEO incidence and severity (Rival et al., 2008). The phenotype of macrophages present in the testis in EAEO are mostly of a pro-inflammatory phenotype (Rival et al., 2008). Under the influence of activin A, which is increased in EAEO, macrophages acquire a pro-fibrotic role and contribute to the testicular fibrosis by increasing fibronectin, collagen I and CXCR4 (Peng et al., 2022). In contrast to the immature tolerogenic dendritic cells found in the normal testis, the dendritic cells present in EAEO are of mature phenotype, express higher level of MHC class II molecules and IL-12a mRNA and are capable of enhancing proliferation of naïve T cells (Guazzone et al., 2011; Rival et al., 2006). The amplification of the autoimmune response can lead to continuous antigen presentation by dendritic cells to lymphocytes in lymph nodes and the testis. In the inflamed testis, there is an increase of certain pro-inflammatory cytokines and chemokines, including TNF, IL-23, IL-17A, IL-6, CCR2, CCL2 and CXCL12 (Jacobo et al., 2015; Nicolas et al., 2017a; Peng et al., 2022), as well as activins, which exhibit pro-inflammatory and pro-fibrotic roles (Nicolas et al., 2017a; Nicolas et al., 2017b).

1.4. Acute bacterial epididymitis model

Epididymitis of infectious origin is commonly caused by uropathogenic *E. coli* (UPEC) infection resulting from bacterial ascension in patients (Pilatz et al., 2015). Taking biopsies from epididymitis patients is not recommended as this would allow the bacteria to disseminate and lead to irreversible damage (Fijak et al., 2018). In order to better mechanistically understand how UPEC infection affects the epididymis, a routinely used murine model can be utilized to mimic acute bacterial epididymitis. In these studies, UPEC strain CFT073 is inoculated by injection into the ligated vas deferens, either unilaterally or bilaterally, in adult mice (Bhushan et al., 2008; Pleuger et al., 2020, 2022). As in humans, the epididymal regions respond differently to the infection with fundamentally

disparate immune responses observed. Following the infection, the proximal regions of the epididymis seem to be largely unaffected, while the cauda is severely damaged and presents with interstitial fibrosis, loss of epithelial integrity, increase in luminal diameter, immune cell infiltration and abscess formation. A massive infiltration of neutrophils and macrophages is observed, especially in the cauda. An increase of activation factors specific for B and T cell populations occurs (Pleuger et al., 2020, 2022, Klein et al., 2020). Moreover, there is also an alteration in production of molecules associated with apoptosis signaling, integrin and interleukin signaling pathways, as well as inflammation mediated by chemokine and cytokine signaling pathway, such as TNF, activin A, IL-6, IL-17A, CCL2, CCL3, and CCL4 (Michel et al., 2016; Pleuger et al., 2022).

1.5. Fibrosis

Sustained inflammation can lead to continuous activation of cytotoxic and repair pathways causing progressive tissue fibrosis and adverse tissue remodeling that, in the case of male reproductive tract involvement, can lead to infertility. In EAEO, there is accumulation of extracellular matrix components and thickening of the lamina propria in the testis (Lustig et al., 2020; Nicolas et al., 2017a). Collagen content is increased along with fibronectin. Importantly, levels of collagens and macrophages expressing fibronectin are also elevated in patients with impaired spermatogenesis accompanied by leukocytic infiltration compared to biopsies with intact spermatogenesis (Kauerhof et al., 2019; Peng et al., 2022). In addition, infection of mice with UPEC leads to an increase of pro-fibrotic markers and cytokines in the epididymis along with visible fibrotic changes demonstrated by thickening of the smooth muscle layer and increase of collagen deposits around tubules. Activin A, increased in testicular and epididymal inflammation, is postulated to play a major role in the progression of fibrosis, as well as regulation of chemokines expression which could impact the course of the disease (Kauerhof et al., 2019; Michel et al., 2016; Peng et al., 2022).

1.6. Activins

Activins, which are members of the TGF-β family of cytokines, have a role in regulating spermatogenesis and steroidogenesis, but also in inflammation, tissue homeostasis and repair (Hedger, 2011; Werner & Grose, 2003; Wijayarathna & de Kretser, 2016). Activins are homodimers and heterodimers of β subunits of the gonadal hormone, inhibin, linked by single covalent disulfide bond. The type of activins formed depends on the type of inhibin β subunits (β_A, β_B and β_C). Of the activins, activin A, a homodimer of β_A subunit, is the best characterized in terms of regulation and function (Phillips et al., 2009; Tompkins et al., 1998). Activins were initially studied for their ability to regulate the pituitary gonadotropin, FSH (follicle-stimulating hormone), which has a vital role in regulating reproductive processes. In males, FSH is critical for the initiation and maintenance of spermatogenesis, promoting testicular growth and Sertoli cells maturation (Nieschlag et al., 1999; Wijayarathna & de Kretser, 2016). Like other members of the TGF-β family, they exert their function through surface transmembrane receptors exhibiting intrinsic serine/threonine kinase activities. The biological activity of activin A is mainly regulated by follistatin (FST), which binds irreversibly with high affinity to all activins leading to their endocytosis and lysosomal degradation. Inhibin can also regulate the biological activity of activin A acting as a competitive antagonist (Gray et al., 2005). The affinity of FST binding to activin A is almost as strong as activin A binding to its receptors. FST can bind to other members of the TGF-β superfamily, particularly activin B, myostatin and bone morphogenetic proteins, but with lower affinity compared to activin A (Gray et al., 2005; Hedger et al., 2011). Alternative splicing generates two main forms of FST: (i) FST315 - the main circulating form, and (ii) FST288 - mostly tissue-bound (Wijayarathna & Hedger, 2019).

1.6.1. Activin A regulates functions of the immune and testicular cells under normal and inflammatory conditions

Activin A plays essential roles in testicular and epididymal functions. Given its wide range of functions, activin A can be produced by almost all cell types, but especially by epithelial, mesenchymal and immune cells (Phillips, 2003). Several

cell types in the testis are regarded as producers of activin A, particularly the Sertoli cells and TM, but the Leydig cells, PTC and spermatogenic cells also contribute (Barakat et al., 2008; Hedger, 2011; Kauerhof et al., 2019; Okuma et al., 2005; Winnall et al., 2011). In the epididymis, there is a gradient of activin A expression, with very high expression in the caput that decreases gradually towards the cauda. Epithelial cells and macrophages present in the epididymis are the major producers of activin A (Wijayarathna et al., 2017).

The Sertoli cells are regarded as a main source of activin A in the testis under normal conditions, and its expression can be stimulated by activation of TLR/IL-1 or TNF inflammatory signalling pathways (Hedger & Winnall, 2012; Kazutaka et al., 2011; Okuma et al., 2005). PTC stimulated with activin A showed increased production of collagen I and fibronectin (Kauerhof et al., 2019). Activin A can also stimulate proliferation and collagen production by fibroblasts (Hedger et al., 1989), and stimulates bone marrow derived macrophages to acquire a pro-fibrotic profile by expressing CCR2, fibronectin, and matrix metalloproteases (Peng et al., 2022). Moreover, activin A can inhibit Leydig cells steroidogenesis (Lin et al., 1989; Mauduit et al., 1991). These actions initiated by activin A are regarded as driving forces for the development of severe fibrosis (Hardy et al., 2015), which in case of testicular inflammation is detrimental to testis function (Kauerhof et al., 2019; Nicolas et al., 2017a; Nicolas et al., 2017b). The ability of IL-1, TNF and TLR ligands, like lipopolysaccharide (LPS), to potently stimulate activin A in a plethora of cell types (Antsiferova & Werner, 2012; Arai et al., 2011; Wilson et al., 2006; Wu et al., 2013), explains the elevated expression of activins in pathologies of inflammatory origin, such as chronic central nervous system inflammation, inflammatory bowel disease and rheumatoid arthritis (Hardy et al., 2015; Hedger et al., 2011; Jones et al., 2004, 2007).

Activin A is increased in the testis and epididymis under inflammatory conditions and also plays a role in the inflammatory and fibrotic responses (Kauerhof et al., 2019; Michel et al., 2016; Nicolas et al., 2017b). For example, the extent of leukocytic infiltration, collagen levels (Kauerhof et al., 2019) and the EAEO severity score correlate with testicular activin A levels in the EAEO model (Nicolas et al., 2017b). Furthermore, blocking activin A action in EAEO by overexpression

of FST in mice decreased expression of pro-fibrotic factors in the testis (Peng et al., 2022). Addition of activin A to the organ cultures of the mouse epididymis, especially the cauda, caused fibrotic changes that could be reversed by addition of recombinant FST (Michel et al., 2016).

1.6.2. Activin A influences the expression of several chemokines and cytokines

Activin A can regulate several members of the chemokine network that display a crucial role in leukocyte migration under both homeostatic and inflammatory conditions. The CCL2-CCR2 axis, which regulates macrophage polarization, can be controlled by activin A. Activin A increases *Ccr2* expression in colony stimulating factor (CSF)1 or CSF2-generated macrophages, but inhibits CCL2 expression (Peng et al., 2022, Sierra-Filardi et al., 2014). Moreover, activin A enhances the migration of bone marrow derived macrophages along a CCL2 gradient and increases the expression of CXCR4 (Peng et al., 2022). It also shows potent autocrine effects on immune responses in dendritic cells. Blocking activin A signaling in dendritic cells using FST after CD40 ligand (CD40L) stimulation not only enhances cytokine secretion (IL-6, IL-10, IL-12p70, and TNF), but also upregulates chemokine production (CXCL8, CXCL10, CCL5, CCL2) (Robson et al., 2008). Activin A can induce CXCL12 and CXCL14 dependent dendritic cell recruitment to areas of inflammation (Salogni et al., 2009). On the other hand, activin A can exert an anti-inflammatory action thought to protect from joint damage by inhibiting the TNF-induced release of CXCL10 (Kuranobu et al., 2020), and it can influence B cell migration by promoting the production of CXCL13 by T cells (Locci et al., 2016). Furthermore, activin A can decrease the expression of CXCL9/10 by myeloid cells, which can subsequently impair cytotoxic T cell infiltration into melanoma sites (Pinjusic et al., 2022).

1.7. Chemokines

Cytokines are signaling molecules that exhibit immune modulatory actions regulating inflammation and affecting cellular activities, such as growth, survival,

and differentiation (Oppenheim, 2013). Chemokines are a special class of chemotactic cytokines that can induce immune cell migration and trafficking (Stone et al., 2017). Chemokine members are divided into 4 groups (CXC, CC, C and CX3C), depending on the number of amino acids located between the N-terminal cysteine residues. Their receptors are G-protein-coupled receptors (GPCR), which are found on several cell types. Because of the similarity in structure between chemokines, the chemokine network is extremely complex and redundant **(Fig. 4)**. This enables accurate fine-tuning of leukocyte responses to various inflammatory stimuli (Stone et al., 2017).

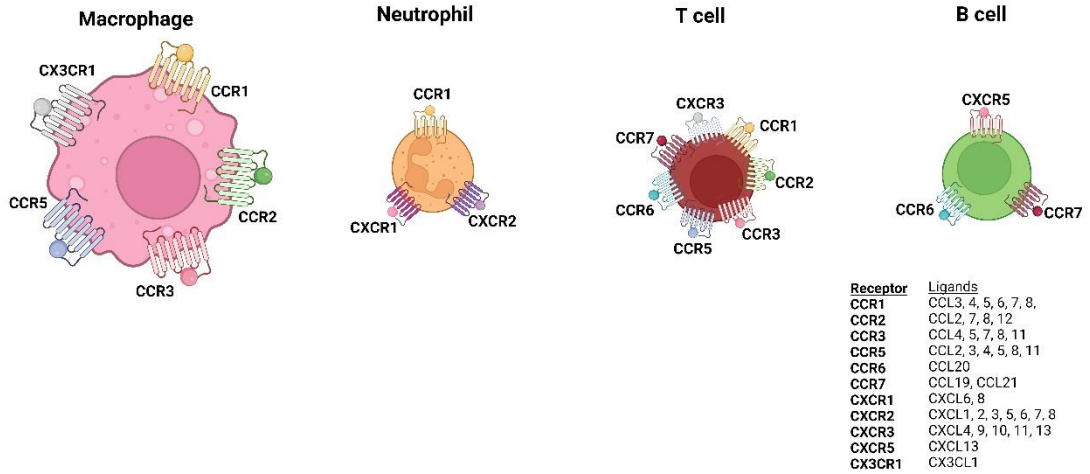

Figure 4. Chemokine network is extremely complex and promiscuous. Scheme demonstrating the expression of chemokine receptors on macrophages, neutrophils, T and B cells. The corresponding ligands are also included. Figure created with BioRender.

Chemokines and their receptors are critical elements in regulating the trafficking of cells to inflammatory sites (Springer, 1994). CCR2 and CCR5 are involved in both monocyte- and macrophage-mediated recruitment, and in the regulation of T cell migration and activation (Tokuyama et al., 2005). CCR2 and its main ligand CCL2, is regarded as one of the key chemokines regulating migration and infiltration of monocytes/macrophages (Deshmane et al., 2009). CCR1 and its ligands regulate trafficking of macrophages and neutrophils (Hughes & Nibbs, 2018). The CCR5-binding chemokines, CCL3, CCL4 and CCL5, play major roles in recruiting Th1 inflammation-promoting T cells and macrophages (Schrum et

al., 1996). CCR3 and CCR4, on the other hand, are involved in recruitment of Th2 cells which play a role in inhibition of inflammation (Hughes & Nibbs, 2018).

On the other hand, CXCR2-binding chemokines, CXCL1 and CXCL2, are potent neutrophil chemoattractants (Girbl et al., 2018). CXCR3 is a chemokine receptor that is highly expressed on effector T cells and plays a potent role in Th1 cell trafficking and function. CXCL9, CXCL10, CXCL11 are responsible for the recruitment of effector, CXCR3- positive T cells to inflammatory sites (Groom & Luster, 2011). CX3CR1 and its ligand CX3CL1 play an important role in monocyte homeostasis and macrophage polarization and function (Zheng et al., 2013). Fibroblasts, which are central to promoting lung fibrosis, highly express CXCR4 and its corresponding ligand CXCL12. Exogenous CXCL12 was found to significantly stimulate the migration and proliferation of fibroblasts, while potentiating the expression of CXCR4 (Li et al., 2020). CXCR5 and its ligand CXCL13 play significant roles in B cell trafficking, facilitating the establishment of lymphoid follicles and germinal center formation (Ghafouri-Fard et al., 2021).

1.7.1. Chemokines in testicular and epididymal physiology and inflammation

In addition to immune cells, somatic testicular cells, including Sertoli cells, PTC and Leydig cells produce a number of chemokines and cytokines (Gerdprasert, 2002; Guazzone et al., 2003, 2009; Rival et al., 2007). Chemokines produced by testicular cells under physiological conditions are mainly involved in maintenance and migration of spermatogonia (Diao et al., 2018). CCL3, found in both germ cells and Leydig cells, participates in the regulation of spermatogonial proliferation (Hakovirta et al., 1994). CCL2 is expressed by PTC and can be stimulated by many pro-inflammatory mediators and cytokines. Moreover, Leydig cells express CCL2 when stimulated by IL-1β (Aubry et al., 2000, Gerdprasert et al., 2002). Sertoli cells also secrete CCL2 in response to TLR agonists (Riccioli et al., 2006). CXCL10 is expressed in Leydig cells and it has an inhibitory effect on Leydig cells steroidogenesis. CXCL1 and CXCL10 can be induced in Leydig cells, PTC and Sertoli cells by pro-inflammatory cytokines (Guazzone et al., 2009; Hu et al., 1998). Moreover, the only ligand in the CX3C chemokine family,

CX3CL1, is expressed in Sertoli cells, spermatogonia, pachytene spermatocytes and elongated spermatids, but to a higher extent in Leydig cells (Habasque, 2003). The epididymis as well acts as source of chemokines under steady state. Clear cells, under physiological conditions, express chemokines involved in pro-inflammatory responses such as CCL17, CXCL10, CXCL1 and CXCL31. Mononuclear phagocytes, which are in close association with clear cells, express the receptors for these ligands. Given how clear cells are strategically located, these chemokines can prime mononuclear phagocytes to mount inflammatory responses (Battistone et al., 2023).

The chemokines secreted by these cells under physiological condition are necessary for several functions mainly growth and differentiation of cells. However, an excess of these mediators can have deleterious effects on fertility. An increase of several pro-inflammatory cytokines especially TNF, IL-1β, Il-1α and IL-6 can drastically alter lymphocyte activation and proliferation, destroy germ cells as well as disrupt spermatogenic cell differentiation and testicular steroidogenesis (Guazzone et al., 2009; Hedger & Meinhardt, 2003; Mealy et al., 1990; Oritani et al., 1999). Modulating the chemokine network might represent a potential strategy to limit or attenuate macrophage and T cell activation in inflammatory pathologies, including testicular and epididymal inflammatory disease.

In the testis, increased CCL2, CCR2 and CCR5 can contribute to leukocyte infiltration in EAEO (Guazzone et al., 2003, 2012; Peng et al., 2022). CCL2, a crucial chemokine in monocyte migration and extravasation, is increased in testicular fluid and in the conditioned medium obtained from cultures of TM in EAEO (Guazzone et al., 2003). Importantly, it was recently shown that mice deficient in CCR2 demonstrate reduced testicular damage and are protected from fibrotic remodeling (Peng et al., 2022). Other CC chemokine ligands play a role in EAEO. High levels of CCL3 and CCL4 in testicular fluid coincide with the onset of EAEO (Guazzone et al., 2012). The increase in monocyte and T cell recruiting chemokines correlates with an influx in number of CCR5-induced lymphocytes infiltrating the EAEO testis (Guazzone et al., 2009) and this is associated with the severity of testicular lesions (Guazzone et al., 2012). In addition, in the inflamed

testis, there is an up-regulation of CCR7 and a down-regulation of CCR2 on dendritic cells, which denotes a migratory phenotype (Rival et al., 2007). In the epididymis, induction of EAEO increases CCL2 and CX3CL1 in the cauda (Wijayarathna et al., 2020). The cauda epididymidis is also affected in UPEC infection and some chemokines are also altered, such as CCL2, CCL3, CCL4, CXCL13 and CXCL2 (Pleuger et al., 2022). Moreover, LPS intravasal–epididymal injection increases pro-inflammatory chemokines by clear cells such as CXCL10, CXCL1, CXCL2 and CCL5 (Battistone et al., 2020).

1.8. Lymphoid chemokines

Lymphoid organs are classically divided into primary and secondary organs. Primary lymphoid organs, including the bone marrow and thymus, are responsible for lymphocyte generation, while SLO including the spleen, tonsils, lymph nodes as well as mucosa-associated lymphoid tissue (such as in the lung and the gastrointestinal tract), are recognized as the hub for adaptive immune response where immune cells become functionally activated and specialized. These immune cells are introduced to different antigens, which subsequently allows them to differentiate into effector and memory T cells that are critical for antigen encounter and subsequent elimination of the antigen if needed (Bery et al., 2022; Ruddle, 2020).

CCL19, CCL21 and CXCL13, referred to as lymphoid chemokines, are expressed in secondary lymphoid organs (SLO), such as the lymph nodes, spleen and Peyer's patches, contributing to lymphoid tissue microanatomical organization (Luther et al., 2002). Chemokine ligands, CCL19 and CCL21, which are produced by stromal cells, bind to CCR7 on T cells and dendritic cells and allow T cells to reside in the paracortical area of SLO. CXCL13, on the other hand, is produced by follicular dendritic cells and is involved in B cell attraction and germinal center formation, which is a site essential for high affinity antibody production. B cells are primarily found in regions known as lymphoid follicles (Drayton et al., 2006; Förster et al., 1996; Lalor & Segal, 2010). These chemokines mentioned above, which play essential roles in SLO formation, can also be expressed during

inflammation driving the ectopic organization of immune cells and stromal elements into structured aggregates called tertiary lymphoid organs (Ruddle, 2020).

1.9. Tertiary lymphoid organs (TLO)

In addition to primary and secondary, a third type of lymphoid organs - termed tertiary lymphoid organs (TLO) - was first coined in 1992 (Picker & Butcher, 1992) to describe tissues that normally contain few lymphoid elements and in the presence of an inflammatory trigger become organized to perform functions analogous to SLO. Initially, there were only few mentions of TLO, as the concept that inflammation could lead to development of an organized accumulation of cells resembling a lymph node was not immediately accepted. At that time, inflammation was classically regarded as a response embodied by the four clinical characteristics (heat, pain, redness, and swelling) (Ley, 2001). The description of inflammation was not dependent on the histological and functional characteristics observed in the tissue.

A series of studies conducted in the 1990s revolving around the lymphotoxins led to wider acceptance of the existence of TLO. Mice deficient in lymphotoxin-alpha (LTα) lacked lymph nodes (De Togni et al., 1994), while mice with overexpression of LTα developed sites resembling lymph nodes in the pancreas, kidney and skin (Kratz et al., 1996). Since then, the occurrence of TLO driven by inflammation has been described in almost every organ, including the pancreas, lung, kidney, skin, brain, gut, liver, joints, artery, placenta, salivary and lacrimal glands, thymus, vagina, blood vessels, heart, testis, and ovaries (Drayton et al., 2006; Neyt et al., 2012; Pipi et al., 2018; Ruddle, 2020). However, some tissues have been reported to be more susceptible to TLO formation than others (Chen et al., 2002). Their occurrence in the epididymis was never reported before and they have not been well characterized in the testis (Sakai et al., 2014).

1.9.1. Organization and characteristics of SLO and TLO

The SLO is a highly organized encapsulated structure and is embedded in stromal reticular networks. It is clearly separated into T and B cell zones, which contain germinal centers (GC). It is highly vascularized and comprises lymphatic vessels, which permit collected lymph and cellular contents to enter the SLO as well as high endothelial venules (HEV), specialized blood vessels, which facilitate naïve and central memory T and B cell homing to the tissue (Bery et al., 2022; Neyt et al., 2012). Its functions include sampling antigens from blood and lymph, permitting dendritic cells to enter and allowing T and B cells, which have encountered antigen, to proliferate and differentiate (Turley et al., 2010). SLO develop in a predefined place before birth and this is governed by a lymphoid tissue inducer cell interacting with a lymphoid tissue organizer via lymphotoxin beta receptor (LTβR), which allows the latter cell to express adhesion molecules in addition to the chemokines CCL19, CCL21 (T cell ligands) and CXCL13 (B cell chemoattractant). Local fibroblasts receive an initial signal to start producing CXCL13 attracting the lymphoid tissue inducer (Van De Pavert et al., 2009). Following the interaction, lymphoid tissue organizer develops into follicular dendritic cells (FDC) and fibroblastic reticular cells (FRC) permitting the conduit framework to develop. Production of lymphangiogenetic growth factors allows lymphatic vessels to form (Vondenhoff et al., 2009).

Unlike SLO, which are developmentally pre-programed, TLO lack a capsule and do not form at pre-determined locations. They can be induced by inflammation resulting from infection, autoimmunity, cancer, aging as well as allograft rejection (Drayton et al., 2006; Ruddle, 2020). TLO follows similar pathways to those utilized by the SLO (Neyt et al., 2012). Overexpression of LTα, CCL21 or CXCL13 can induce the formation of TLO (Chen et al., 2002; Drayton et al., 2003; Neyt et al., 2012). In addition, LTα plays a role in developing stromal cells into FDC and HEV (McDonald et al., 2005; Neyt et al., 2012). The TLO can form in an antigen-dependent or -independent manner (Sato et al., 2023). It is believed that once the antigen exposure is cleared, TLO formation is resolved (Drayton et al., 2006). A very recent study, however, showed that loss of NOTCH signaling in mice can modify arterial endothelial cells shifting their identity to a HEV-like phenotype.

This was associated with the spontaneous formation of TLO in multiple organs, such as kidney, liver and lung (Fleig et al., 2022). At this stage of research, several studies are still needed to delineate the mechanisms that allow TLO development and maintenance in an antigen-independent manner (Sato et al., 2023).

Inflammation that allows TLO development is mainly driven by innate immune cells, specifically neutrophils, natural killer cells, dendritic cells and macrophages, which can prime endothelial cells and stromal cells (e.g. fibroblasts). Stromal cells once primed can release chemokines CCL19, CCL21, and CXCL13 that mediate further immune cell recruitment and spatial organization within the forming TLO (Bery et al., 2022; Ruddle, 2020). The extent of TLO organization depends on the inflammatory stimulus, the tissue type, and where they develop (Sato et al., 2023). This ectopic organ first appears as loose B cell- T cell clusters, mostly intermingling, but occasionally forming clearly segregated zones of B cells and T cells, as observed in SLO **(Fig. 5)**.

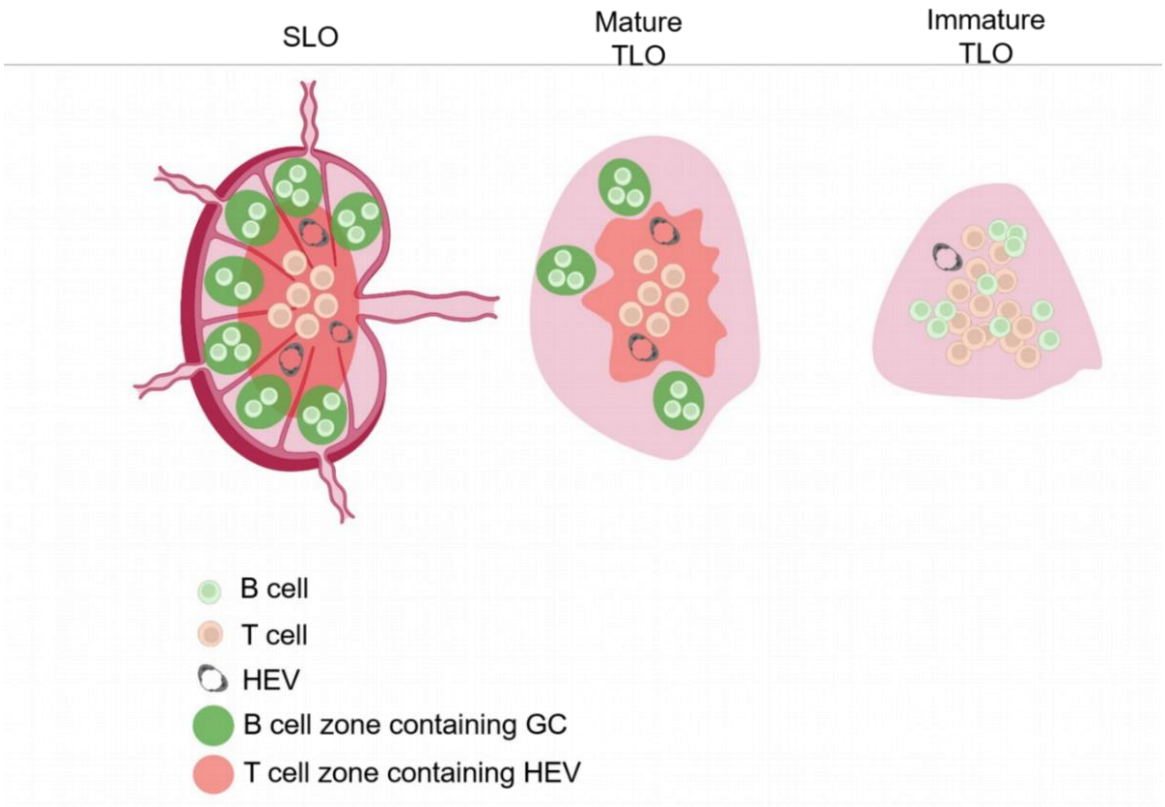

Figure 5. Comparison between secondary lymphoid organ (SLO) and tertiary lymphoid organ (TLO). Both mature TLO and SLO are divided into distinct zones of T and B cells. While an SLO is capsulated, a TLO lacks a capsule. The B cells are proliferating in the germinal center (GC) and are capable of producing high affinity class switched B cells and plasma cells. The T

cell zone is rich in CCL19 and CCL21 and contains high endothelial venule (HEV). An immature TLO, on the other hand, includes the elements of a TLO but is not well organized and lacks a clear GC. Note: the SLO schematic acts as a representation of a lymph node and not a spleen as the spleen, although regarded as an SLO, lacks the presence of HEV. Figure created using Bio Render.

This compartmentalization of B and T cells is achieved by chemokine gradients of B cell chemoattractants (CXCL13) and T cell ligands (CCL19 and CCL21). An early form of TLO can be differentiated during acute inflammation, where it generally contains few granulocytes and contains B and T cells (Borregaard, 2010). Later advanced mature stages of TLO include the presence of CD21+ FDC within the B cell areas. (Bery et al., 2022; G. Jones et al., 2016; Ruddle, 2020). Finally, FDC allow for an activation of GC reactions in the B cell areas, which are then responsible for the production of high affinity antibody secreting plasma cells and memory B cells. The immune cells are recruited by HEV, which develop from activated endothelial cells **(Fig. 5)** (Bery et al., 2022; Drayton et al., 2006; Jones et al., 2018; Neyt et al., 2012; Ruddle, 2020).

1.9.2. High endothelial venules (HEV) in inflammatory conditions

HEV are regarded as specialized portals adapted for the trafficking of large numbers of lymphocytes. HEV are formed by cuboidal endothelial cells, have a thick basal lamina made of fibronectin, collagen IV, and laminins and are enclosed by concentric layers of fibroblastic reticular cells (FRC). Within their lumen they contain numerous lymphocytes and accumulate chemokines, such as CCL21, CCL19, CXCL10, CXCL12 and CXCL13 (Blanchard & Girard, 2021; Girard & Springer, 1995). HEV are found in all SLO except those of the spleen. They are fully integrated in organs during embryogenesis. Under homeostatic conditions, they act as guardians regulating the outcome of the immune response where they are responsible for delivering naïve and memory lymphocytes from the blood stream to lymphoid organs. Lymphocytes circulating in the blood directly enter a lymph node via HEV, where they scan antigen-presenting cells (Blanchard & Girard, 2021; Girard & Springer, 1995; Hayasaka et al., 2010). The immune cells roll on the surface of the HEV by binding via L-selectin to 6-sulfo

sialyl Lewis X motifs present on the HEV cells. They interact with chemokines presented by heparin sulfate on the HEV luminal surface. Chemokine receptor-ligand binding activates lymphocyte integrins which mediate firm binding, leading to arrest of the lymphocytes followed by transmigration across the HEV endothelium and allowing them to enter the lymphoid tissue (Blanchard & Girard, 2021; Girard & Springer, 1995).

These specialized blood vessels can also develop postnatally in non-lymphoid organs during chronic inflammation driven by autoimmunity, infection and allografts. Their appearance in non-lymphoid organs was first reported in the synovium of rheumatoid arthritis patients (Freemont et al., 1983). They are commonly observed when pronounced infiltration is present and are frequently associated with TLO. HEV are regarded as critical for the maintenance and function of TLO (Blanchard & Girard, 2021). Several mechanisms related to the development of HEV in lymphoid organs under physiological conditions seem to also be involved in HEV formation in ectopic locations. A series of studies showed that stimulation of tumor necrosis factor receptor 1 (TNFR1) signaling pathway can lead to the formation of MECA-79 (Mouse Endothelial Cell Antigen-79) positive HEV. MECA-79 is a highly specific HEV sulfated antigen. The activation of LTβR signaling is required for HEV to acquire mature phenotypes with improved ability to capture L-selectin-expressing lymphocytes **(Fig. 6)** (Drayton et al., 2003; Sacca et al., 1998).

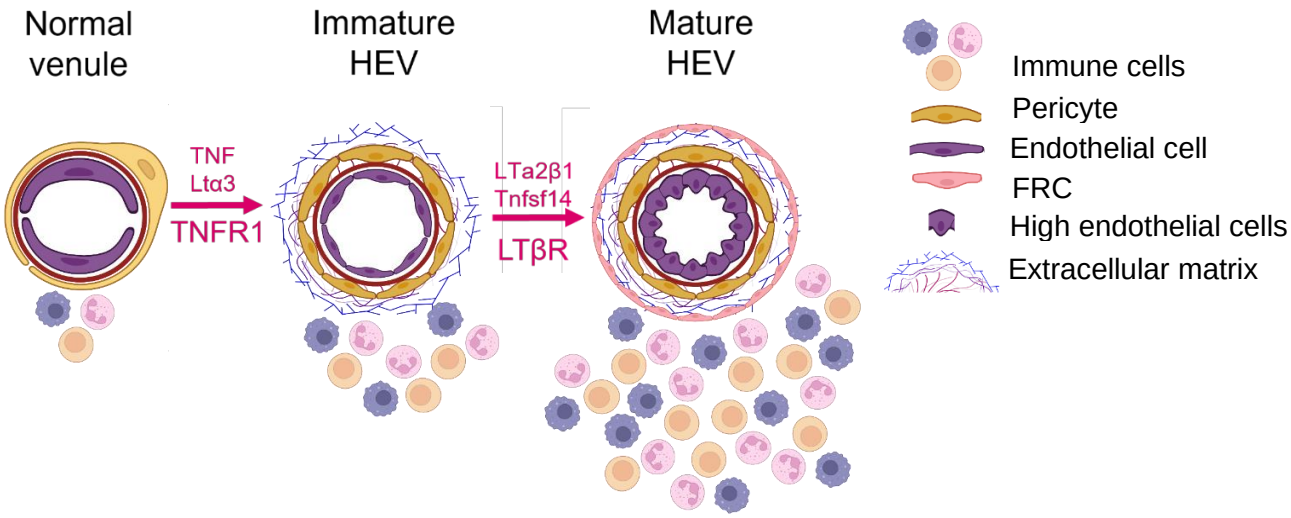

Figure 6. Mechanisms involved in the ectopic formation of High endothelial venule (HEV). HEV develop from post-translation modifications of normal venules. Normal venules lacking MECA-79 can recruit few immune cells. Under inflammatory conditions, triggering of the TNFR1 pathway via LTα3 changes the normal vessel into an immature HEV still displaying flat endothelial cells. Prolonged inflammatory signals can stimulate the LTβR pathway, which allow the HEV to acquire a mature phenotype. A mature HEV possesses cuboidal endothelial cells, is enclosed by concentric layers of fibroblastic reticular cells (FRC) and is also capable of recruiting massive amounts of lymphocytes compared to its predecessors. Figure created using Bio Render.

Lymphocytes, especially CD4+T cells, play major roles in induction of HEV formation. HEV forming as a result of ectopic expression of CCL21 are lost when lymphocytes are experimentally depleted, but are restored when CD4+T cells are transferred to the mice (Blanchard & Girard, 2021; Marinkovic et al., 2006).

1.9.3. TLO function

The function and clinical relevance of TLO are context-dependent. TLO seems to develop to accommodate an increased demand for a localized immune response (Neyt et al., 2012). Understanding the prognosis of TLO formation in different disease conditions is necessary to formulate future experimental manipulation strategies. The formation of TLO can be induced when it provides a benefit or limited when it is detrimental.

In the context of cancer, the presence of TLO is often associated with a better outcome. Patients, who develop TLO show higher survival rates, lower relapses and in some cases respond better to immunotherapy (Cabrita et al., 2020; Sautès-Fridman et al., 2019; Schumacher & Thommen, 2022; Vanhersecke et al., 2021). The presence of a TLO in the vicinity of the cancer shortens the time for priming T and B cells to generate efficient immune responses as this bypasses the need to traffic to the lymph nodes. Moreover, the presence of a TLO may strengthen, diversify and amplify the immune responses generated against the tumor antigens as there is a higher chance of antigen encounter with lymphocytes. Likewise, lymphocytes fighting against cancer may have better survival as they are located in an environmental niche that supports their survival (Sautès-Fridman et al., 2019; Schumacher & Thommen, 2022). Patients with

seminoma, a germ cell tumor, have HEV-like vessels that are likely contributing to T cell recruitment (Sakai et al., 2014).

In cases of autoimmune diseases, the presence of TLO is associated with breaking of self-tolerance, progression of the disease and a worse outcome due to their ability to act as sites of antigen-presentation (Pipi et al., 2018). In rheumatoid arthritis, TLO support the local production of anti-citrullinated protein/peptide antibodies, which are highly specific markers of rheumatoid arthritis and predict a poor prognosis (Humby et al., 2009). Moreover, the kidneys of patients with systemic lupus erythematosus contain GC that support *in situ* antibody production, clonal expansion and somatic hypermutation (Chang et al., 2011). TLO can contribute to the progression of Sjögren's syndrome, an autoimmune disease that affects the body's moisture-producing glands, where they are involved in increased production of auto-antibodies by B cells in the salivary gland (Salomonsson & Wahren-Herlenius, 2003).

In the context of infections, TLO develop quickly and are considered essential for providing protective immune responses (Sato et al., 2023). Mice experimentally lacking SLO develop TLO in response to influenza infection, facilitating clearance of the virus and enhanced survival (Moyron-quiroz et al., 2004; Sato et al., 2023). In addition, TLO that develop due to influenza infection promote local antibody production, thereby providing efficient protection. Infection with *Mycobacterium tuberculosis* leads to granuloma formation followed by TLO development in murine models (Kahnert et al., 2007). Patients with latent tuberculosis develop TLO and patients with reactivated tuberculosis usually lack TLO (Ulrichs et al., 2005). TLO also form in response to fungal infections such as *Pneumocystis jirovecii* resulting in a lower fungal burden in mice (Eddens et al., 2017). Infection with *Helicobacter pylori,* on the other hand, can induce the formation of TLO, but this was associated with gastritis and development of mucosal associated lymphoma in mice (Shomer et al., 2003).

1.10. Aims and hypotheses of the study

The fact that infiltration of immune cells leads to testicular and epididymal destruction during inflammatory response, paving the way for infertility, highlights the importance of understanding the mechanisms that govern leukocyte migration and attraction in these tissues (Fijak et al., 2018; Loveland et al., 2017).

EAEO is a model of chronic testicular inflammation and it shares many similar pathological features reported in some patients with infertility. CCR2 and its ligand CCL2 are increased in EAEO testis and mice deficient in CCR2 are protected from EAEO induced damage (Peng et al., 2022). Activin A, which is also elevated in testicular inflammation, induces CCR2 expression and migration of macrophages. Moreover, there is a positive correlation between the severity of disease and testicular activin A concentration. Importantly, inhibition of activin A bioactivity by overexpression of follistatin reduces EAEO-induced testicular damage (Peng et al., 2022; Nicolas el al., 2017a, Nicolas et. Al 2017b).

In many instances, disturbances in homeostasis, accompanied by alterations in the chemokine network can drive the formation of organized immune cell infiltrates. Tertiary lymphoid organs develop ectopically in non-lymphoid locations during inflammation and they resemble secondary lymphoid organs in their structure, vasculature, chemokine expression and functionality. Sustained inflammation can trigger the formation of these ectopic structures in certain locations (Neyt et al., 2012; Sato et al., 2023; Schumacher & Thommen, 2022). However, their occurrence in the male reproductive tract has not been previously reported. The testis and epididymis are prone to insults, where infection and inflammation are causes of concern (Jequier, 2000; Weidner et al., 2013). The testis and the epididymis respond differently to inflammation (Fijak el al., 2018). In addition, the individual regions of the epididymis react differently to inflammation. While the proximal regions of the epididymis remain unaffected in presence of bacterial infection, the cauda epididymidis is severely damaged and presents with interstitial fibrosis, loss of epithelial integrity, increase in luminal diameter, immune cell infiltration and abscess formation (Pleuger et al., 2020, 2022, Klein et al., 2020).

Therefore, the aims of this thesis are:

(1) to investigate how the chemokine network responds during testicular inflammation in normal wild-type and CCR2-deficient (*Ccr2*$^{-/-}$) mice;

(2) to elucidate how activin A influences the expression of chemokines and their receptors; and

(3) to examine the potential formation of tertiary lymphoid organs fueled by inflammatory responses in the testis and epididymis.

The following hypotheses were examined:

- Disruption of the chemokine network paves the way for the destruction of the testis, but depletion of CCR2 signaling can ameliorate tissue damage and preserve fertility.
- Systemic and testicular activin A are increased in EAEO and regulate chemokine and chemokine receptor expression, with detrimental outcomes.
- Disturbances in the chemokine network driven by inflammatory stimuli can induce tertiary lymphoid organs to develop in the male reproductive tract.

2. Methods

2.1. Methods

2.1.1. Animals

10- to 12-week-old male wild-type (*WT*) *C57BL/6J* and *B6.129P2-Ccr2*$^{tm1Mae/tm1Mae}$ (*Ccr2*$^{-/-}$) mice were purchased from Charles River Laboratories, Sulzfeld, Germany. The mice were housed in specific pathogen-free (SPF) conditions under 12 h light/dark cycle, 20–22 °C ambient temperature and 50 ± 5% relative humidity at the animal facility of Justus Liebig University, Giessen. The mice were supplied with autoclaved water and food *ad libitum*. All experiments involving animals were carried out in strict accordance with the recommendations for the Care and Use of Laboratory Animals of the German animal welfare law. Animal experiments were approved by the responsible local ethics committee for animal care (Regierungspraesidium Giessen GI 58/2014 — Nr. 735-GP and V54 – 19 c 20 15 h 01 GI20/25 Nr. G60/2017 and Nr. G71/2019) and were performed in strict accordance with the German animal welfare law and the European legislation for the protection of animals used for scientific purposes (2010/63/EU). Mice were euthanized using isoflurane inhalation followed by cervical dislocation. Testis, epididymis, bone (femur and tibia) and blood were collected.

2.1.2. Induction of EAEO

EAEO was induced in 10- to 12-week-old male *WT C57BL/6J* and *B6.129P2-Ccr2*$^{tm1Mae/tm1Mae}$ (*Ccr2*$^{-/-}$) mice as described previously (Nicolas et al., 2017a; Peng et al., 2022). Briefly, mice (n = 6) were immunized with testicular homogenate mixed at 1:1 ratio with complete Freund's adjuvant (CFA) containing heat killed *Mycobacterium tuberculosis.* Testicular homogenate was obtained from decapsulated *WT C57BL/6J* mice testis in sterile 0.9% NaCl using a Potter S homogenizer. Each animal was immunized with a total volume of 200 µl of the prepared mixture by four s.c. injections on the back in the area of the shoulders and the hind limbs in the proximity of the lymph nodes. This was followed by *i.p* injection of 100 ng *Bordetella pertussis* toxin in 100 µl Munõz Buffer (25 mM Tris,

0.5 M NaCl, 0.017% Triton X-100, pH 7.6). Mice were immunized using this protocol three times, 14 days apart **(Fig. 7).**

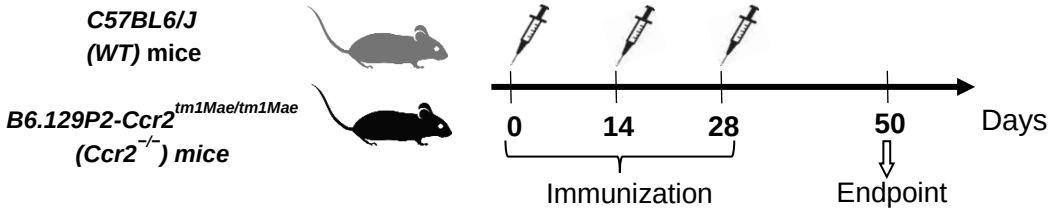

Figure 7. Scheme representing the time points for EAEO induction and organ collection in *C57BL6/J* (*WT*) and *Ccr2*$^{-/-}$ mice. Mice were immunized with testis homogenate (TH) in Complete Freund's Adjuvant (CFA) three times, 14 days apart. Testis, epididymis and blood were collected at day 50 after first immunization. Adjuvant control mice received CFA in NaCl without TH. Untreated age-matched control mice were also included.

Mice received analgesia in form of tramadol (STADApharm GmbH, Bad Vilbel, Germany) in drinking water (2.5 mg/ml) starting 24 h before each immunization and for 3 following days. Age-matched untreated and adjuvant control mice were also included. Adjuvant control mice were immunized with 0.9% NaCl instead of testicular homogenate following the same scheme. During immunization, mice were anesthetized by inhalation of 3-5% isoflurane and all efforts were made to minimize suffering. 50 days after the first immunization, animals were euthanized by inhalation of 5% isoflurane followed by cervical dislocation and the testis, epididymis and blood (using cardiac puncture) were collected. The blood was allowed to clot and then centrifuged at 1000 x g for 15 min at 4 °C. Sera were collected and stored at -80 °C for further analysis. The collected testis and epididymis were weighed, and either snap-frozen in liquid nitrogen or fixed in Bouin's solution for embedding in paraffin.

2.1.3. Induction of acute bacterial epididymitis

This part was completed in collaboration with project 9 of the International Research Training Group (Molecular Pathogenesis of Male Reproductive Disorders).

Uropathogenic *E. coli* (UPEC) strain CFT073 (Welch et al., 2002) was provided by the Institute of Medical Microbiology (Justus-Liebig-University Giessen, Germany).

To elicit an ascending infection, vasa deferentia were bilaterally ligated followed by an intravasal injection of 5 µl sterile 0.9% NaCl containing 1-2 x 10^5 colony forming units proximal to the ligation using a Hamilton syringe (Pleuger et al., 2022). Control 'sham' mice were subjected to the same surgical procedure, but with an intravasal injection of 5 µl sterile 0.9% NaCl without bacteria. Mice were sacrificed at different time points after the infection (1, 3, 5, 7, 10, 14, 21 and 28 days) by isoflurane inhalation followed by cervical dislocation **(Fig. 8).** For each time point, three mice were used per experimental approach.

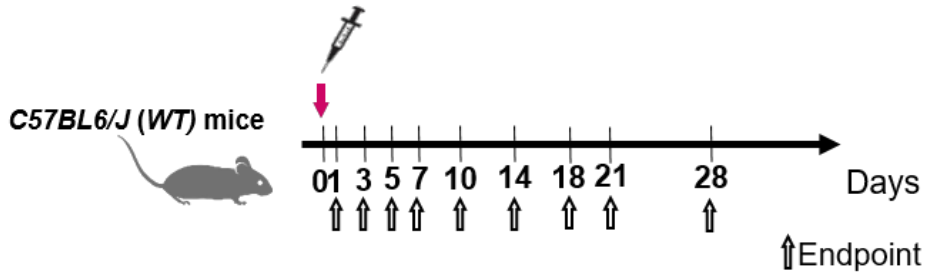

Figure 8. Scheme representing the time points for organ collection following UPEC infection in *C57BL6/J (WT)* strain. Mice were intravasally injected with UPEC or saline alone (sham) after ligation of the vas deferens. Testis, epididymis and blood were collected at 1, 3, 5, 7, 10, 14, 18, 21 and 28 days after UPEC or saline injection.

.

2.1.4. Paraffin embedding of tissues

Collected organs were fixed in Bouin's solution for 2 h. After fixation, organs were washed using 70% ethanol and subsequently dehydrated in an increasing ethanol series (70%, 96% and 100%) for more than 2 h in each ethanol gradient. Afterwards, organs were transferred into benzoic acid methyl ester (>99%) for 2 h and this step was followed by incubation in xylol for 2 h. After that, organs were transferred into a mixture of xylol and paraffin (1:1) for 1 h at 60 °C. Subsequently, organs were transferred to pre-warmed liquid paraffin at 60 °C overnight. Finally, the tissues were embedded in paraffin wax

2.1.5. Azo-carmine and aniline blue (azan) staining

Azan staining was used to evaluate the histology and collagen content (Kikui & Miki, 1995) in the tissues. 8 µm thin paraffin sections were deparaffinized in xylene (10 min, 2 changes) and incubated in 100% ethanol (10 min, 2 changes). After that, the sections were rehydrated through a series of decreasing ethanol concentrations from 96% to 50%, and then rinsed in distilled water. Sections were stained for 5 min in aniline alcohol (0.1% aniline oil in 90% ethanol). After rinsing the sections in distilled water, they were stained with preheated azo-carmine G solution (0.1% azo-carmine G, 1% acetic acid in distilled water) for 10 – 15 min. The sections were washed with distilled water and then differentiated for 1 min in aniline alcohol followed by 1% glacial acetic acid in 96% ethanol for one minute and then washed again with distilled water. The sections were then placed for 2 h in 5% phosphotungstic acid to stain connective tissues. After rinsing, the sections were stained for 2 h in aniline blue-orange mixture (0.5% aniline blue, 2% Orange G, 8% glacial acetic acid). The sections were differentiated in 96% ethanol. Finally, sections were dehydrated in isopropanol and xylene and then mounted on glass slides using Eukitt Quick hardening mounting medium and glass coverslips.

2.1.6. Human testicular biopsies

Bouin's-fixed paraffin-embedded human testicular biopsies and cyrosections were provided by the Giessen Testicular Biopsy Repository (courtesy of Profs. Hans-Christian Schuppe, Daniela Fietz). The specimens were obtained from infertile men with non-obstructive azoospermia and a histological diagnosis of focal inflammatory lesions associated with disturbed spermatogenesis (Schuppe and Bergmann, 2013). Biopsies from patients with obstructive azoospermia, i.e. intact spermatogenesis without any signs of inflammation, served as controls. Written informed consent was obtained from all men undergoing testicular biopsy. The study was approved by the local institutional review board (Ref. No. 100/07).

2.1.7. Immunofluorescence localization of activin A with macrophage and T cell markers in mouse testis

Double staining for activin A and F4/80 (a universal macrophage antigen) or activin A and CD3 (a universal T cell antigen) was performed. 8 µm paraffin sections were deparaffinized in xylene, rehydrated in decreasing series of ethanol and then rinsed in distilled water. Antigen retrieval was performed using pre-warmed (37 ^{o}C) proteinase K antigen retrieval solution (20 µg/ml Proteinase K, 2.5% Glycerol, TE buffer ((50 mM Tris Base, 1 mM EDTA, 0.5% Triton X-100) pH 8.0) for 3 min. After antigen retrieval, slides were washed in 1X TBS (10X TBS: 15 mM Tris-HCl, 137 mM NaCl, pH 7.6) buffer. Sections were then processed using MaxFluorTM Mouse on Mouse Fluorescence Detection Kit (MaxFluor 488) following the manufacturer's instructions. Briefly, sections were blocked with ready-to-use protein blocking solution for 10 min, then with the MaxMOM blocking reagent for 1 h at room temperature (RT). Sections were washed with 1X TBS and incubated with the mouse anti-mouse activin A and rat anti-mouse F4/80 or CD3 antibodies, all diluted in 1X TBS and incubated overnight at 4 °C. Sections were then washed with 1X TBS and incubated with the Fluorescence Signal Enhancer for 30 min, washed again and incubated for 1 h in dark at RT with the MaxFluor 488 labeled linker concentrate and AF546 goat anti-rat IgG diluted in the fluorescent diluent. The slides were then washed with 1X TBS. To reduce auto-fluorescence, sections were incubated with 0.3% Sudan Black B in 70% ethanol for 5 min. Finally, slides were washed and mounted with coverslips in ProLong Gold Antifade mountant with DAPI. One section of each sample served as a negative control and was incubated with the antibody diluent in place of the primary antibody and showed no immunofluorescence signal. Fluorescence images were taken using confocal laser scanning microscope 710 (Carl Zeiss, Göttingen, Germany). The number of triple positive cells in the testicular sections was counted in fields chosen randomly. Each section was quantified by two observers.

2.1.8. Immunofluorescence staining of macrophages and CCR2 in human testicular sections

Double immunofluorescence staining for CCR2 and CD68 (a universal human macrophage antigen) was performed on human testicular sections. 5 µm paraffin sections were deparaffinized in xylene, rehydrated in decreasing series of ethanol and then rinsed in distilled water. Antigen retrieval was performed using pre-warmed (37 ^{o}C) working proteinase K antigen retrieval solution (0.6 units/ml in TE buffer) for 3 min. Afterwards, slides were washed in 1X TBS buffer and blocked using 10% normal goat serum (NGS), 5% bovine serum albumin (BSA) in TBS for 1.5 h. Finally, sections were then incubated with mouse anti- human CD68 and rabbit anti - human CCR2 antibodies in 1X TBS overnight at 4 °C. Next day, slides were washed in 1X TBS and incubated with AF546 goat anti-rabbit IgG and AF488 goat anti-mouse IgG F(ab)2, both diluted in 1X TBS for 1.5 h in dark at RT. Sections were then washed and incubated with 0.3% Sudan Black B in 70% ethanol for 5 min. Subsequently, slides were washed once more and incubated with DAPI diluted 1:1000 in 1X TBS for 20 min. Finally, the slides were washed once again and mounted with ProLong Gold Antifade mountant. One section of each sample served as a negative control and was incubated with the antibody diluent in place of the primary antibody and showed no immunofluorescence signal. Fluorescence images were taken using confocal laser scanning microscope 710. The number of triple positive cells in the testicular sections was counted in fields chosen randomly. Each section was quantified by two observers.

2.1.9. Immunofluorescence staining to detect cells and other elements involved in the formation tertiary lymphoid organs (TLO) in mouse tissues

In order to examine the presence of cells and factors important for TLO composition, tissues were stained for several specific makers **(Table 1).** The sections were deparaffinized and rehydrated as mentioned above, unspecific binding sites were blocked and a panel of specific antibodies was utilized **(Table 1)**. After adding the appropriate secondary antibodies and washing, 0.3% Sudan

black in 70% ethanol was added to the sections for 5 min before finally washing the slides and mounting with ProLong Gold Antifade Mountant containing DAPI. All antibodies were diluted in 1X TBS. One section of each sample served as a negative control and was incubated with the antibody diluent in place of the primary antibody and showed no immunofluorescence signal.

Table 1. List of blocking reagents, antigen retrieval method and combination of antibodies used for staining of TLO elements.

Antibodies	**Blocking**	**Antigen retrieval buffer**	**Notes**
Rat anti- mouse CD3e, rabbit anti-mouse CD19	10% NGS and 5% BSA	Proteinase K solution (0.6 units/ml in TE buffer pH 8.0) for 3 min	
Rabbit anti- mouse CD45	10% NGS and 5% BSA	Proteinase K solution	
Rabbit anti-mouse CD19, rat anti-mouse CD3e rat anti-mouse MECA-79 Alexa Fluor 647-conjugated	10% NGS and 5% BSA	Citrate buffer (10 mM, pH 6.0) for 3 min in microwave at full power	Citrate Buffer (87.4 mM sodium citrate dehydrate, 12.6 mM citric acid, pH 6.0)
Rat anti-mouse MECA-79, goat anti-mouse CXCL13	10%BSA	Citrate buffer	
Rabbit anti-mouse CD19, mouse anti-mouse PCNA	MaxMOM blocking reagent	Proteinase K solution	MaxFluorTM Mouse on Mouse Fluorescence Detection Kit (MaxFluor 488) was used

Rabbit- anti mouse CD45, goat anti-mouse PDPN	10%BSA	Proteinase K solution	
Rabbit anti-mouse CD19, rat anti-mouse F4/80	10% NGS and 5% BSA	Proteinase K solution	

2.1.10. Immunofluorescence staining of plasma cells and IgA in mouse tissues

Frozen epididymal sections (10 µm) from adult mice were fixed in ice-cold methanol for 10 min and washed with 1X TBS 3 times for 5 min. Subsequently, slides were blocked with 10% NGS and 5% BSA in TBS at RT for 1.5 h. Afterwards, slides were incubated with a rat anti-mouse CD138 antibody. Next day, sections were washed with 1X TBS and incubated with AF546 goat anti-rat IgG at RT for 1 h. After washing, an FITC conjugated anti-mouse IgA antibody was then added for 4 h before finally washing the slides and mounting with ProLong Gold Antifade Mountant containing DAPI. One section of each sample served as a negative control and was incubated with the antibody diluent in place of the primary antibody and showed no immunofluorescence signal.

2.1.11. Generation of bone marrow-derived macrophages

In order to generate bone marrow derived macrophages (BMDM), BM progenitor cells were isolated from femurs and tibias of 8-10 weeks old *WT* male mice. Briefly, the tibia and femur were dissected using sterile instruments and muscles were removed. The bones were washed multiple times in ice cold Dulbecco's phosphate buffered saline (DPBS). The femur and tibia were separated from each other at the knee joint and were placed in DPBS containing 50 µg/ml gentamicin. Both ends of the femur and tibia were removed, and then the cells were flushed out with PBS containing gentamicin using a syringe with a needle (femur – 24G, tibia - 30G). Progenitor cells were filtered through a 70 µm strainer.

The cells were centrifuged at 300 x g for 10 min. The supernatant was discarded and red blood cells were lysed by the addition of RBC lysis buffer for 5 min at RT. The pellet was resuspended in complete RPMI-1640 (containing 10% FBS, 1% penicillin/ streptomycin, 1% non-essential amino acids, 1 mM sodium pyruvate, 10 mM HEPES and 50 µM β-mercaptoethanol) and centrifuged again for 10 min at 300 x g. Finally, the cells were diluted in complete RPMI-1640 and counted using a Bürker chamber. 1 × 10^6 cells/ well were seeded in 6 well plates in a volume of 2 ml of complete RPMI-1640 for 5 or 6 days. BMDM were generated by using 50 ng/ml mouse recombinant macrophage-colony stimulating factor (M-CSF). Moreover, the cells were stimulated with 50 ng/ml human recombinant activin A or left untreated. After three days of culture, media were changed and M-CSF and activin A were replaced. The supernatants were collected for protein analysis using a Proteome Profiler assay. Cells were used either for RNA isolation (6-day culture) or for co-culture with T cells (5-day culture).

2.1.12. Bulk RNA sequencing

A previously published transcriptomic dataset from BMDMs treated with activin A, which was generated in previous study and is available in the GEO database under accession code GSE210004 (Peng et al., 2022), was used to analyze the chemokine expression changes in BMDMs after activin A treatment. RNA sequencing was performed by Dr. Stefan Günther at ECCPS Bioinformatics and Deep Sequencing Platform in Max Planck Institute for Heart and Lung Research (Bad Nauheim, Germany). The detailed method for Bulk RNA sequencing can be found in (Peng et al., 2022).

2.1.13. Isolation of T cells

Spleens obtained from 8-10 weeks old *WT* male mice were placed in a Petri dish and splenocytes were flushed out by injecting the tissue with DPBS. The cell suspension containing splenocytes was aspirated using a syringe and filtered through a 100 µm strainer. After centrifugation (300 x g) and red blood cell lysis as mentioned above, cells were washed in PBS and centrifuged again for 10 min.

The obtained cell pellet was resuspended in sterile MACS Quant buffer (0.5% BSA + 2 mM EDTA in DPBS) and the cells were counted. T cells were isolated by negative selection using a mouse Pan T Cell Isolation Kit II according to the manufacturer's instructions. This antibody cocktail labels unwanted cells, while T cells are left unstained and can be used for subsequent cell culture. A maximum of 1 x 10^8 splenocytes were used. The splenocytes were resuspended in MACS Quant buffer and were filtered using 30 µm strainer before proceeding with the magnetic cell isolation. A biotin-labeled antibody cocktail (containing cocktail of biotin-conjugated monoclonal antibodies against CD11b, CD11c, CD19, CD45R (B220), CD49b (DX5), CD105, Anti-MHC class II, and Ter-119), was added and the cell suspension was incubated for 5 min at 4 ^oC. This labels all cells except T cells. Afterwards MACS Quant buffer and magnetic anti-biotin microbeads were added and incubated for 10 min at 4 ^oC. The cells were then subjected to magnetic cell separation using MidiMACS™ Separator and LS columns. The LS column was placed in magnetic field of the separator. The column was rinsed with MACS Quant Buffer before the cell mixture was added to the column and the flow through containing the T cells was collected. The column was washed with MACS Quant Buffer. T cell purity (defined as $CD45^+CD3^+$) was evaluated after T cell isolation and staining with appropriate antibodies (anti-CD45 VioGreen and anti-CD3ε APC) by flow cytometry using MACS Quant 10 flow cytometer. The purity of T cells ranged between 94 - 97%.

2.1.14. T cell stimulation

Isolated T cells were co-cultured with BMDM. 96 well flat - bottomed plates were coated with 50 µl 10 µg/ml anti-mouse CD3 antibody in PBS overnight at 4 ^oC. The following day, the wells were washed with 200 µl DPBS three times. 2 x 10^6 T cells in 200 µl complete RPMI-1640 were added to each well containing 1µg/ml anti-mouse CD28 antibody. T cells were cultured for 2 days before they were collected, counted and used for co-culture with BMDM.

2.1.15. Co-culture of T cells and BMDM

1 x 10^6 activated T cells diluted in 200 µl complete RPMI-1640 were added to 5 day old cultures of BMDM. T cells and BMDM were co-cultured for 2 days. In order to block cytokine secretion, the cells were stimulated with cell stimulation cocktail (CSC), a cocktail of phorbol 12-myristate 13-acetate (PMA) and ionomycin used for polyclonal cell activation, for 6 h and addition of brefeldin A, protein transport inhibitor, during the last 5 h of culture. No CSC or brefeldin A were added for the collection of the conditioned media from co-culture experiments.

2.1.16. Flow cytometry staining (co-culture)

Co-cultured cells were collected for flow cytometry analysis. 1 x 10^6 cells were diluted in 1 ml DPBS and stained with 1 µl Fixable Viability Dye eFluor 450 for 30 min at 4 ^oC in the dark. Cells were centrifuged for 10 min at 300 x g. Cell surface staining using anti-mouse CD45 VioGreen and anti-mouse CD3ε APC conjugated antibodies was performed in a total volume of 50 µl MACS Quant Buffer for 20 min at 4 ^oC in the dark **(Table 2).** After that, MACS Quant buffer was added to the staining reaction. The cells were then centrifuged at 300 x g for 10 min and the pellet was resuspended in MACS Quant buffer and Inside Fix (Inside Stain Kit) for 20 min at RT in the dark to fix the cells. The cells were centrifuged at 300 x g for 5 min, washed with MACS Quant buffer and then centrifuged again. Inside Perm solution was added to permeabilize the cells and the cells were centrifuged once more for 5 min. After that, cells were stained with the cytokine antibodies (anti-TNF PerCP/Cy5.5 and anti-IFNγ PE) resuspended in 100 µl Inside Perm for 10 min at RT in the dark **(Table 2).** Subsequently, Inside Perm was added, cells were centrifuged and then resuspended in 100 µl MACS Quant buffer for measurement by flow cytometry (MACSQuant Analyzer 10). Data was analyzed using FlowJo V10 software. After gating out cell debris, doublets and nonviable cells, the cell population of interest was selected according to isotype or negative controls.

Table 2. Antibody panel used for flow cytometry analysis of murine T cells from co-culture setting.

Laser	Filter	Channel	Antibody and/or fluorescent label
Violet 405 nm	450/50 nm	V1	Fixable Viability Dye eFluor™ 450
	525/50 nm	V2	anti-CD45 VioGreen
Blue 488 nm	585/40 nm	B2	anti-IFNγ PE
	655-730 nm	B3	anti-TNF PerCP/Cy5.5
Red 638nm	655-730 nm	R1	anti-CD3ε APC

2.1.17. Flow cytometry staining of cell suspension from cauda epididymis

Cauda epididymides were digested in DPBS containing 1.5 mg/ml collagenase A for 45 min at 37 °C in a heat block with shaking. After that, the cell suspension was vortexed and using a syringe with 20G needle filtered through 70 µm strainer. Afterwards, DPBS was added and the cells were centrifuged for 10 min at 300 x g. 1 x 10^6 cells were diluted in 1 ml DPBS and stained with 1 µl Fixable Viability Dye eFluor 450 for 30 min at 4 °C in the dark. Cells were centrifuged and incubated with mouse FcR blocking reagent for 10 min at 4 °C. This was followed by staining with appropriate antibodies for 20 min at RT in the dark **(Table 3).** Cells were centrifuged and then resuspended in 200 - 300 µl MACS Quant buffer for flow cytometry measurement (MACSQuant Analyzer 10). Data was analyzed by using FlowJo V10 software.

Table 3. Antibody panel used for flow cytometry analysis of murine B cells in the epididymis

Laser	Filter	Channel	Antibody and/or fluorescent label
Violet 405 nm	450/50 nm	V1	Fixable Viability Dye eFluor™ 450
	525/50 nm	V2	anti-CD45 VioGreen
Blue 488 nm	585/40 nm	B2	anti-CD3ε PE
	655-730 nm	B3	anti-CD45R PE-Vio615
	750 nm LP	B4	anti-CD19 PE-Vio770
Red 638 nm	655-730 nm	R1	anti-CD138 APC

2.1.18. Proteome Profiler Mouse Chemokine Array

Conditioned media from BMDM and T cell co-cultures were collected and the expression levels of selected mouse chemokines were analyzed using a Mouse Chemokine Array Kit according to the manufacture's protocol. Mouse Chemokine Array is a rapid and sensitive proteome profiler assay to simultaneously detect 25 chemokines (CCL2, CCL3/CCL4, CCL5, CCL6, CCL8, CCL9, CCL11, CCL12, CCL21, CCL22, CCL27, CCL28, CXCL1, CXCL2, CXCL9, CXCL10, CXCL11, CXCL12, CXCL13, CXCL16, CX3CL1, Complement Component C5, Chemerin, IL-16 and LIX) in conditioned media, cell and tissue lysates, and serum samples. Briefly, Array Buffer 6 (blocking buffer) was added into each well of the 4-well multi-dish along with the nitrocellulose membrane, captured with 25 different antibodies which are printed in duplicate on the nitrocellulose membrane, and incubated for 1 h at RT in a shaker. The conditioned media from the co-culture experiments were mixed with the detection cocktail containing biotinylated antibodies and incubated at RT for 1 h. After aspiration of the Array Buffer 6 from the multi-dish, the prepared samples were added and incubated on a shaker overnight at 4 ^{o}C. The membranes were then washed three times with wash buffer on a shaker and streptavidin-HRP conjugate diluted in Array Buffer 6 was

added and incubated for 30 min at RT. The membranes were washed and Chemi Reagent Mix was added onto each membrane and incubated for 1 min at RT before detecting the chemiluminescence signals on membranes using Fusion Fx Imaging System. The average signal intensity of the spot duplicates was determined, as follows. For each chemokine spot, the mean of background signal was subtracted from the averaged integrated pixel density. The final signal density was calculated by dividing the averaged integrated pixel density of each chemokine spot by the averaged integrated pixel density of the reference spots.

2.1.19. RNA isolation from mouse testis, epididymis, BMDM and human testicular biopsies

Total RNA was isolated from frozen mouse testis using the RNeasy Fibrous Tissue Mini Kit and from mouse epididymis, BMDM and human testicular biopsies using the RNeasy Mini Kit according to the manufacturer's instructions.
Briefly, about 10 mg of each frozen mouse testis and epididymis or human testis was homogenized in 350 µl RLT lysis buffer containing 1% β-mercaptoethanol using stainless steel beads and a tissue lyser at 30 oscillations/ second for a minimum of 3.5 min. The lysates were collected after centrifugation for 3 min at 20,000 x g.

For BMDM, the cell pellet was collected in 350 µl RLT Lysis buffer containing 1% β-mercaptoethanol. Equal volume of 70% ethanol was added and then transferred to RNeasy mini spin column. Columns were centrifuged at 14,000 x g for 1 min and washed with RW1 wash buffer DNase digestion was performed to get rid of genomic DNA (gDNA) on column using RNAase-Free DNase Set for 30 min at RT. Columns were washed once more with RW1 buffer, twice with RPE buffer to precipitate RNA, followed by centrifugation for 2 min at 14,000 x g. RNA was eluted in 20 – 30 µl RNase free water after centrifugation for 1 min at 14,000 x g. RNA concentration and quality was determined using NanoDrop ND2000.

2.1.20. Reverse cDNA transcription

RNA isolated from human testicular samples and mouse BMDM, testis and epididymis was reverse transcribed, as follows. 1 µg RNA was mixed with 2 µl 10 pM oligo dT and RNase-free water to final volume of 22 µl. The mixture was heated for 10 min at 70 ^{o}C and then cooled on ice. A master mix was prepared as follows: 8 µl M-MLV 5x RT buffer, 2 µl dNTP (10mM), 1 µl recombinant RNasin ribonuclease inhibitor, and 7 µl of RNase free water. 22 µl of prepared RNA – oligo dT reaction was mixed with 18 µl of master mix before adding 1 µl of M-MLV reverse transcriptase (RNase (H-), point mutant) to each sample. Reverse transcription was performed at 42 °C for 75 min. The enzyme was inactivated at 72 °C for 15 min and cDNA samples were stored at -20 °C for further analysis.

Note: RNA from UPEC-infected cauda epididymides was already isolated by Dingding Ai, a PhD student working in our lab on P9 from IRTG, on the UPEC model. I used this RNA for subsequent analysis.

2.1.21. Testing for presence of genomic DNA contamination and for successful cDNA synthesis

The isolated RNA was checked for presence of contaminating gDNA and the generated cDNA was checked for successful reverse transcription by amplification of β-actin. Briefly, a master mix was prepared containing the following: 5 µl 5X Green Go Taq Flexi buffer, 2 µl MgCl2 (25 mM), 0.5 µl dNTPs (10 mM), 0.25 µl Go Taq Flexi polymerase and 0.5 µl of each β-actin forward and reverse primer (10 pM), 15.25 µl distilled water. 1 µl of RNA or cDNA was added to 24 µl of the master mix and PCR was run on a PCR thermocycler for 25 cycles as presented in Table 4.

Table 4. PCR program for β-actin amplification.

Cycles	Step	Time	Temperature (°C)
1x	Denaturation	4 min	94
25x	Denaturation	40 sec	94
	Annealing	40 sec	55
	Elongation	40 sec	72
1x	Inactivation	10 min	72

The amplified products obtained from the PCR reaction were examined by using an agarose gel. Briefly, 1.5% agarose gels were prepared by dissolving agarose in 1X TAE buffer (10X TAE buffer: 40 mM Tris base, 20 mM acetic acid, 1 mM EDTA, pH 8.0) in the microwave. After cooling, a few drops of ethidium bromide (250 µg/ ml) were added to the agarose solution and gels were cast. The amplified PCR products were mixed with 1X Blue/orange DNA loading dye and were loaded next to a 100 bp DNA ladder. Gels were run in 1X TAE buffer at 110 V. The gel was examined using a UV transilluminator and photographed in a Gel Jet Imager 2000 documentation system. Successfully reverse transcribed cDNA samples showed a band with a β-actin amplification product of 156 bp. RNA samples showed no PCR product as expected **(Fig. 9)**.

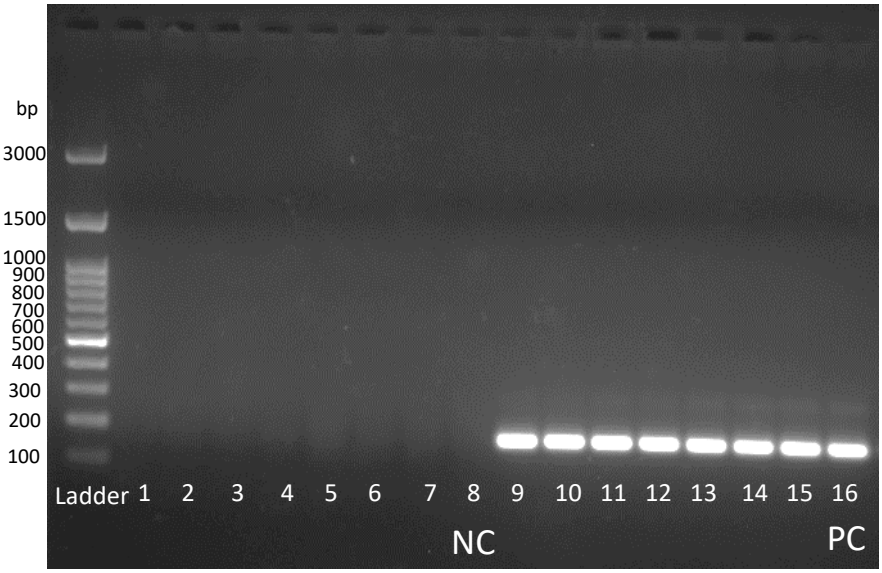

Figure 9. Representative agarose gel demonstrating successful digestion of genomic DNA and cDNA synthesis. Total RNA was isolated from untreated, adjuvant-control and EAEO mouse testis. The PCR products were amplified using β-actin primers. The representative agarose gel of PCR amplicons for β-actin in RNA samples showed no product amplification for β -actin in untreated (lane 1, 2), adjuvant-control (lane 3, 4) and EAEO testis (lane 5, 6, 7), which indicated no genomic DNA contamination. The cDNA from the respective RNA samples showed a β-actin band in untreated (lane 9, 10), adjuvant (lane 11, 12) and EAEO testis (lane 13, 14, 15), which indicated that cDNA was successfully reverse transcribed. Splenocytes (lane 16) was used as a positive control (PC) and a negative control (NC) containing RNase-free water (lane 8) instead of RNA or cDNA template. 100 bp DNA ladder was used. The amplicon size of β-actin is 156 bp.

2.1.22. Quantitative RT - PCR (qRT-PCR)

qRT-PCR was performed using the CFX96 Touch real-time PCR detection system. The master mix was prepared, as follows: 10 µl 2 X iTaq Universal SYBR Green supermix, 0.5 µl of 10 pM forward and reverse primers and 8 µl RNase free water. 1 µl cDNA was used for the q-PCR. Relative gene expression was calculated using the $2^{-\Delta\Delta Ct}$ method (Livak & Schmittgen, 2001). The relative

expression (RE) was normalized to *GAPDH* for human testicular samples, to *Hprt* for mouse BMDM and to *Rplpo* for mouse epididymis.

Note: Results for relative expression of *Tnf* in UPEC-infected cauda epidiymides (all days excluding 21 and 28) were determined by Dingding Ai.

Table 5. qRT-PCR conditions

Number of cycles	Step	Temperature	Time
1	Denaturation	95	30
45	Denaturation	95	15
	Annealing	55, 60 or 65	30
	Elongation	72	30
Melt curve	Dissociation	50 - 95	5

A melting curve analysis allowed for assessing the specificity of the qRT-PCR assay. A single distinct peak in the plot indicates that the amplified double-stranded DNA product is specific. A representative melting curve is shown in **Fig. 10**, which indicates a single specific peak for CCR5 product during the amplification by qRT-PCR.

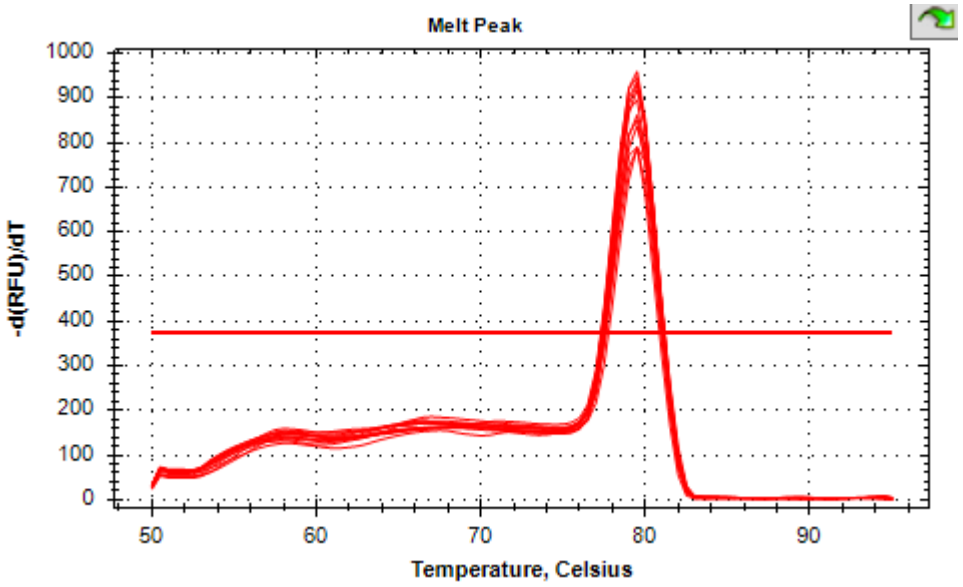

Figure 10. Representative melting curve for CCR5 transcript using as a template cDNA from mouse bone marrow cells. Single peak represents single amplicon at 78°C.

Primer efficiency was validated by performing dilution series of cDNA samples and by generating a linear standard curve **(Fig. 11).** Primer efficiencies were 90% - 110% and R^2>0.98.

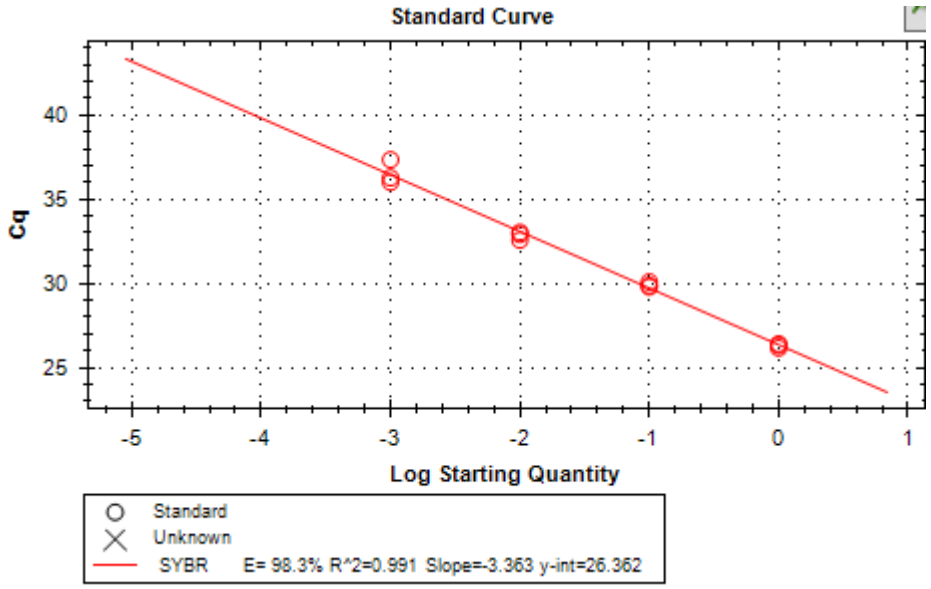

Figure 11. Representative qRT-PCR standard curve of CCR5 primer by using cDNA template from mouse bone marrow cells. Dilutions (0, 1/10, 1/100, 1/1000) of cDNA were used as the template for qRT-PCR reaction (triplicates). A standard linear curve was generated by plotting Cq values against the log of dilution series. Primer efficiency for CCR5 was 98.3 % and R^2 = 0.991.

2.1.23. Screening of chemokines and receptors mRNA expression by PCR array in mouse testis

RNA isolated from the mouse testis was used to analyze the mRNA expression of chemokines and their receptors using a Mouse Chemokines & Receptors RT² Profiler PCR Array. This array profiles the expression of 84 selected genes that encode chemokines and their receptors. RT² Profiler PCR Arrays 96-well plates contain customizable primer assays for 84 genes of interest **(Table 6)**. In addition to selected primers for the genes of interest, the array includes 5 different housekeeping genes (*Actb, B2m, Gapdh, Gusb* and *Hsp90ab1*) **(Table 6)**.

Table 6. List of gene included in Mouse Chemokines & Receptors RT² Profiler PCR Array

UniGene	GenBank	Symbol	Description
Mm.247623	NM_007577	*C5ar1*	Complement component 5a receptor 1
Mm.258105	NM_021609	*Ccbp2*	Chemokine binding protein 2
Mm.1283	NM_011329	*Ccl1*	Chemokine (C-C motif) ligand 1
Mm.4686	NM_011330	*Ccl11*	Chemokine (C-C motif) ligand 11
Mm.867	NM_011331	*Ccl12*	Chemokine (C-C motif) ligand 12
Mm.41988	NM_011332	*Ccl17*	Chemokine (C-C motif) ligand 17
Mm.424740	NM_011888	*Ccl19*	Chemokine (C-C motif) ligand 19
Mm.290320	NM_011333	*Ccl2*	Chemokine (C-C motif) ligand 2
Mm.116739	NM_016960	*Ccl20*	Chemokine (C-C motif) ligand 20
Mm.12895	NM_009137	*Ccl22*	Chemokine (C-C motif) ligand 22
Mm.31505	NM_019577	*Ccl24*	Chemokine (C-C motif) ligand 24
Mm.7275	NM_009138	*Ccl25*	Chemokine (C-C motif) ligand 25
Mm.376459	NM_001013412	*Ccl26*	Chemokine (C-C motif) ligand 26
Mm.143745	NM_020279	*Ccl28*	Chemokine (C-C motif) ligand 28
Mm.1282	NM_011337	*Ccl3*	Chemokine (C-C motif) ligand 3
Mm.244263	NM_013652	*Ccl4*	Chemokine (C-C motif) ligand 4

Mm.284248	NM_013653	*Ccl5*	Chemokine (C-C motif) ligand 5
Mm.137	NM_009139	*Ccl6*	Chemokine (C-C motif) ligand 6
Mm.341574	NM_013654	*Ccl7*	Chemokine (C-C motif) ligand 7
Mm.42029	NM_021443	*Ccl8*	Chemokine (C-C motif) ligand 8
Mm.416125	NM_011338	*Ccl9*	Chemokine (C-C motif) ligand 9
Mm.274927	NM_009912	*Ccr1*	Chemokine (C-C motif) receptor 1
Mm.8021	NM_007721	*Ccr10*	Chemokine (C-C motif) receptor 10
Mm.423532	NM_007718	*Ccr1l1*	Chemokine (C-C motif) receptor 1-like 1
Mm.6272	NM_009915	*Ccr2*	Chemokine (C-C motif) receptor 2
Mm.57050	NM_009914	*Ccr3*	Chemokine (C-C motif) receptor 3
Mm.1337	NM_009916	*Ccr4*	Chemokine (C-C motif) receptor 4
Mm.14302	NM_009917	*Ccr5*	Chemokine (C-C motif) receptor 5
Mm.8007	NM_009835	*Ccr6*	Chemokine (C-C motif) receptor 6
Mm.2932	NM_007719	*Ccr7*	Chemokine (C-C motif) receptor 7
Mm.442098	NM_007720	*Ccr8*	Chemokine (C-C motif) receptor 8
Mm.440604	NM_009913	*Ccr9*	Chemokine (C-C motif) receptor 9
Mm.269254	NM_145700	*Ccrl1*	Chemokine (C-C motif) receptor-like 1
Mm.7336	NM_017466	*Ccrl2*	Chemokine (C-C motif) receptor-like 2
Mm.5196	NM_008153	*Cmklr1*	Chemokine-like receptor 1
Mm.272746	NM_027022	*Cmtm2a*	CKLF-like MARVEL transmembrane domain containing 2A
Mm.390108	NM_024217	*Cmtm3*	CKLF-like MARVEL transmembrane domain containing 3
Mm.383258	NM_153582	*Cmtm4*	CKLF-like MARVEL transmembrane domain containing 4
Mm.41614	NM_026066	*Cmtm5*	CKLF-like MARVEL transmembrane domain containing 5
Mm.28858	NM_026036	*Cmtm6*	CKLF-like MARVEL transmembrane domain containing 6
Mm.103711	NM_009142	*Cx3cl1*	Chemokine (C-X3-C motif) ligand 1
Mm.44065	NM_009987	*Cx3cr1*	Chemokine (C-X3-C) receptor 1
Mm.21013	NM_008176	*Cxcl1*	Chemokine (C-X-C motif) ligand 1

Mm.877	NM_021274	*Cxcl10*	Chemokine (C-X-C motif) ligand 10
Mm.131723	NM_019494	*Cxcl11*	Chemokine (C-X-C motif) ligand 11
Mm.303231	NM_021704	*Cxcl12*	Chemokine (C-X-C motif) ligand 12
Mm.10116	NM_018866	*Cxcl13*	Chemokine (C-X-C motif) ligand 13
Mm.30211	NM_019568	*Cxcl14*	Chemokine (C-X-C motif) ligand 14
Mm.64326	NM_011339	*Cxcl15*	Chemokine (C-X-C motif) ligand 15
Mm.425692	NM_023158	*Cxcl16*	Chemokine (C-X-C motif) ligand 16
Mm.4979	NM_009140	*Cxcl2*	Chemokine (C-X-C motif) ligand 2
Mm.244289	NM_203320	*Cxcl3*	Chemokine (C-X-C motif) ligand 3
Mm.4660	NM_009141	*Cxcl5*	Chemokine (C-X-C motif) ligand 5
Mm.766	NM_008599	*Cxcl9*	Chemokine (C-X-C motif) ligand 9
Mm.337035	NM_178241	*Cxcr1*	Chemokine (C-X-C motif) receptor 1
Mm.234466	NM_009909	*Cxcr2*	Chemokine (C-X-C motif) receptor 2
Mm.12876	NM_009910	*Cxcr3*	Chemokine (C-X-C motif) receptor 3
Mm.1401	NM_009911	*Cxcr4*	Chemokine (C-X-C motif) receptor 4
Mm.6246	NM_007551	*Cxcr5*	Chemokine (C-X-C motif) receptor 5
Mm.124289	NM_030712	*Cxcr6*	Chemokine (C-X-C motif) receptor 6
Mm.6522	NM_007722	*Cxcr7*	Chemokine (C-X-C motif) receptor 7
Mm.6393	NM_010045	*Darc*	Duffy blood group, chemokine receptor
Mm.56951	NM_013521	*Fpr1*	Formyl peptide receptor 1
Mm.391108	NM_001025381	*Gpr17*	G protein-coupled receptor 17
Mm.3879	NM_010431	*Hif1a*	Hypoxia inducible factor 1, alpha subunit
Mm.240327	NM_008337	*Ifng*	Interferon gamma
Mm.10137	NM_010551	*Il16*	Interleukin 16
Mm.222830	NM_008361	*Il1b*	Interleukin 1 beta
Mm.276360	NM_021283	*Il4*	Interleukin 4
Mm.1019	NM_031168	*Il6*	Interleukin 6
Mm.262106	NM_008401	*Itgam*	Integrin alpha M
Mm.1137	NM_008404	*Itgb2*	Integrin beta 2

Mm.196581	NM_011949	*Mapk1*	Mitogen-activated protein kinase 1
Mm.311337	NM_011951	*Mapk14*	Mitogen-activated protein kinase 14
Mm.332490	NM_019932	*Pf4*	Platelet factor 4
Mm.293614	NM_023785	*Ppbp*	Pro-platelet basic protein
Mm.289739	NM_178804	*Slit2*	Slit homolog 2 (Drosophila)
Mm.248380	NM_011577	*Tgfb1*	Transforming growth factor, beta 1
Mm.87596	NM_011905	*Tlr2*	Toll-like receptor 2
Mm.38049	NM_021297	*Tlr4*	Toll-like receptor 4
Mm.1293	NM_013693	*Tnf*	Tumor necrosis factor
Mm.287977	NM_138302	*Tymp*	Thymidine phosphorylase
Mm.190	NM_008510	*Xcl1*	Chemokine (C motif) ligand 1
Mm.390241	NM_011798	*Xcr1*	Chemokine (C motif) receptor 1
Mm.328431	NM_007393	*Actb*	Actin, beta
Mm.163	NM_009735	*B2m*	Beta-2 microglobulin
Mm.343110	NM_008084	*Gapdh*	Glyceraldehyde-3-phosphate dehydrogenase
Mm.3317	NM_010368	*Gusb*	Glucuronidase, beta
Mm.2180	NM_008302	*Hsp90ab1*	Heat shock protein 90 alpha (cytosolic), class B member 1

Moreover, one well was used for genomic DNA control to detect non-transcribed genomic DNA contamination with a high level of sensitivity, 3 wells contained reverse-transcription controls to test the efficiency of the reverse-transcription reaction and additional 3 wells incorporated positive PCR controls, which consists of a predispensed artificial DNA sequence. This control is needed to estimate the efficiency of the polymerase chain reaction itself.

Testicular RNA was subjected to genomic DNA elimination step according to the protocol for RT^2 First Strand Kit, which contains a proprietary buffer to eliminate any residual genomic DNA contamination in RNA samples. Briefly, 1 µg RNA was treated to digest genomic DNA. 2 µl buffer GE was used and RNase-free water was added to a final volume of 10 µl. The reaction mixture was incubated for 5 min at 42 ^{o}C and placed on ice for at least one minute. Reverse transcription mix

was prepared as follows: 4 µl 5X buffer BC3, 1 µl control P2, 2 µl RE3 reverse transcriptase mix, 3 µl RNase-free water. 10 µl of the reverse transcriptase mix was added to 10 µl genomic DNA elimination mix. This was followed by incubation at 42 ^{o}C for 15 min. The reaction was stopped by incubating at 95 ^{o}C for 5 min, followed by adding 91µl RNase-free water. Before proceeding with the PCR, the generated cDNA was checked for successful reverse transcription by β-actin amplification as mentioned above. The PCR components mix was prepared as follows: 1350 µl 2X RT^{2} SYBR Green Mastermix, 102 µl cDNA, 1248 µl RNase-free water. 25 µl of PCR components mix was added to each well of the 96-well array plate.

Based on the preliminary results obtained from the Mouse Chemokines & Receptors RT² Profiler PCR Array, a customized PCR array was also used to assess the relative expression of 27 selected chemokines and receptors (*Ccr1, Ccr2, Ccr3, Ccr5, Ccr6, Ccr10, Cx3cr1, Cx3cl1, Ccl1, Ccl3, Ccl4, Ccl5, Ccl6, Ccl7, Ccl8, Ccl9, Ccl11, Ccl12, Ccl22, Cxcr3, Cxcr5, Cxcl1, Cxcl4, Cxcl9 Cxcl13, Cxcl14 and Cxcl16)* that were changed more than three-fold in EAEO testis compared to adjuvant controls. Relative gene expression was calculated using the $2^{-\Delta\Delta Ct}$ method as mentioned above. The relative expression was normalized to β-actin.

2.1.24. Statistical analysis

Statistical analysis was performed using GraphPad Prism 6 software (GraphPad Software, San Diego, USA). All data are presented as mean ± standard error of mean (SEM) and were tested for normal distribution and equal variance. Statistical differences between two groups was determined using student's *t*-test (Gaussian distribution) or Mann Whitney test (non-parametric distribution). Differences between multiple groups were determined using one-way or two-way Analysis of Variance (ANOVA) followed by Tukey's comparisons test (Gaussian distribution) or Kruskal-Wallis test followed by Dunn's multiple comparisons test (non-parametric distribution). *p*-values <0.05 were considered as significantly different.

3. Results

3.1. The chemokine network was altered in EAEO testis

Induction of EAEO in *WT* mice led to destruction of the seminiferous tubules and severe alteration of the testicular morphology, as previously reported (Kauerhof et al., 2019; Nicolas et al., 2017a; Peng et al., 2022). The atrophic seminiferous tubules displayed sloughing of germ cells and thickened lamina propria accompanied by extensive interstitial fibrosis and immune cell infiltration **(Fig. 12).**

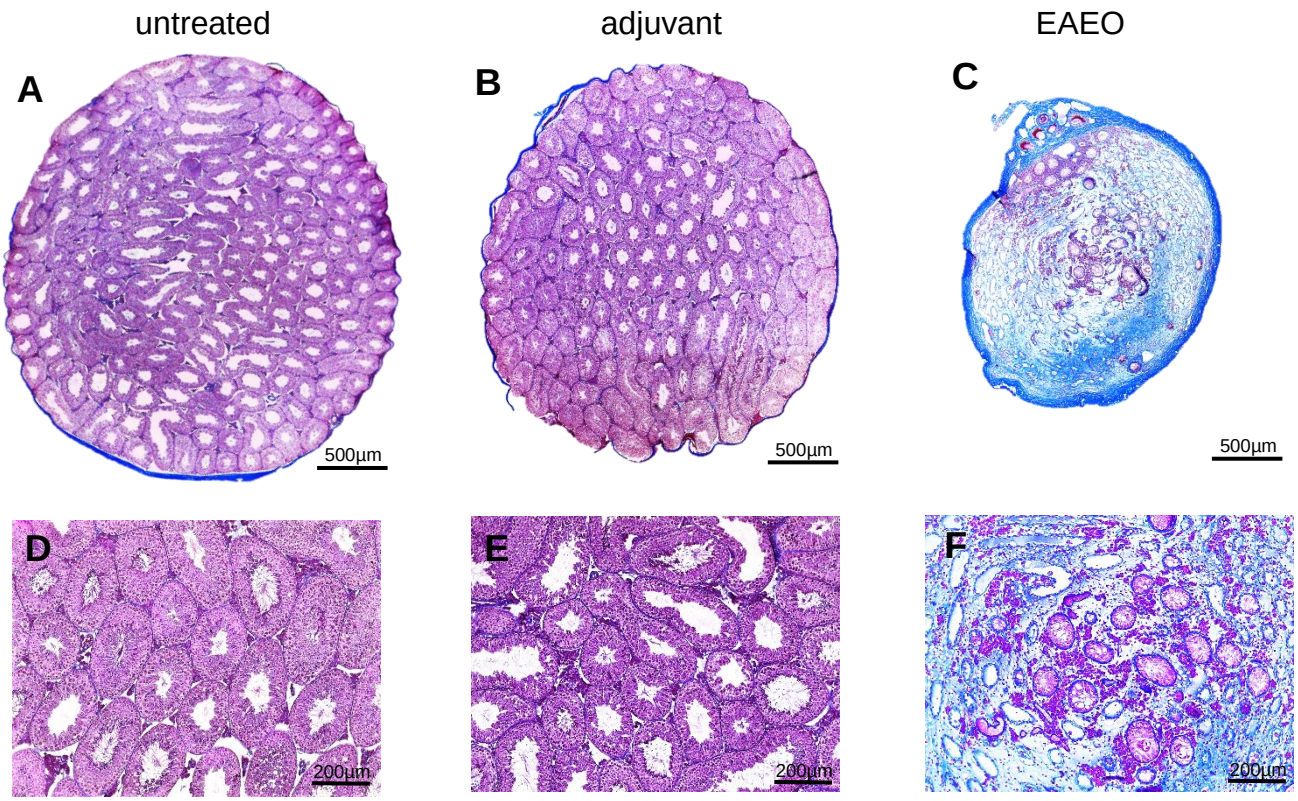

Figure 12. EAEO damages the testicular architecture. Representative photomicrographs of azan stained paraffin sections from untreated **(A, D)**, adjuvant control **(B, E)** and EAEO **(C, F)** testis in *WT* mice 50 days from the immunization.

In order to determine whether EAEO affects the expression of chemokines and their receptors in the testes, an initial mRNA screen using a RT^2 Profiler PCR Array was performed. A preliminary analysis of 84 chemokine and chemokine receptor related genes (**Fig. 13)** was performed on one EAEO and one adjuvant

control testis. This preliminary analysis was performed in order to select from the chemokines which would be of interest to investigate in EAEO testis.

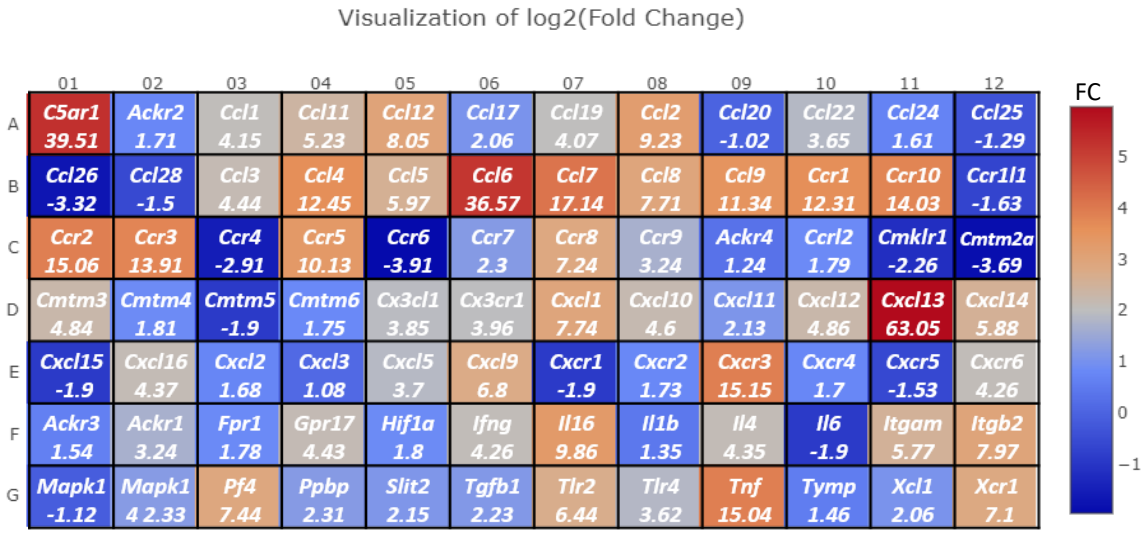

Figure 13. Expression of several chemokines and their receptors was altered in EAEO testis. Heatmap generated from the analysis of mRNA expression of one EAEO and one adjuvant control testis 50 days from the immunization using the Mouse Chemokines & Receptors RT² Profiler PCR Array profiling the expression of 84 genes encoding selected mouse chemokines and their receptors. The numbers represent the log2 fold change (FC) from control.

A total of 27 genes that were more than 3-fold changed and identified as important for macrophage and T cell trafficking were selected for further analysis using a customized RT² Profiler PCR Array (**Table 7**). *Cxcr5* (-1.53 fold regulation) was selected because it is the receptor for Cxcl13, which was the gene with the largest increase among the 84 genes analyzed. *Ccl2, Cxcl12* and *Cxcr4*, which changed by more than 3-fold and are essential for macrophage trafficking, were not selected as they had been assessed previously in published studies from our lab (Peng et al., 2022).

Table 7. List of genes selected for further analysis using a customized RT² Profiler PCR Array

Gene Symbol	log2FC
Cxcl13	63.05

Ccl6	36.57
Ccl7	17.14
Cxcr3	15.15
Ccr2	15.06
Ccr10	14.03
Ccr3	13.91
Ccl4	12.45
Ccr1	12.31
Ccl9	11.34
Ccr5	10.13
Ccl12	8.05
Cxcl1	7.74
Ccl8	7.71
Pf4	7.44
Cxcl9	6.8
Ccl5	5.97
Cxcl14	5.88
Ccl11	5.23
Ccl3	4.44
Cxcl16	4.37
Ccl1	4.15
Cx3cr1	3.96
Cx3cl1	3.85
Ccl22	3.65
Cxcr5	-1.53
Ccr6	-3.91

The mRNA expression of CC chemokine receptors (*Ccr1, Ccr2, Ccr3* and *Ccr5*), known to be expressed on macrophages and T cells **(Fig. 14),** was significantly increased in EAEO testis as compared to control samples. Moreover, mRNA expression of the respective ligands, *Ccl3, Ccl4, Ccl5, Ccl6, Ccl7, Ccl8, Ccl9, Ccl11, Ccl12 and Ccl22* (Hughes and Nibbs, 2018), was also significantly elevated in EAEO testis in comparison to controls**.**

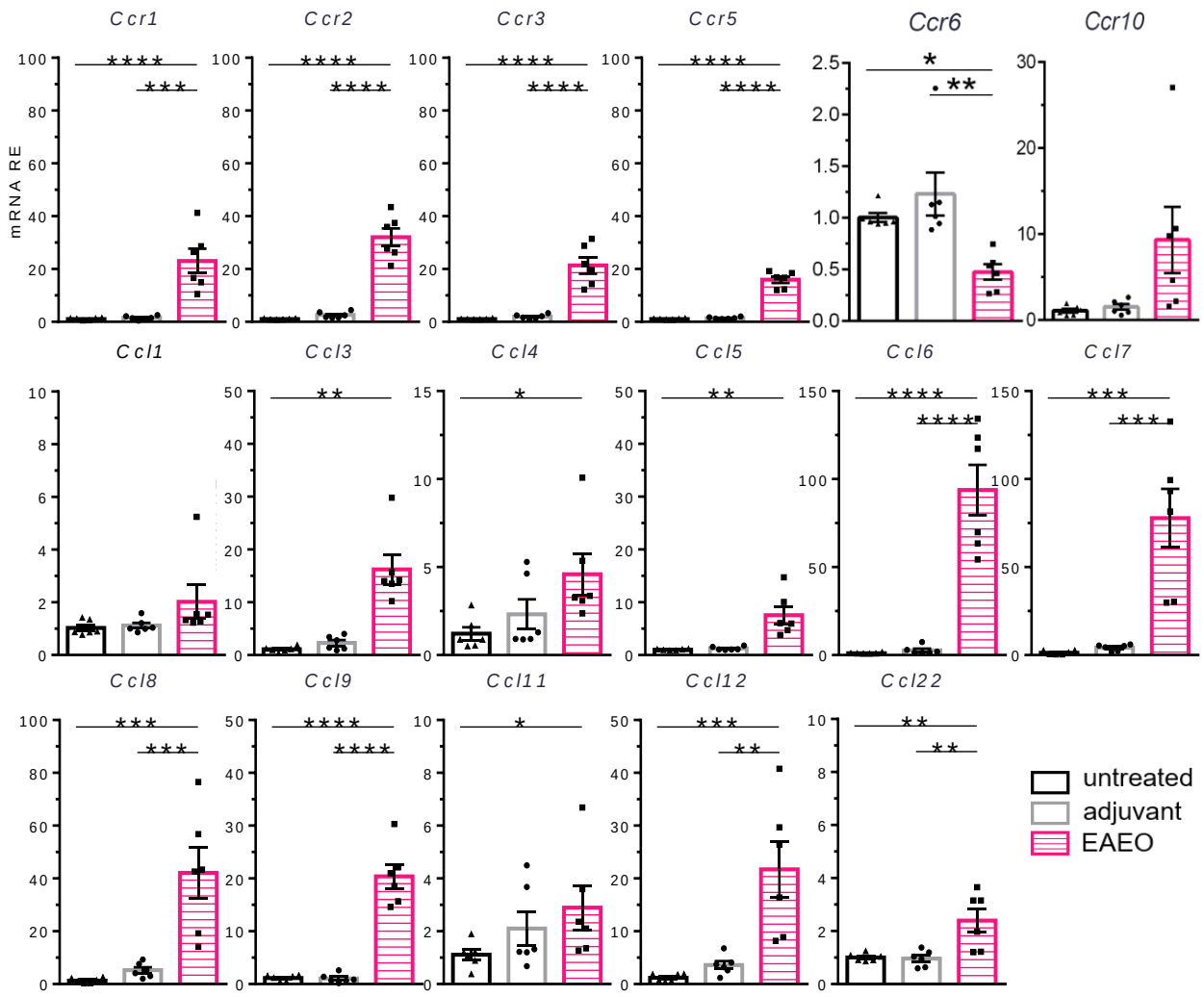

Figure 14 Expression of CC chemokines responsible for macrophages and T cell chemotaxis increased in EAEO *WT* testis. Relative expression (RE) of *Ccr1, Ccr2, Ccr3, Ccr5, Ccr6, Ccr10, Ccl1, Ccl3, Ccl4, Ccl5, Ccl6, Ccl7, Ccl8, Ccl9, Ccl11, Ccl12* and *Ccl22* mRNA was analyzed by a customized Mouse Chemokines & Receptors RT² Profiler™ PCR Array in untreated, adjuvant control and EAEO testis from *WT* mice 50 days from the immunization and normalized to β-actin (n = 6; mean ± SEM). Statistical analyses used Kruskal–Wallis test followed by Dunn's multiple comparison test or one-way ANOVA followed by Tukey's multiple comparison test (**P*<0.05, ***P*<0.01, ****P*<0.001, *****P*<0.0001).

Furthermore, mRNA expression of *Cx3cr1* and its ligand *Cx3cl1,* which are essential for migration and adhesion of macrophages (Bazan et al., 1997) was significantly increased in EAEO testis as compared to control testis **(Fig. 15)**. The mRNA expression of *Cxcr3*, a member of the CXC chemokine receptors, which plays a key role in T cell trafficking (Hughes and Nibbs, 2018), as well its ligands *Cxcl4* and *Cxcl9* was significantly increased in EAEO testis as compared to

control groups. The mRNA expression of other members of the CXC chemokine ligand family involved in monocyte and T cell migration and in angiogenesis, including *Cxcl1, Cxcl14 and Cxcl16* was significantly increased as well **(Fig. 15)**.

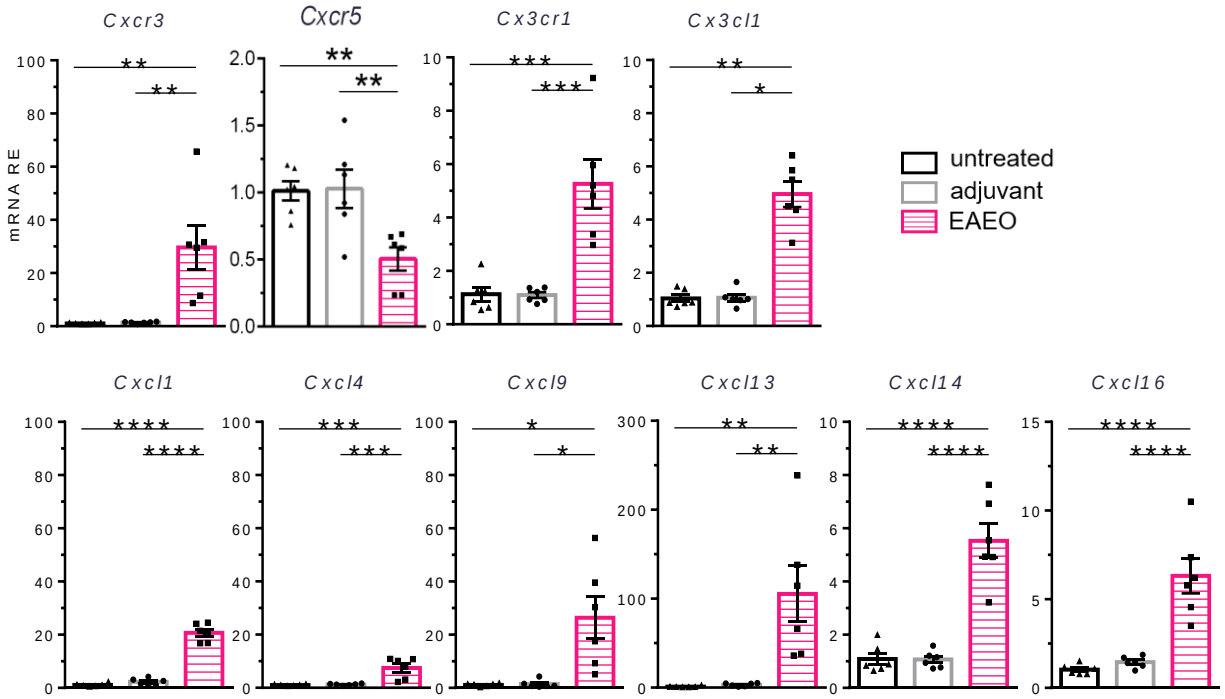

Figure 15. Expression of CXC and CX3C chemokines was altered in EAEO *WT* testis. Relative expression (RE) of *Cxcr3, Cxcr5, Cx3cr1, Cx3cl1, Cxcl1, Cxcl4, Cxcl9, Cxcl13, Cxcl14* and *Cxcl16* mRNA was analyzed by customized Mouse Chemokines & Receptors RT² Profiler™ PCR Array in untreated, adjuvant control and EAEO testis from *WT* mice 50 days from the immunization and normalized to *β-actin* (n = 6; mean ± SEM). Statistical analyses used Kruskal–Wallis test followed by Dunn's multiple comparison test or one-way ANOVA followed by Tukey's multiple comparison test (**P*<0.05, ***P*<0.01, ****P*<0.001, *****P*<0.0001).

The mRNA expression of receptors involved in B -cell (*Ccr6, Cxcr5*) and T -cell (*Ccr4, Ccr6*) trafficking was decreased in EAEO testis as compared to controls **(Fig. 13, 14, 15)**. The mRNA expression of ligand for *Cxcr5* - *Cxcl13*, was more than 100-fold increased in EAEO testis compared to control testis **(Fig. 15)**. Relative expression of *Ccl1*, a ligand for *Ccr8* expressed on T cells, as well as *Ccr10*, important for homing of plasma cells, was not significantly changed **(Fig. 15)**. These results indicate enhanced expression of the chemokine–chemokine

receptor axis involved in monocyte/macrophage and T cell migration and thus enhanced trafficking of these immune cells to the inflammatory site.

3.2. Chemokines responsible for macrophage trafficking, specifically CCR2, were highly elevated in human testicular biopsies with impaired spermatogenesis and focal leukocytic infiltrates

In order to define the clinical relevance of the findings from the mouse model outlined in the previous section, the expression of chemokines and their receptors involved in the trafficking of monocytes/macrophages and T cells was evaluated in human biopsies with diagnosed signs of testicular inflammation. The mRNA expression of the monocyte/macrophage chemoattractant *CCL2* and its receptor *CCR2* was significantly increased by 10- and 5–fold, respectively, in human biopsies with impaired spermatogenesis and focal leukocytic infiltrates compared to biopsies with intact spermatogenesis lacking leukocyte infiltration (controls) **(Fig 16)**. Notably, the comparison of mRNA expression levels of all chemokine receptors analyzed in mouse testis revealed that *Ccr2* shows the highest expression (above 30 - fold increase) in EAEO *WT* testis **(Fig 14)**. Consistent with the mouse data, *CCR1*, *CCR5* and *CXCL13* mRNA expression were significantly increased in the testis of patients with disturbed spermatogenesis **(Fig. 16)**.

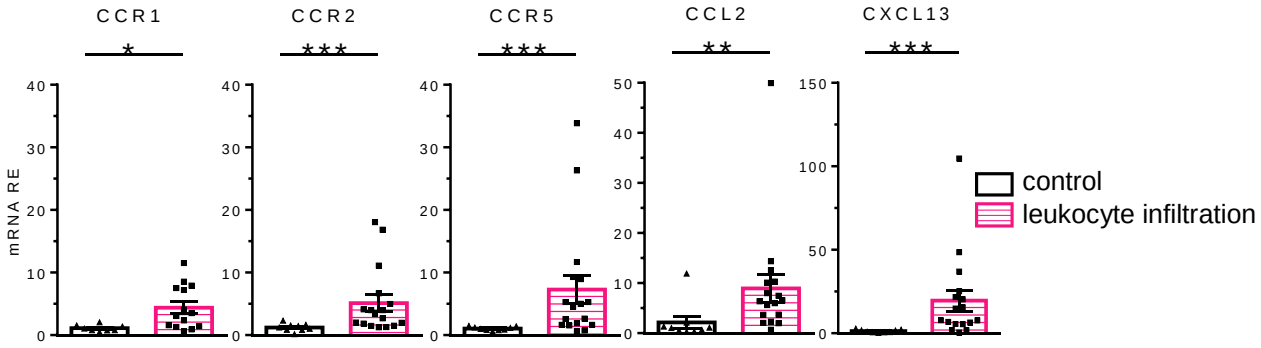

Figure 16. Expression of chemokines involved in macrophage trafficking was increased in human testicular biopsies with focal leukocyte infiltrates. Relative expression (RE) of CCR1, CCR2, CCR5, CCL2 and CXCL13 mRNA was determined by qRT-PCR in human testicular biopsies with impaired spermatogenesis and focal leukocytic infiltrates (n = 17, except for CCR1

n = 14) and control testicular samples with normal spermatogenesis and no signs of inflammation (n = 9, except for CCR1 n = 8), normalized to GAPDH; (mean ± SEM). Statistical test used Mann-Whitney test (*P<0.05, **P<0.01, ***P<0.001).

Considering that CCR2 was significantly increased in EAEO testis as well as in human testicular biopsies accompanied by leukocytic infiltration, it was of interest to examine the identity of cells expressing CCR2 in inflammatory conditions. Histology of biopsies with impaired spermatogenesis showed that immune cell infiltrates were present in several locations (in interstitial space, inside tubule) and patterns (scattered, diffuse) in the testis (**Fig. 17**).

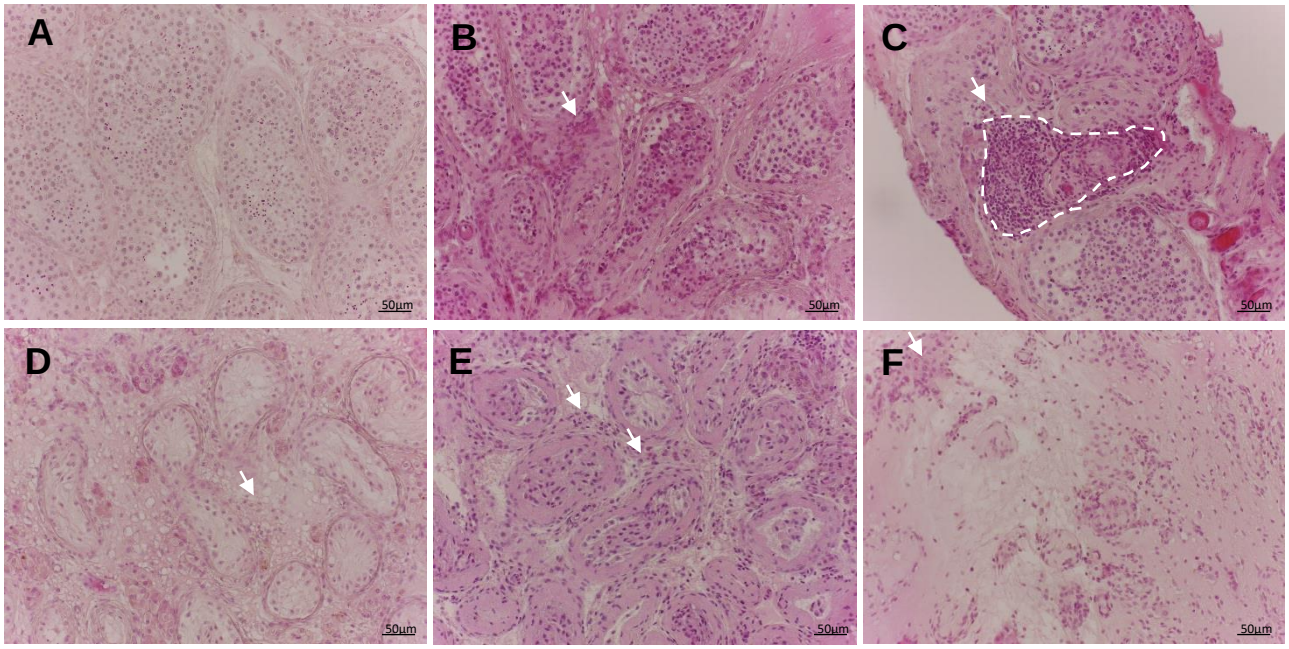

Figure 17. Hematoxylin & Eosin staining of representative human testicular biopsies. Intact spermatogenesis and no signs of inflammation **(A)** and biopsies with impaired spermatogenesis and leukocyte infiltrates **(B, C, D, E, F).** Arrows and broken lines highlight the presence of immune cell infiltration.

Immunofluorescence staining of testicular macrophages ($CD68^+$) in combination with CCR2 in human biopsies revealed that, in sections showing intact spermatogenesis, the majority of $CD68^+$ cells were negative for CCR2 **(Fig. 18A)**. However, in human testicular biopsies with signs of inflammation, CCR2 expression was visibly increased and $CD68^+$ macrophages expressing CCR2 were located within interstitial spaces and peritubular niches **(Fig. 18B, C, D, E,**

G) and, in some patients, within the seminiferous tubules **(Fig. 18B)**. In sections displaying severe fibrosis, the macrophages did not show CCR2 expression **(Fig. 18F).**

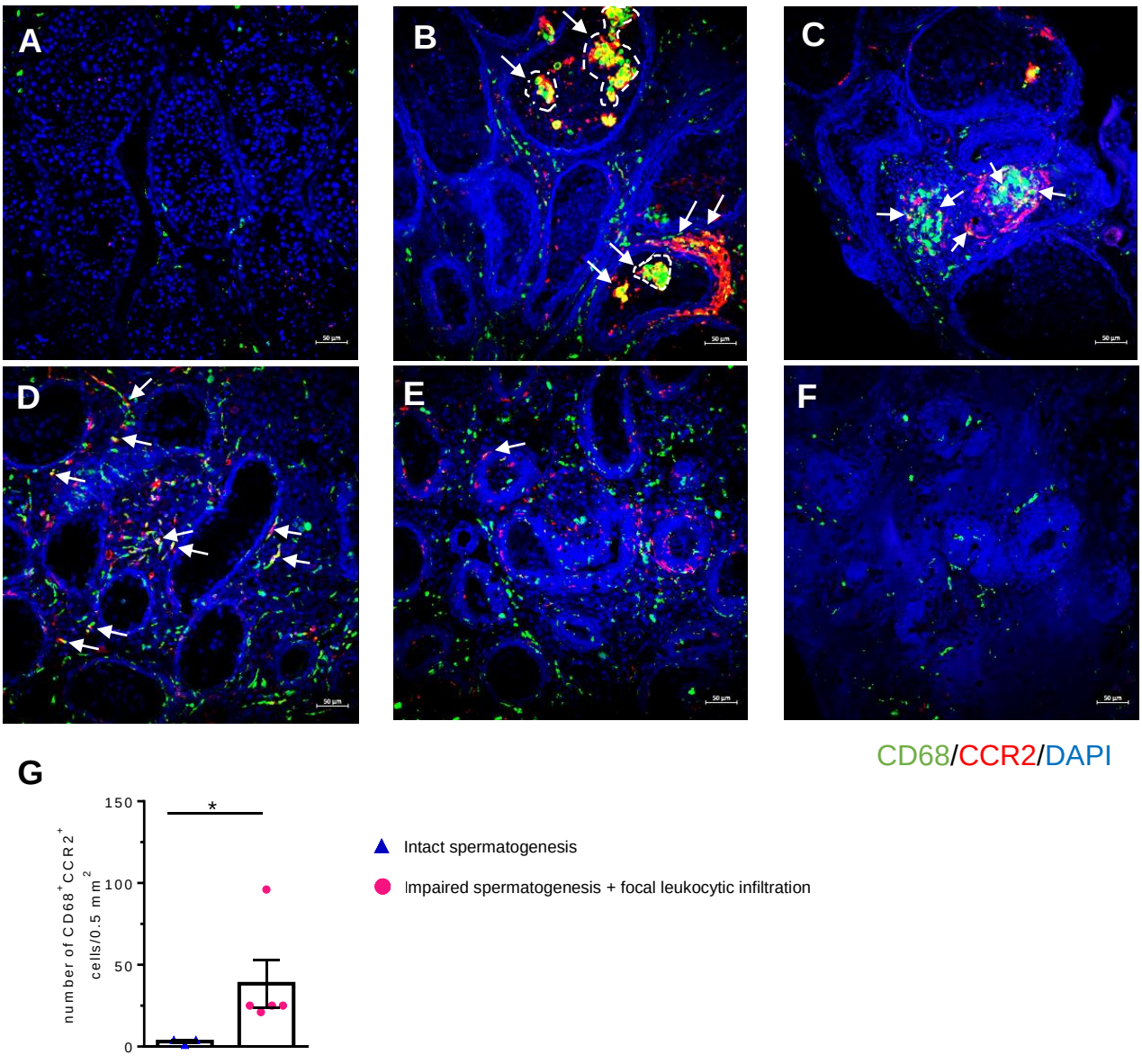

Figure 18. Macrophages expressing CCR2 were increased in human testicular biopsies with focal leukocytic infiltrates. Immunofluorescence staining of macrophages (CD68, green) and CCR2 (red) and DAPI fluorescence (blue) of representative human testicular biopsies showing intact spermatogenesis and no signs of inflammation **(A)** and biopsies with impaired spermatogenesis and leukocytic infiltrates **(B, C, D, E, F).** Arrows point to macrophages positive for CCR2. Scale bars represent 50 µm. Negative control sections were incubated only with the antibody diluent in place of the primary antibody and showed no immunofluorescence signal. Quantification of CD68+CCR2+ macrophages determined by counting of triple positive immunofluorescence stained cells (CD68, green; CCR2, red; DAPI, blue) in paraffin sections from

human testicular biopsies (**G**; n = 3 - 5 ± SEM). Statistical analysis was performed using the Mann-Whitney test (*P<0.05).

3.3. In the absence of CCR2, EAEO-induced alterations in the expression of chemokines and their receptors involved in macrophage and T cell migration were reduced

Since the results in EAEO testis and human testicular biopsies containing focal inflammatory infiltrates showed increased expression of chemokines, especially CCR2, it became of interest to elucidate the importance of CCR2 signaling in the recruitment of immune cells to the testis and expression of chemokines and their receptors during testicular inflammation. In order to do so, the expression of previously analyzed molecules was examined in EAEO mice deficient for *Ccr2*, which exhibit defective monocyte macrophage infiltration. Absence of CCR2 protected mice from the destructive characteristics of EAEO and demonstrated decreased testicular inflammatory responses **(Fig. 19)** (Peng et al., 2022).

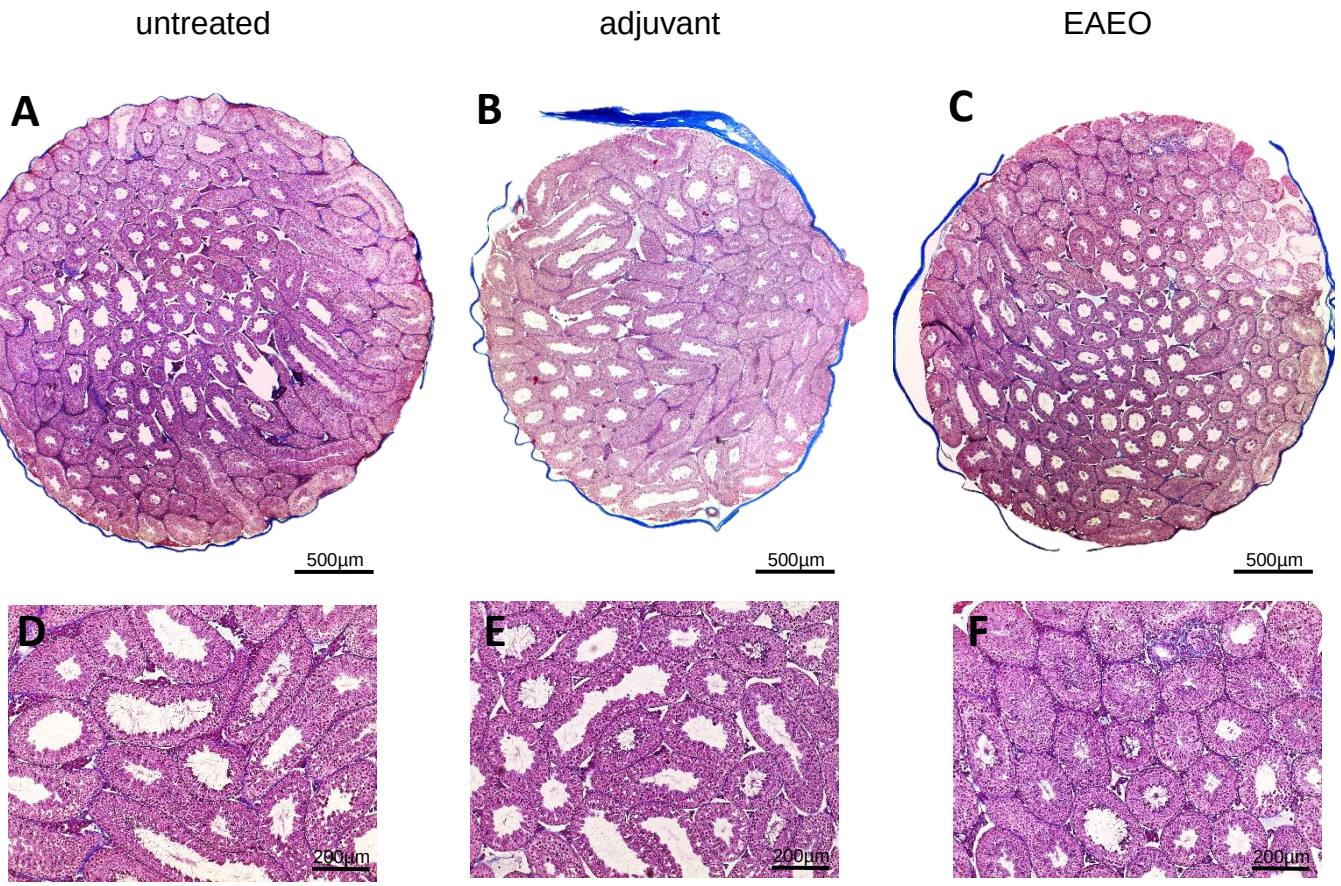

Figure 19. CCR2 deficiency protected the testis from inflammation. Representative photomicrographs of azan staining in paraffin sections from untreated **(A, D)**, adjuvant control **(B, E)** and EAEO **(C, F)** testis in *Ccr2*$^{-/-}$ mice 50 days from the immunization.

EAEO testis from *Ccr2*$^{-/-}$ mice exhibited lower mRNA expression of *Ccr1*, *2, 3*, *5* and *10* along with some of their ligands *Ccl4, Ccl5* and *Ccl11* compared to *WT* EAEO testis **(Fig. 20)**. In contrast, *Ccr6* mRNA expression was not significantly changed in absence of *Ccr2* in EAEO testis as compared to *WT* EAEO controls. Ablation of *Ccr2* significantly downregulated the mRNA expression of *Ccr2* ligands *Ccl8* and *Ccl12,* but not *Ccl7* in EAEO testis*.* In the absence of *Ccr2,* mRNA expression of *Ccl22*, produced by macrophages, was significantly downregulated in EAEO testis. The ablation of *Ccr2* did not affect the mRNA expression of *Ccl1* nor Cc*l3, Ccl6* and *Ccl9,* ligands for *Ccr1.* The expression of *Cx3cr1* and its ligand *Cx3cl1* was significantly downregulated in *Ccr2*$^{-/-}$ EAEO testis compared to *WT* EAEO mice. The mRNA expression of *Cxcr3* as well as its ligand *Cxcl4,* but not *Cxcl9,* was significantly decreased in the absence of *Ccr2.* Chemokines known to be secreted by macrophages, *Cxcl13* and *Cxcl16,* but not *Cxcl1* or *Cxcl14* demonstrated lower mRNA expression in *Ccr2*$^{-/-}$ EAEO testis compared to *WT* EAEO testis. Finally, the relative expression of *Cxcr5* (the receptor for *Cxcl13*) was not significantly changed. These data indicate that CCR2 signaling is required for the recruitment of macrophages and T cells to the testis during inflammatory conditions.

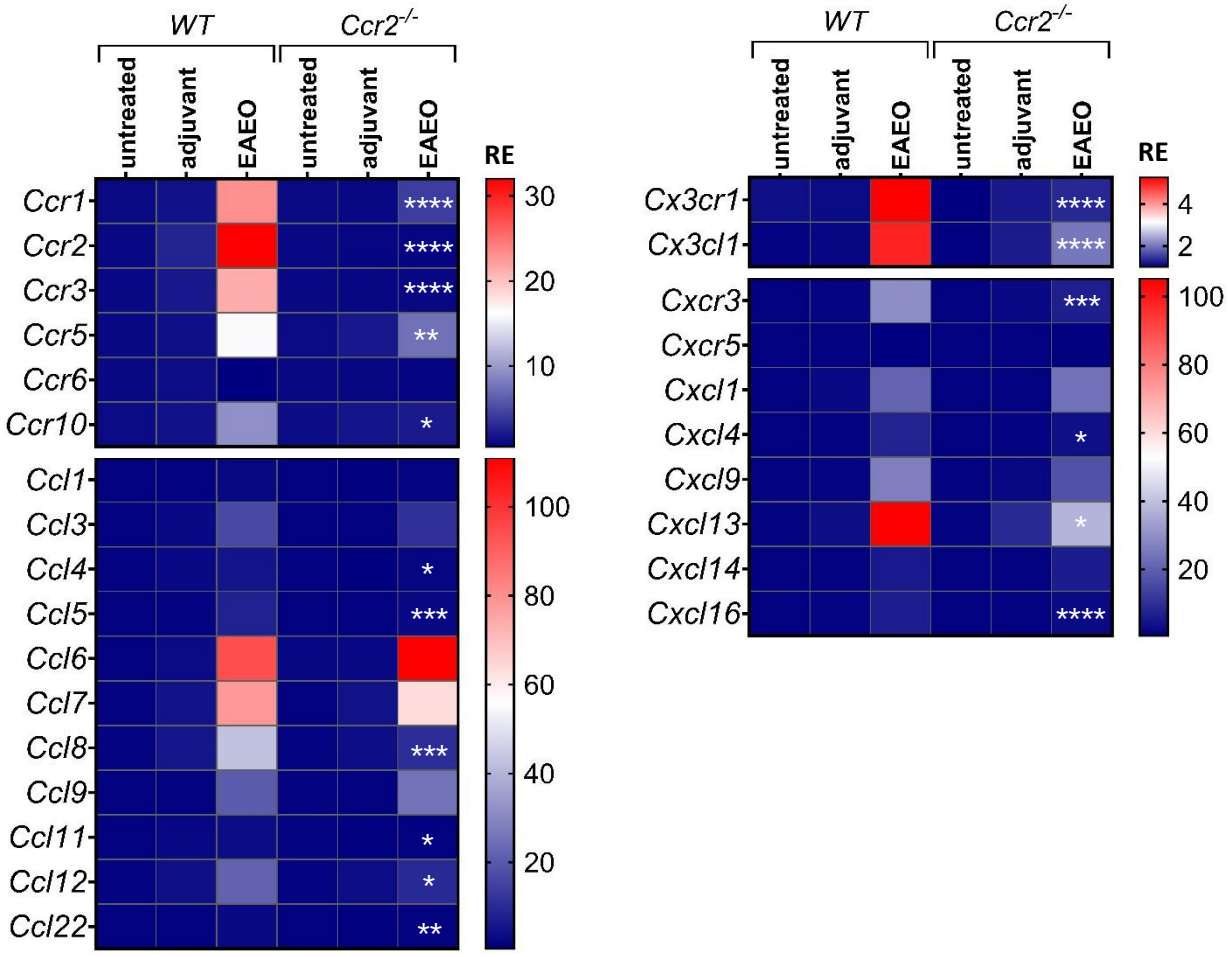

Figure 20. Expression of macrophage and T cell chemokines was reduced in EAEO testis in the absence of CCR2 signaling. Relative expression (RE) of *Ccr1, Ccr2, Ccr3, Ccr5, Ccr6, Ccr10, Ccl1, Ccl3, Ccl4, Ccl5, Ccl6, Ccl7, Ccl8, Ccl9, Ccl11, Ccl12, Ccl22, Cx3cr1, Cx3cl1, Cxcr3, Cxcr5, Cxcl1, Cxcl4, Cxcl9, Cxcl13, Cxcl14* and *Cxcl16* mRNA was determined using customized Mouse Chemokines & Receptors RT² Profiler™ PCR Array in untreated, adjuvant control and EAEO testis from *WT* and *Ccr2*$^{-/-}$ mice 50 days from the immunization and normalized to *β-actin* (n = 6). The results are presented as a heatmap. For simplicity, statistical analysis displayed in the heatmap are limited to between EAEO group from *WT* and *Ccr2*$^{-/-}$, however, the statistical analysis was performed on whole data sets from all investigated groups (untreated, adjuvant control and EAEO) using two-way ANOVA followed by Tukey's test (**P*<0.05, ***P*<0.01, ****P*<0.001, *****P*<0.0001).

3.4. Activin A altered expression of chemokines involved in macrophage trafficking

Recently, we have demonstrated that activin A plays an active role in the testicular inflammatory response and fibrotic remodeling and is able to induce CCR2 expression in macrophages (Nicolas et al., 2017a; Nicolas et al., 2017b; Kauerhof et al., 2019, Peng et al., 2022). Based on these observations, the direct effect of activin A on macrophages using an established *in-vitro* culture of bone

marrow-derived macrophages (BMDM) acting as a surrogate of testicular macrophages (TM) was investigated (Peng et al., 2022) **(Fig. 21A)**. Although BMDM and TM mostly display similar gene expression profiles when not stimulated, differences exist between the two. TM display IL-10 expression as opposed to BMDM when not stimulated. TM exhibit reduced pro-inflammatory responses following LPS stimulation as evident by their lower expression of TNF-α, IL-1β and IL-6 compared to BMDM. Stimulation of TM seems to favor an alternatively activated phenotype over classically activated phenotype. BMDM, on the other hand, are capable of being classically activated as well as being alternatively activated (Winnall et al., 2011).

Whole transcriptomic analysis of previously generated dataset (GSE210004; Peng et al. 2022) revealed that activin A regulated the expression of multiple chemokine receptors and their ligands in BMDM (**Fig. 21B, C)**. Dr. Stefan Günther (ECCPS Bioinformatics and Deep Sequencing Platform, Max Planck Institute for Heart and Lung Research, Bad Nauheim, Germany) performed the analysis. In the presence of activin A during BMDM differentiation, gene expression of *Ccr1, Ccr2, Ccr5* and *Cx3cr1* was elevated. In contrast, chemokines *Ccl2, Ccl3, Ccl4, Ccl6, Ccl7, Ccl8, Ccl12 and Ccl22* were downregulated **(Fig. 21B, C)**. Upon activin A treatment, CXC ligands *Cxcl9* and *Cxcl14* were upregulated, but their receptor *Cxcr3* was downregulated. These effects were abolished by addition of follistatin (FST). Notably, untreated (CTRL), FST-alone or FST + activin A-treated BMDM showed similar gene expression levels, which differed from those in activin A-treated BMDM **(Fig. 21B)**. These results indicate an important role of activin A in the regulation of the chemokine network in the macrophages.

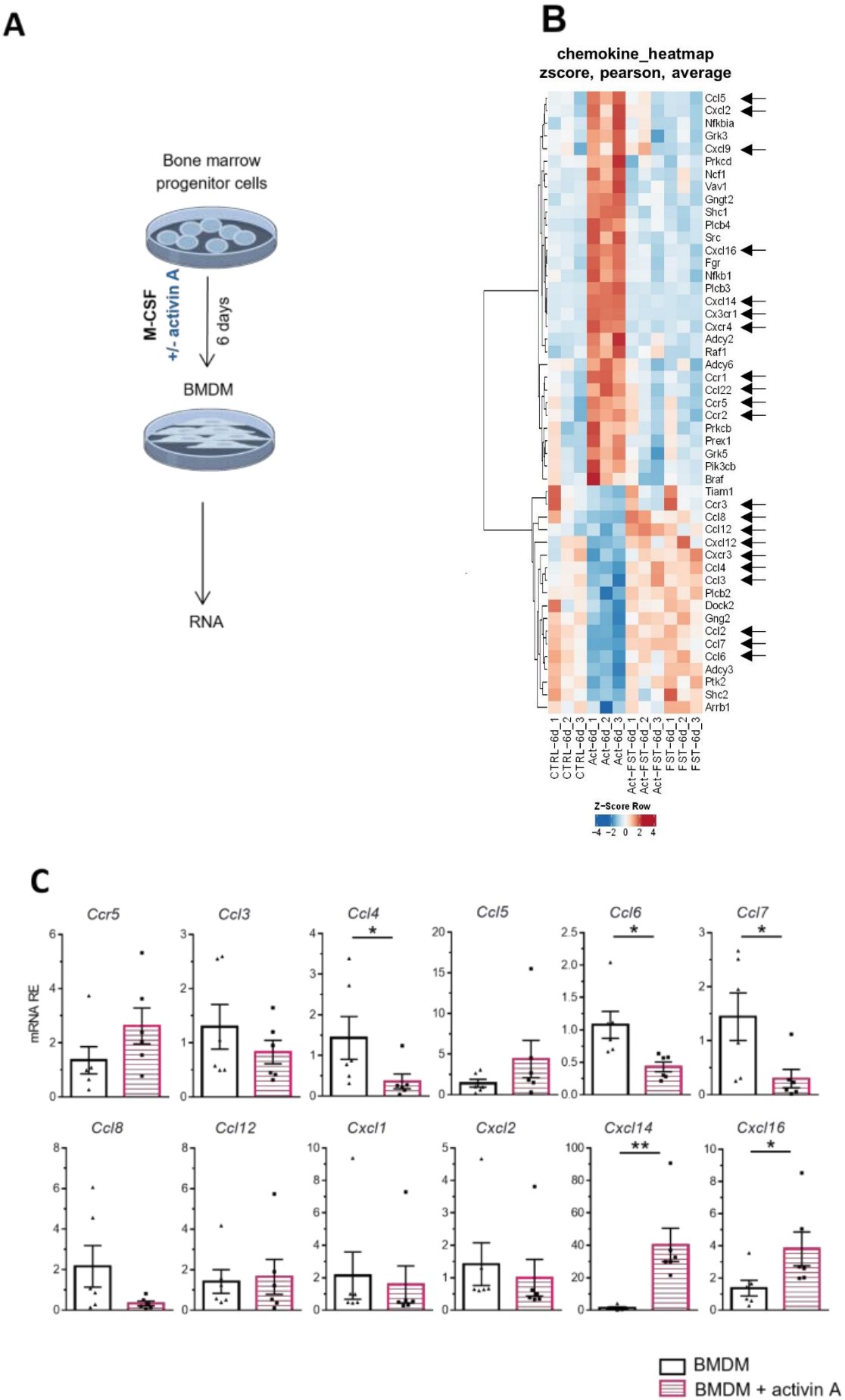
A
Bone marrow progenitor cells
M-CSF
+/- activin A
6 days
BMDM
RNA
B
chemokine_heatmap
zscore, pearson, average
Ccl5
Cxcl2
Nfkbia
Grk3
Cxcl9
Prkcd
Ncf1
Vav1
Gngt2
Shc1
Plcb4
Src
Cxcl16
Fgr
Nfkb1
Plcb3
Cxcl14
Cx3cr1
Cxcr4
Adcy2
Raf1
Adcy6
Ccr1
Ccl22
Ccr5
Ccr2
Prkcb
Prex1
Grk5
Pik3cb
Braf
Tiam1
Ccr3
Ccl8
Ccl12
Cxcl12
Cxcr3
Ccl4
Ccl3
Plcb2
Dock2
Gng2
Ccl2
Ccl7
Ccl6
Adcy3
Ptk2
Shc2
Arrb1
CTRL-6d_1
CTRL-6d_2
CTRL-6d_3
Act-6d_1
Act-6d_2
Act-6d_3
Act+FST-6d_1
Act+FST-6d_2
Act+FST-6d_3
FST-6d_1
FST-6d_2
FST-6d_3
Z-Score Row
−4 −2 0 2 4
C
Ccr5
Ccl3
Ccl4
Ccl5
Ccl6
Ccl7
Ccl8
Ccl12
Cxcl1
Cxcl2
Cxcl14
Cxcl16
mRNA RE
BMDM
BMDM + activin A

Figure 21. Activin A altered expression of chemokines involved in macrophage trafficking. Experimental design for BMDM generation and *in-vitro* treatment, created using BioRender (A). Heatmap from whole transcriptomic analysis of the previously generated dataset (GSE210004; Peng et al. 2022). Bone marrow progenitor cells from WT mice were treated with M-CSF and were left untreated or treated with 50 ng/ml activin A (Act), 250 ng/ml FST288 (FST), or a combination of both (Act+FST). (B). Heat map showing expression of the top 50 differentially expressed genes (DEGs) enriched for the term "Chemokine signaling pathway" in CTRL, Act, Act+FST, and FST groups (based on false discovery rate>0.05 and minimal count number>5) from the KEGG pathway database presented with Z-score normalization. Relative expression (RE) of *Ccr5, Ccl3, Ccl4, Ccl5, Ccl6, Ccl7, Ccl8, Ccl12, Cxcl1, Cxcl2, Cxcl14* and *Cxcl16* mRNA measured by qRT-PCR (C) in activin A-treated BMDM or BMDM without activin A treatment (control) and normalized to expression of *Hprt*. (n=6; mean ± SEM). Statistical test used: Mann-Whitney test or student's *t*-test (**P*<0.05, ***P*<0.01).

3.5. Activin A indirectly suppressed the pro-inflammatory profile of T cells

Activin A is a major regulator of macrophage development and function and is also secreted by macrophages (Hedger & de Kretser, 2013). In the testis, activin A secreted by macrophages can influence other immune cells, such as T cells, which are anatomically located in very close proximity to testicular macrophages (Han et al., 2016; Locci et al., 2016; Morianos et al., 2019; Semitekolou et al., 2009). For this reason, the effects of activin A on chemokine expression in a co-culture of isolated T cells with BMDM were further investigated **(Fig. 22, 23)**. The purity of the isolated T cells used in the co-culture ranged between 94 - 97% **(Fig. 22)**.

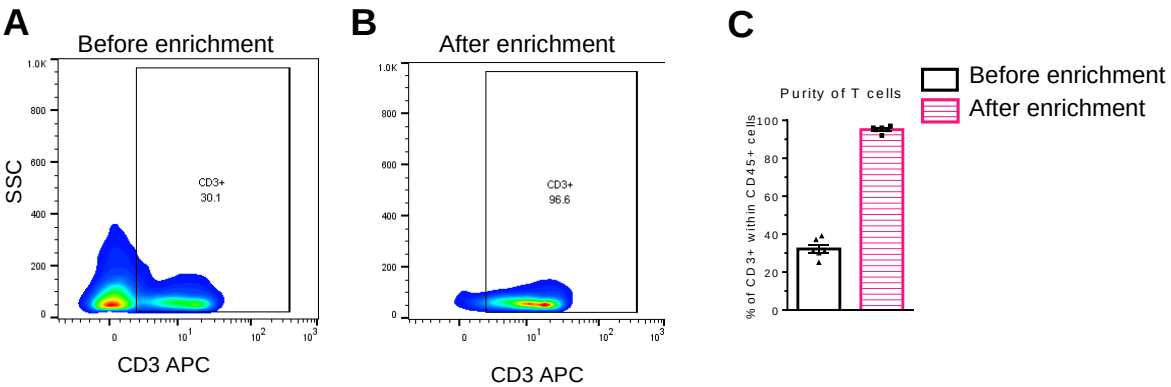

Figure 22. Representative flow cytometry plots of CD3⁺ T cells before (A) and after enrichment (B) using a mouse Pan T Cell Isolation Kit II. Histogram showing the percentages of T cells before and after enrichment using mouse Pan T Cell Isolation Kit II (C) (n=6, mean ± SEM).

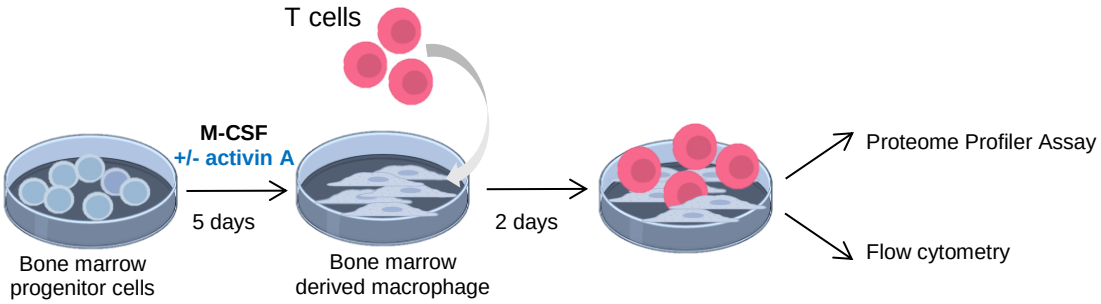

Figure 23. Co-culture of T cells with BMDM. Experimental setting for generation of BMDM and co-culture with T cells. Enriched T cells were added to 5-day-old activin A-treated or untreated BMDM (control) and were co-cultured for 2 days. Figure created with BioRender.

Conditioned media collected from T cells co-cultured with activin A-treated BMDM were applied to a proteome profiler assay, which semi-quantitatively measures released chemokines. Secretion of CCL2, CCL3/4, CCL12, ligands that mainly bind to CCR1 and CCR2, and CXCL2 was significantly lower in the conditioned media from T cells co-cultured with activin A-treated BMDM as compared to co-culture with untreated BMDM **(Fig. 24)**. In contrast, the levels of CXCL16, a chemokine involved in the attraction of T cells, were higher in presence of activin A in co-culture. Treatment of BMDM with activin A had no influence on the production of CCL5, CCL6, CCL8 and CCL9 in co-culture with T cells (**Fig. 24**).

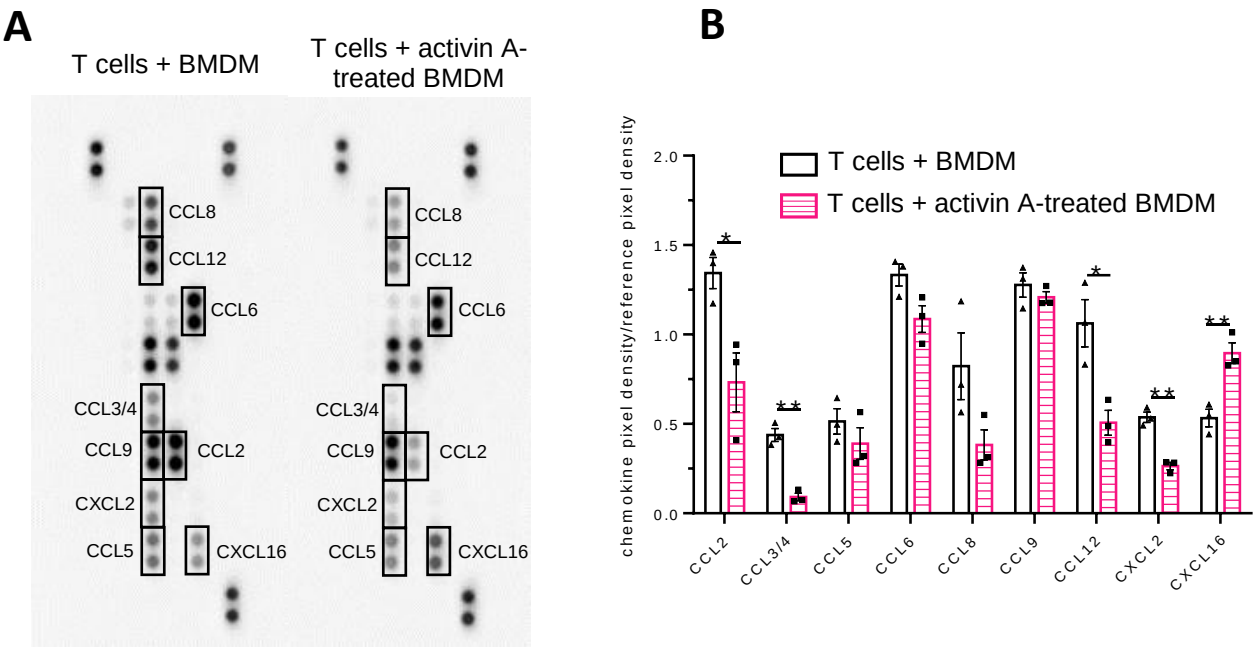

Figure 24. Activin A altered chemokine expression in co-cultures of T cells and BMDM. Representative dot blot membrane incubated with conditioned media from co-cultures of T cells with activin A-treated BMDM or untreated BMDM **(A)**. Profiles of integrated pixel density divided by reference pixel density **(B)** obtained using a chemiluminescence imaging system and image analysis software (ImageJ software). (n = 3; mean ± SEM). Statistical analysis used: unpaired *t*-tests (**P*<0.05, ***P*<0.01).

T cells co-cultured with activin A-treated BMDM were analyzed using flow cytometry for the induction of pro-inflammatory cytokines. T cells co-cultured with activin A-treated BMDM showed significantly lower induction of pro-inflammatory cytokine TNF compared to T cells cultured with untreated BMDM. In contrast, production of IFN-γ was decreased although this decrease was not significant (**Fig. 25A, B**). The importance of macrophages for the effect of activin A on the production of TNF and IFN-γ by T cells was confirmed during stimulation of T cells by activin A alone, where no effect on the induction of both cytokines was observed **(Fig.25C, D)**. These results suggest that activin A related effects on TNF production by T cells are directed through macrophages.

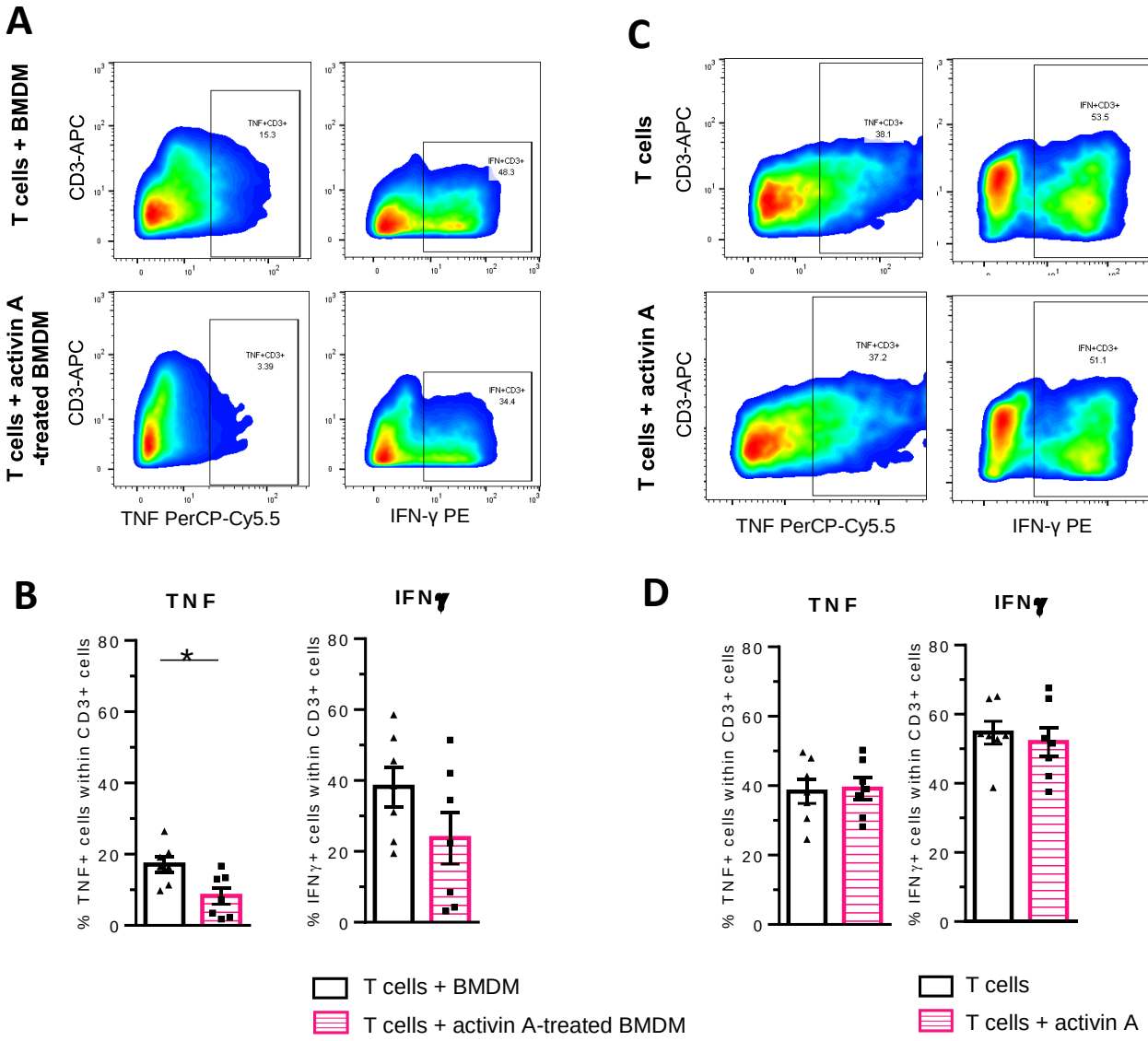

Figure 25. Activin A indirectly decreased the pro-inflammatory profile of T cells. Representative flow cytometry plots for TNF⁺ and IFNγ⁺ CD3⁺ T cells co-cultured with activin A-treated or untreated BMDM **(A)**. Percentages of TNF⁺ and IFNγ⁺ CD3⁺ T cells **(B)** were determined after gating out doublets and nonviable cells (n = 7; mean ± SEM). Statistical test used: Student's *t*-test (**P*<0.05). Representative flow cytometry plots for TNF⁺ and IFNγ⁺ CD3⁺ T cells cultured with or without activin A **(C)**. Percentages of TNF⁺ and IFNγ⁺ CD3⁺ T cells **(D)** were determined after gating out doublets and nonviable cells (n = 7; mean ± SEM). Statistical test used: Student's *t*-test (**P*<0.05).

3.6. Macrophages expressing activin A were increased in EAEO testis

Given that activin A can influence chemokine expression and is implicated in EAEO development and progression (Nicolas et al., 2017a; Kauerhof el al., 2019; Peng et al., 2022), it was of interest to explore the identity of cells expressing activin A in EAEO testis. A double immunofluorescence staining of activin A with macrophage (F4/80) or T cell (CD3) markers was performed in testis sections. Activin A staining in untreated and adjuvant control WT testis was observed in the cytoplasm of Sertoli cells, and interstitial and peritubular macrophages **(Fig. 26A, C, D)**. However, in EAEO testis, activin A staining was not present in all seminiferous tubules, in contrast to tubules in normal testis. Interstitial macrophages expressing activin A were markedly increased in EAEO testis. Some macrophages could also be seen inside the seminiferous tubules and these were also positive for activin A **(Fig. 26B, E, J)**. In *Ccr2*$^{-/-}$ EAEO mice, on the other hand, macrophages expressing activin A were visibly reduced when compared to WT EAEO testis. **(Fig. 26H, I)**.

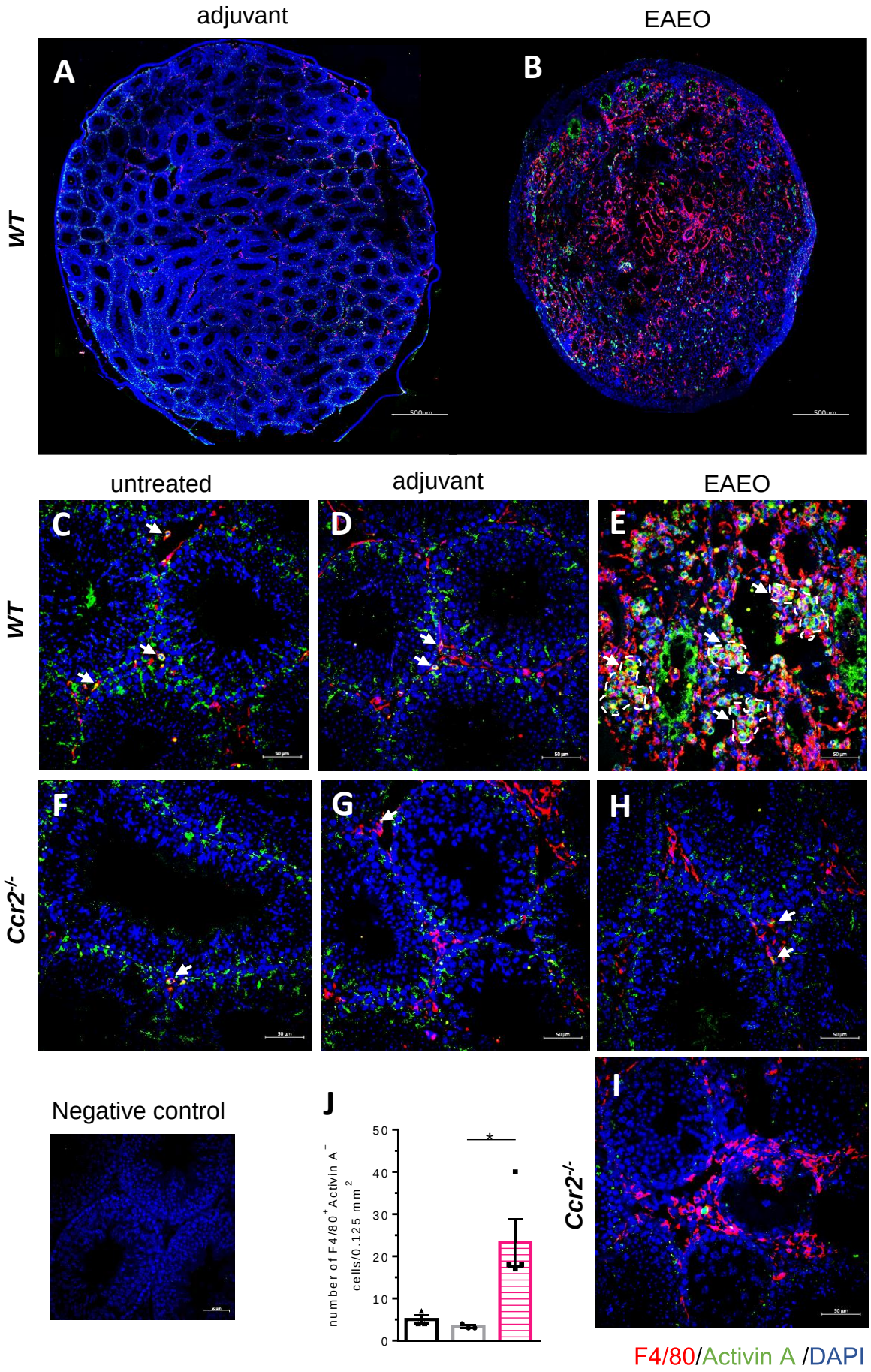
adjuvant
EAEO
A
B
WT
untreated
adjuvant
EAEO
C
D
E
WT
F
G
H
Ccr2-/-
Negative control
J
I
Ccr2-/-
number of F4/80+Activin A+ cells/0.125 mm2
50
40
30
20
10
0
*
F4/80/Activin A /DAPI

Figure 26. Macrophages expressing activin A were increased in EAEO testis. Representative photomicrographs of macrophages (F4/80, red), activin A (green) and DAPI (blue) fluorescence in paraffin sections of untreated **(C)**, adjuvant control **(A, D)** and EAEO **(B, E)** testis from *WT* mice and untreated **(F)**, adjuvant control **(G)** and EAEO **(H, I)** testis from *Ccr2*$^{-/-}$ mice 50 days from the immunization. Arrows and dotted lines point to triple-labelled macrophages. Negative control sections were incubated only with the antibody diluent in place of the primary antibody. Quantification of F4/80+activin A+ positive macrophages **(J)** determined by counting of triple positive immunofluorescence stained cells (activin A, green; F4/80, red; DAPI, blue) in paraffin sections of untreated, adjuvant control and EAEO testes from WT mice (n = 3 - 5 ± SEM); statistical analysis was performed using Kruskal–Wallis test (followed by Dunn's multiple comparison test) (*P<0.05).

3.7. T cells expressing activin A were increased in EAEO testis

Some of the cells positive for activin A in the interstitial space of EAEO testis were not labelled by F4/80 and were checked to see if they could be T cells. Double immunofluorescence of activin A with CD3 revealed that T cells positive for activin A were present in the testis in the absence of inflammation **(Fig 27A, B).** EAEO testis, on the other hand, showed that T cells expressing activin A were increased in the interstitial space **(Fig. 27C, I).** In mice deficient for CCR2, T cells expressing activin A were visibly reduced when compared to *WT* EAEO testis **(Fig. 26F, G)**.

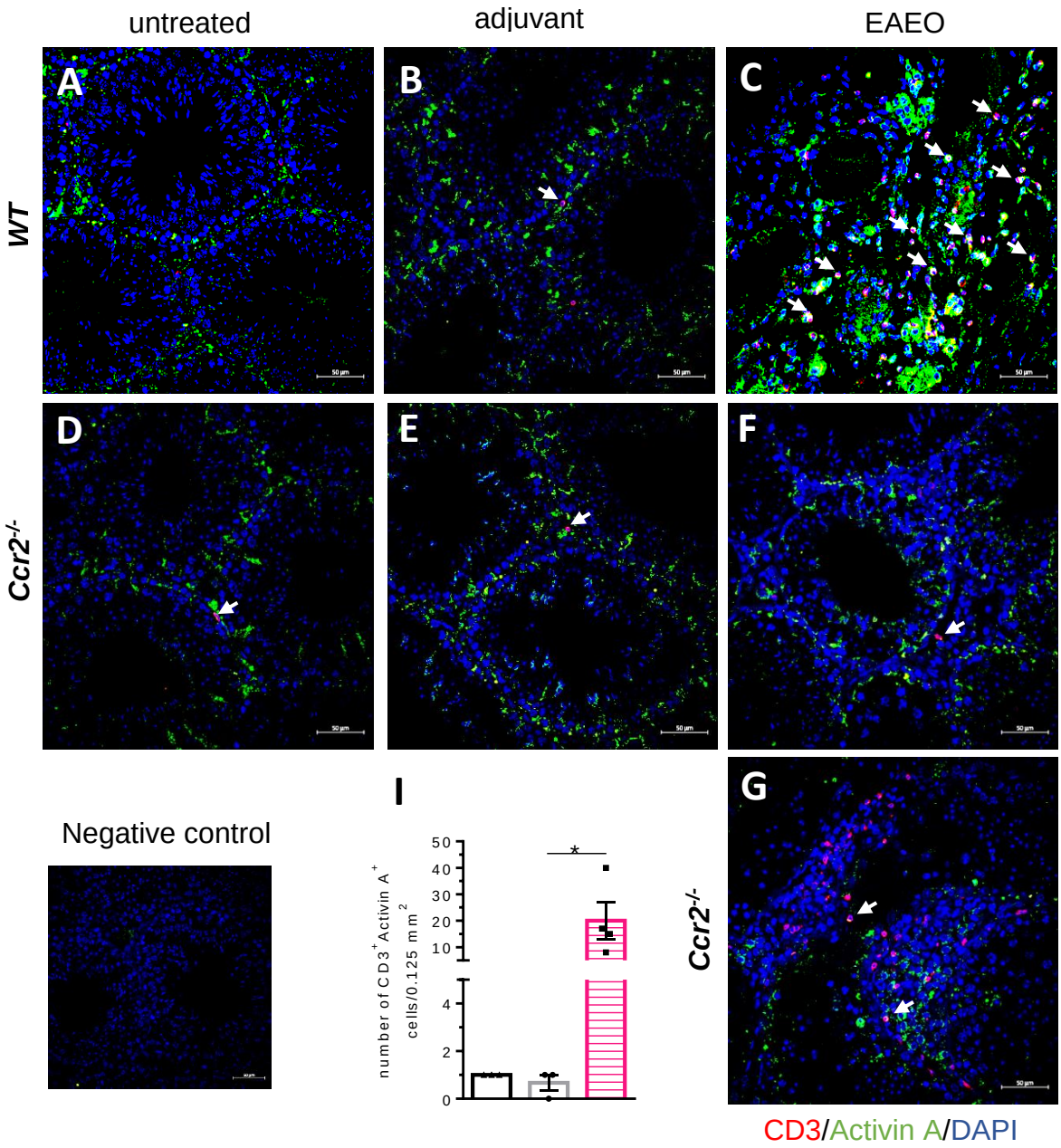

Figure 27. T cells expressing activin A were increased in EAEO testis. Representative photomicrographs of T cells (CD3, red), activin A (green) and DAPI (blue) fluorescence staining in paraffin sections of untreated **(A),** adjuvant control **(B)** and EAEO **(C)** testis from *WT* mice and untreated **(D),** adjuvant control **(E)** and EAEO **(F, G)** testis from *Ccr2*$^{-/-}$ mice 50 days from the immunization. Arrows point to triple-positive T cells. Negative control sections were incubated with the antibody diluent in place of the primary antibody. Quantification of CD3+activin A+ positive T cells **(I)** determined by counting of triple positive immunofluorescence stained cells (activin A, green; CD3, red; DAPI, blue) in paraffin sections of untreated, adjuvant control and EAEO testes from WT mice (n = 3 - 5 ± SEM); statistical analysis was performed using Kruskal–Wallis test (followed by Dunn's multiple comparison test) (**P*<0.05).

3.8. B cells were present in EAEO testis

The data from the PCR array revealed that, out of all 84 genes analyzed, *Cxcl13* mRNA demonstrated the highest fold-increase (100-fold) in comparison to adjuvant control testis. CXCL13 is commonly regarded as a chemoattractant for B cells to lymphoid organs and inflamed sites (Harrer et al., 2022). Therefore, the presence of B cells was investigated in EAEO testis. In contrast to EAEO testis, B cells were not detected in adjuvant or untreated controls **(Fig. 28A, B, C)**. In EAEO testis, B cells were detected as single cells or clusters in the interstitial space **(Fig 28C).** Knockout of Ccr2 reduced the number of B cells in the EAEO testis relative to controls **(Fig. 28F, G).**

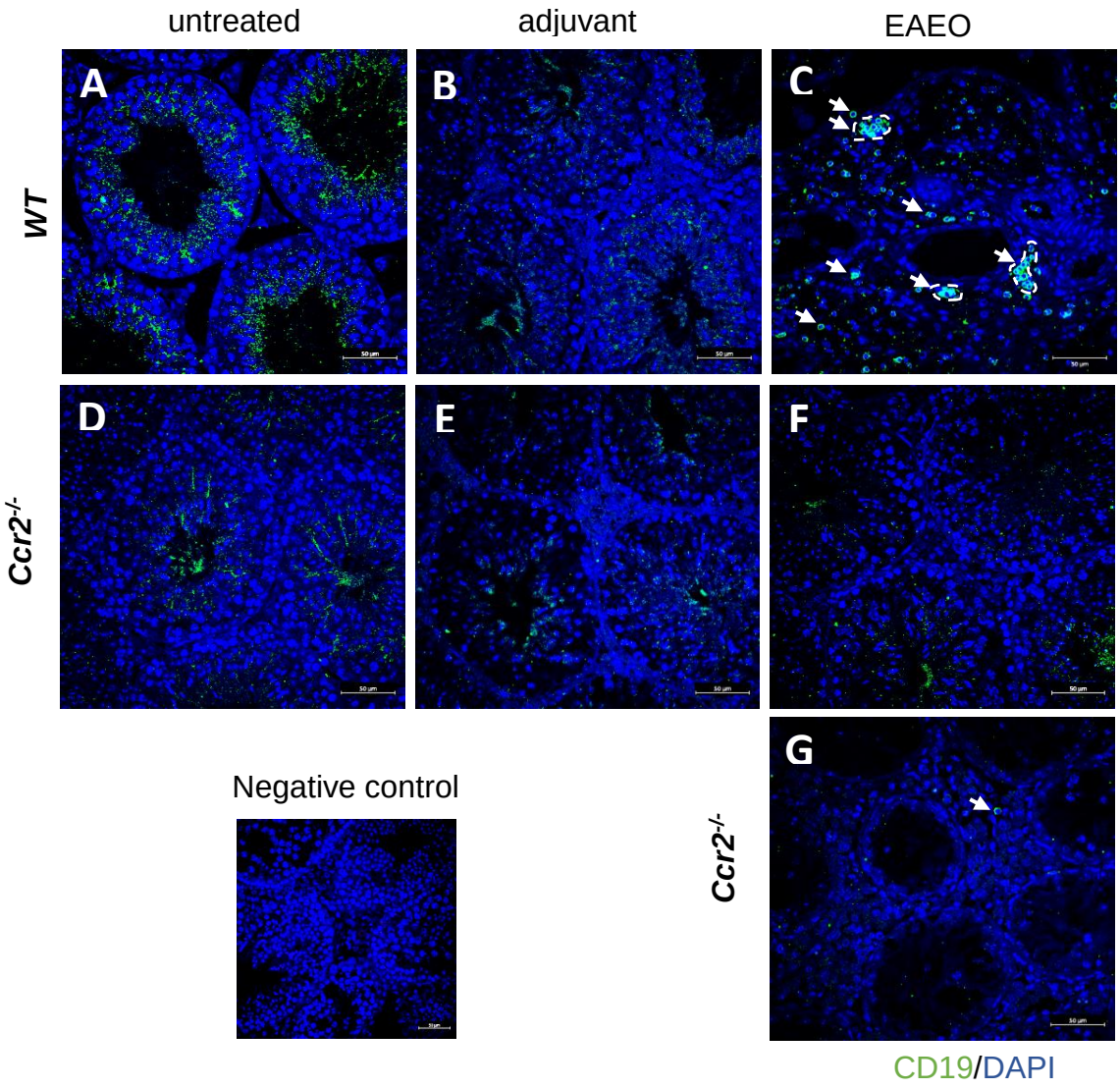

Figure 28. B cells were present in EAEO testis. Representative photomicrographs of B cells (CD19, green) and DAPI (blue) fluorescence staining on paraffin sections of untreated **(A),** adjuvant control **(B)** and EAEO **(C)** testis from *WT* and untreated **(D),** adjuvant **(E)** and EAEO **(F,**

G) testis from *Ccr2*$^{-/-}$ mice 50 days from the immunization. Arrows and dotted lines point to B cells. Negative control sections were incubated with the antibody diluent in place of the primary antibody.

3.9. High endothelial venules (HEV) were not present in EAEO testes but were found in the inflamed epididymis

Given the observation that CXCL13 was elevated and B cell clusters were found in the inflamed testis, it was hypothesized that high endothelial venules (HEV) may be involved in the recruitment of B cells. In EAEO testis, MECA-79 (a marker for HEV) was not detected **(Fig. 29)**. However, in the terminal part of the cauda epididymidis of EAEO mice, immune cell filtrates were present along with fibrotic remodeling affecting the tissue **(Fig. 30C)**. In this part of the epididymis, MECA-79+ HEV were detected, associated with clusters of B cells **(Fig. 29)**.

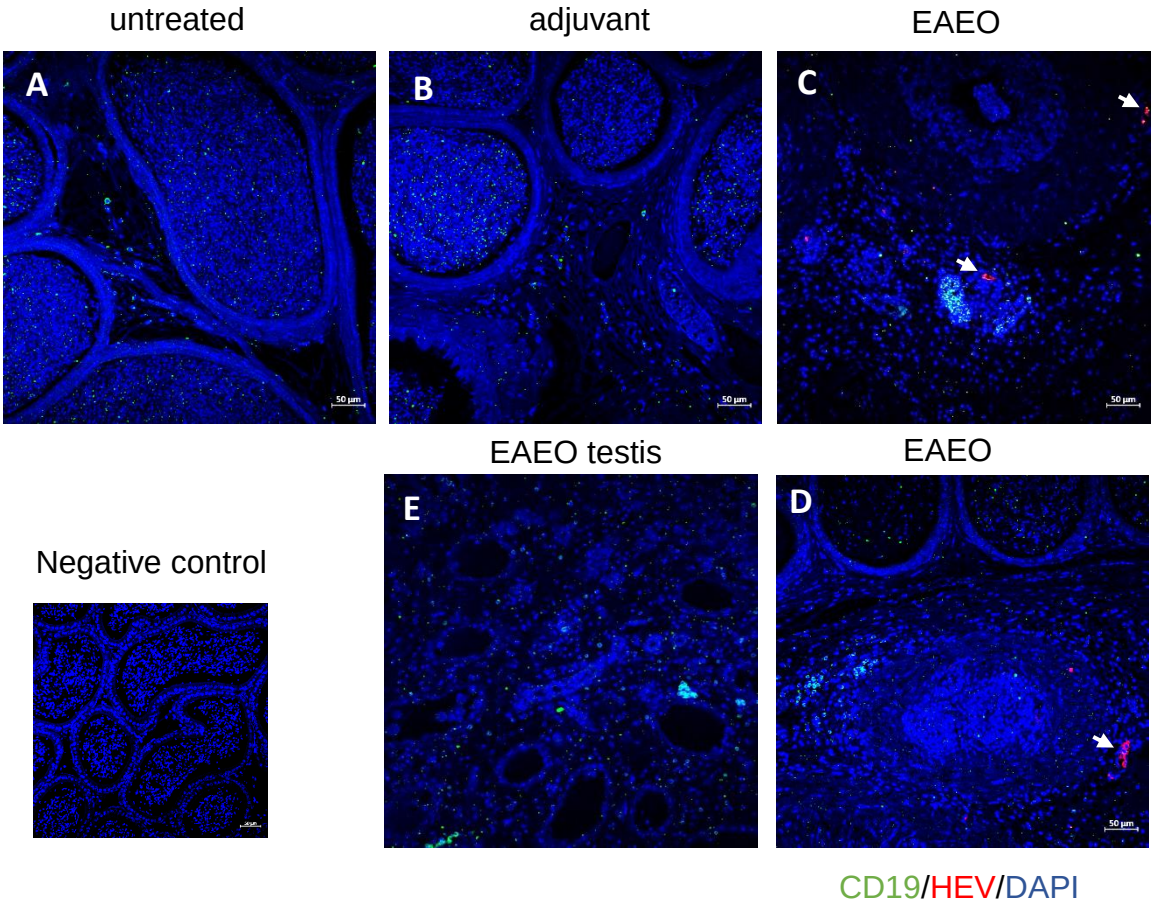

Figure 29. HEV were present in EAEO cauda epididymides. Representative photomicrographs of B cells (CD19, green), HEV (MECA-79, red) and DAPI (blue) fluorescence staining in paraffin sections of untreated **(A)**, adjuvant **(B)**, EAEO epididymides **(C, D)** and EAEO testis **(E)** from *WT*

mice 50 days from the immunization. Arrows point to MECA-79^{+} HEV. Negative control sections were incubated with the antibody diluent in place of the primary antibody.

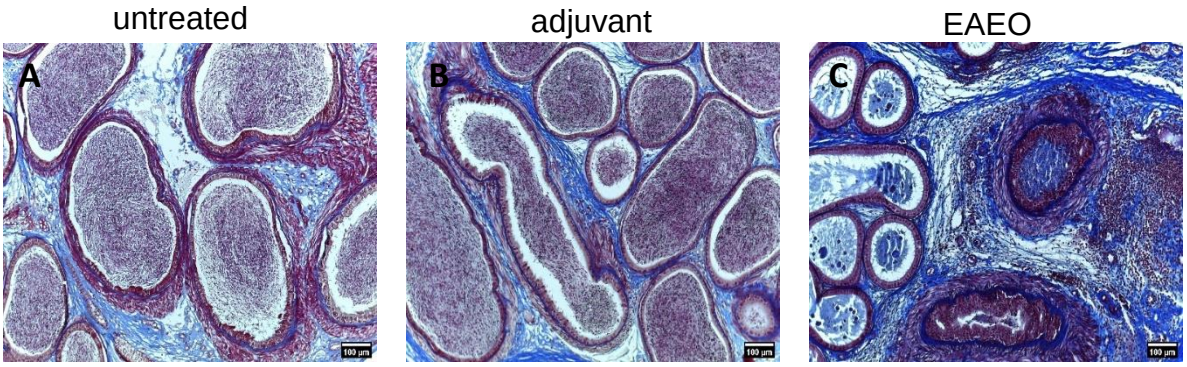

Figure 30. EAEO caused immune cell infiltration and fibrotic remodeling in cauda epididymidis. Representative photomicrographs of azan staining in paraffin sections of untreated **(A)**, adjuvant control **(B)** and EAEO **(C)** cauda epididymides from *WT* mice 50 days from the immunization. Arrows indicates immune cell infiltrate. Magnification bar 100µm.

3.10. T and B cell clusters were present in EAEO cauda epididymides

Since B cells along with HEV were reported in the epididymis of EAEO mice, the presence of other TLO-related elements in the epididymis during inflammation was analyzed. A classical aspect of TLO is the presence of clusters of B cells next to the T cell areas (Ruddle, 2016). Staining of T cells and B cells revealed that clusters of both cell populations next to each other were only found in the EAEO cauda epididymidis, but not in the testis of EAEO mice **(Fig. 31)**.

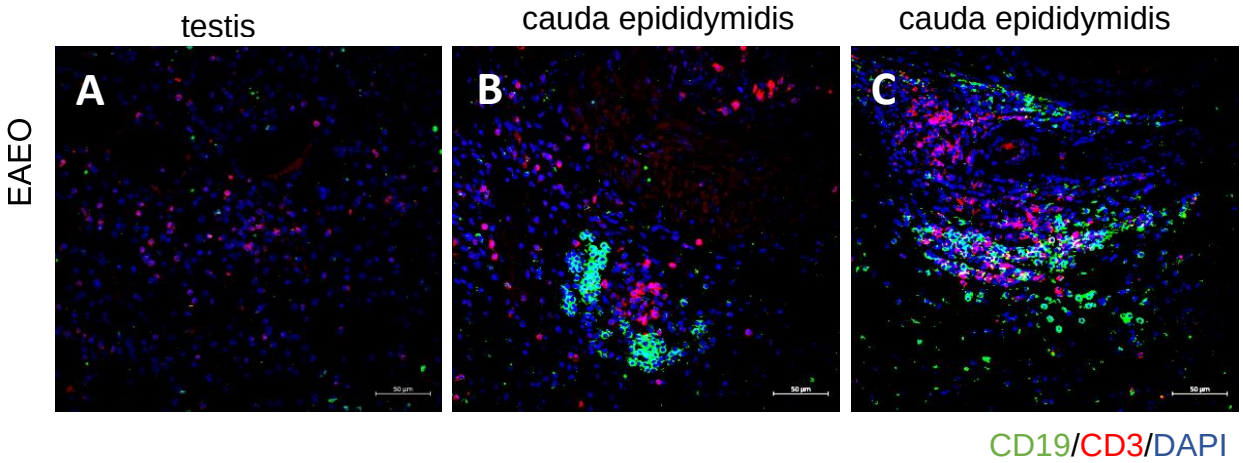

Figure 31. B and T cell clusters are detected in EAEO cauda epididymidis. Representative photomicrographs of CD19 (green), CD3 (red) and DAPI (blue) fluorescence staining in paraffin sections of EAEO testis **(A)** and cauda epididymidis **(B, C)** from *WT* mice 50 days from the immunization.

Clusters of B cells and T cells could only be found in the cauda epididymides, but not in the caput or corpus of the epididymis **(Fig. 32)**.

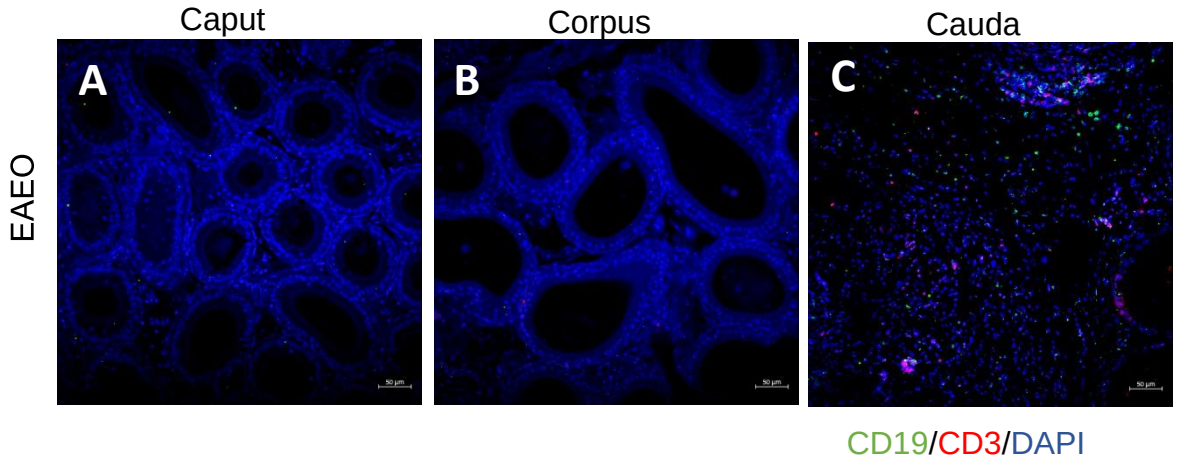

Figure 32. 50 days after first immunization only the cauda epididymidis shows the presence of B and T cell infiltrates. Representative photomicrographs of B cells (CD19, green), T cells (CD3, red) and DAPI (blue) in paraffin sections from caput **(A)**, corpus **(B)** and cauda **(C)** epididymides from *WT* mice 50 days from the immunization.

Subsequently, B cell numbers were determined by flow cytometry, and an increase in B cells ($CD19^{+}CD45R^{+}$) in some EAEO cauda epididymides was noted, but this was highly variable **(Fig. 33).**

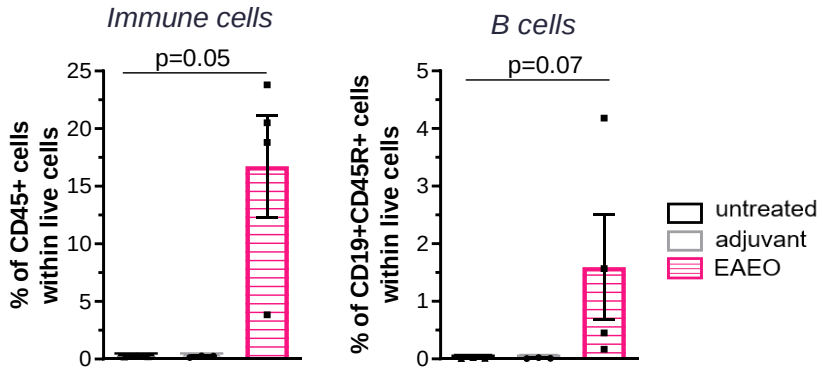

Figure 33. B cells were variably increased in EAEO cauda epididymidis. Proportions of immune cells ($CD45^+$) and B cells ($CD19^+CD45R^+$) were determined in untreated, adjuvant control and EAEO WT epididymides 50 days from the immunization using flow cytometry after gating out doublets and nonviable cells. (n = 3 - 4; mean ± SEM). Statistical analysis used Kruskal–Wallis test followed by Dunn's multiple comparison test.

3.11. Elements of TLO were present in the EAEO cauda epididymidis

In addition to the presence of B and T cell clusters and HEV ($MECA\text{-}79^+$) in the inflamed epididymis **(Fig 29, 31)**, the maturation stage of the TLO was determined. Proliferating B cells are indicators of a mature TLO, which are capable of producing high affinity antibodies (Sato et al., 2023). However, proliferating clusters of B cells were not detected in the EAEO cauda, as detected by PCNA staining **(Fig. 34B).** Macrophages ($F4/80^+$) were found surrounding the B cell clusters **(Fig. 34C).** These macrophages could act as antigen-presenting cells and influence survival and proliferation of B cells (Shabgah et al., 2019). The presence of lymphoid stromal cells were detected using podoplanin (PDPN) as a marker (Astarita et al., 2012). Lymphoid stromal cells provide structural support and spatial arrangement of lymphoid immune cells as well as a reticular network for the lymphoid organ (Astarita et al., 2012; Cinti & Denton, 2021; Mittal et al., 2013). Podoplanin-positive cells were found in the interstitial space between the cauda tubules in the EAEO epididymis **(Fig. 34D)**. However, podoplanin was not expressed within the B cell clusters, indicating that a reticular network had not developed in the lymphoid aggregates present in EAEO cauda epididymidis. These results reveal that the lymphoid aggregates present in EAEO cauda epididymidis contains only some elements necessary for TLO formation and do not represent fully-developed TLO

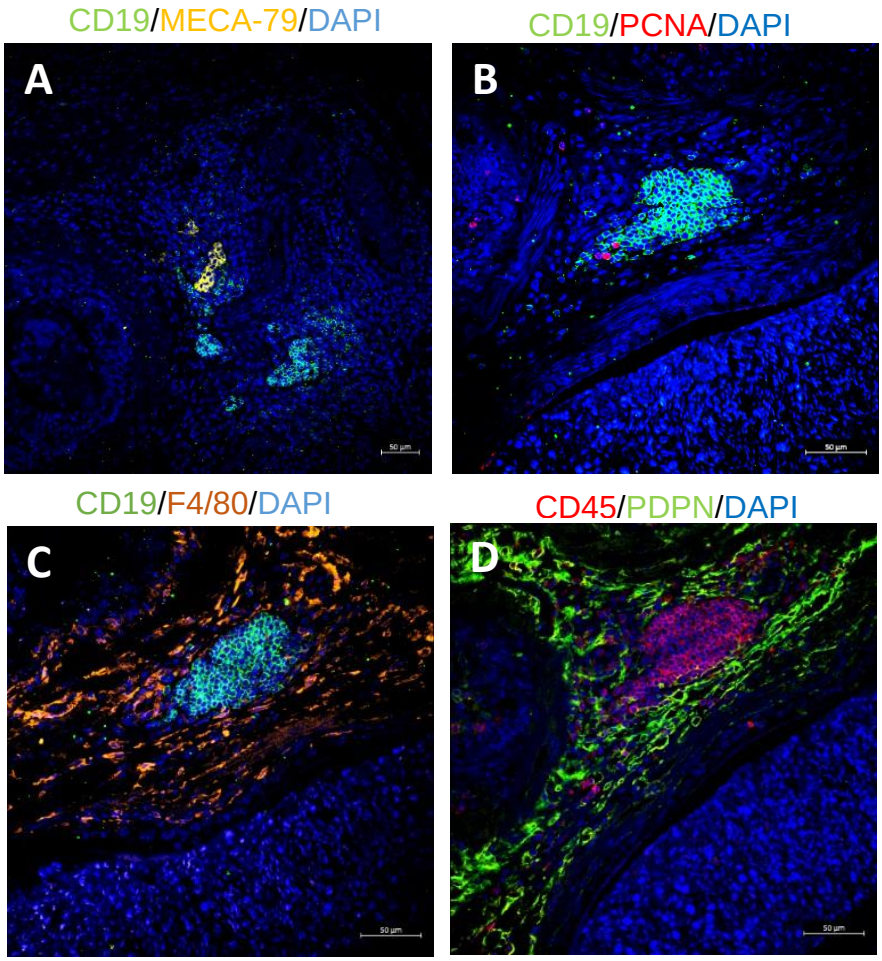

Figure 34. Elements of TLO were detected in EAEO cauda epididymides. Representative photomicrographs of B cells (CD19, green), HEV (MECA-79, yellow) and DAPI (blue) **(A),** B cells (CD19, green), proliferating cells (PCNA, red) and DAPI (blue) **(B),** B cells (CD19, green), macrophages (F4/80, orange) and DAPI (blue) **(C)** podoplanin (PDPN, green), immune cells (CD45, red) and DAPI (blue) **(D)** fluorescence staining in paraffin sections of EAEO cauda epididymidis from *WT* mice 50 days from the immunization.

3.12. Several TLO related chemokines and HEV associated genes were increased in EAEO cauda epididymidis

Correct compartmentalization of B and T cells within lymphoid organs and tissues is achieved partially by the presence of a gradient of the chemokines CCL19 and CCL21 (T cell ligands) and CXCL13 (B cell chemoattractant) (Neyt et al., 2012; Ruddle, 2020). B and T cell clusters found in EAEO cauda epididymides were not well-segregated in all epididymis investigated (n = 5) and were mostly present as B and T cells intermingling together **(Fig. 31C)**. Determination of the mRNA

expression related to TLO chemokines revealed that *Cxcl13* was significantly increased in EAEO cauda epididymides as compared to adjuvant controls **(Fig 35)**. mRNA expression of *Ccl19* and *Ccl21*, on the other hand, was not significantly increased in EAEO cauda epididymides compared to adjuvant controls. These results suggest that the inefficient compartmentalization of B and T cells could be a consequence of the low expression of the chemokines *Ccl19* and *Ccl21*.

Considering that HEV were also present in EAEO cauda epididymides, analysis of the factors leading to their ectopic formation was performed. HEV develop from normal venules by the stimulation of the TNFR1 signaling pathway via a homotrimer of lymphotoxin (LT) α and/or TNF. Transformation into a mature HEV is achieved by stimulation of the LTβ receptor (R) via a heterotrimer of LTα and LTβ as well as TNFSF14 (Blanchard & Girard, 2021). Relative expression of *Ltα* and *Tnf* was significantly increased in EAEO cauda in comparison to untreated controls **(Fig. 35)**. On the other hand, other factors responsible for HEV maturation were not significantly increased in the EAEO cauda epididymidis compared to the untreated cauda epididymidis **(Fig. 35).** mRNA expression of *Ltβ* was increased in most EAEO cauda epididymidis, but the response was highly variable. mRNA expression of *Tnfsf14* was significantly elevated in EAEO cauda epididymides compared to adjuvant controls. These results suggest that factors essential for HEV formation are expressed in EAEO cauda epididymidis, but not all factors responsible for HEV maturation are present.

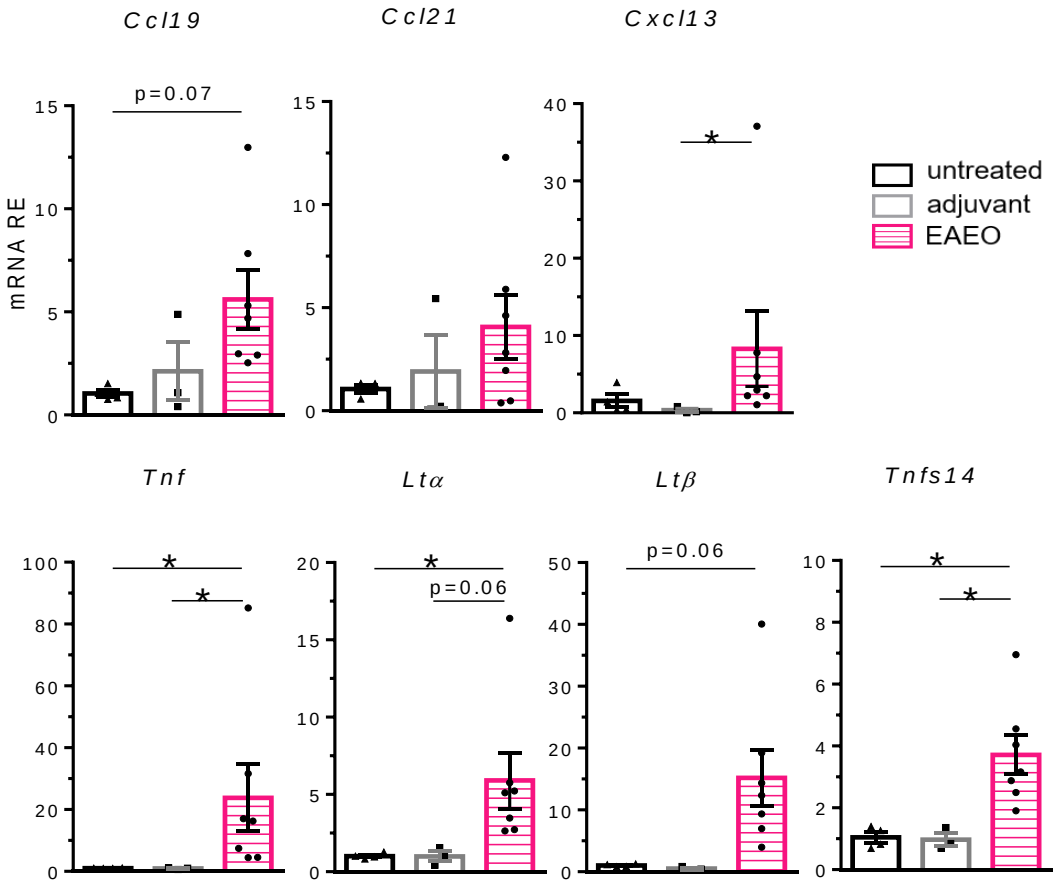

Figure 35. Expression of TLO related chemokines and HEV related genes was increased in EAEO cauda epididymidis. Relative expression (RE) of *Ccl19, Ccl21, Cxcl13, Tnf, Ltα, Ltβ* and *Tnfs14* mRNA was measured by qRT-PCR in untreated, adjuvant and EAEO cauda epididymides from *WT* mice 50 days from the immunization and normalized to *Rplpo* (n = 3 - 7; mean ± SEM). Statistical test used was Kruskal–Wallis test followed by Dunn's multiple comparison test or one-way ANOVA followed by Tukey's multiple comparison test (**P*<0.05).

3.13. TLO-related chemokines and HEV-related genes were increased in UPEC-infected cauda epididymides

Considering the immature stages of TLO were found in the inflamed cauda epididymis in the EAEO model, whether TLO also develop in the cauda epididymidis during acute infection was checked. A commonly used mouse model of acute UPEC-induced epididymitis was investigated (Pleuger et al., 2022). Relative expression of several parameters involved in TLO formation was monitored in the cauda epididymides from UPEC-infected and sham operated

mice during the course of infection (d1, 3, 5, 7, 10, 14, 18, 21, and 28 days post-UPEC inoculation). An initial rise in TLO related chemokines (*Cxcl13, Ccl19* and *Ccl21*) was observed within 5 days, however this was variable and not statistically significant **(Fig. 36)**. A significant peak of *Ccl19* and *Ccl21* mRNA was observed by 14 days compared to sham control mice, and while the expression of *Cxcl13* also appeared to increase, this was not significant at this time-point due to variable results. The expression of *Ccl21* reached another peak at 21 days, and *Ccl19* and *Cxcl13* were again significantly elevated at 28 days post-UPEC infection **(Fig. 36).** These results suggest that possible B and T cell recruitment takes place at time points after UPEC infection, mainly between 14 and 28 days following the initial inoculation.

.

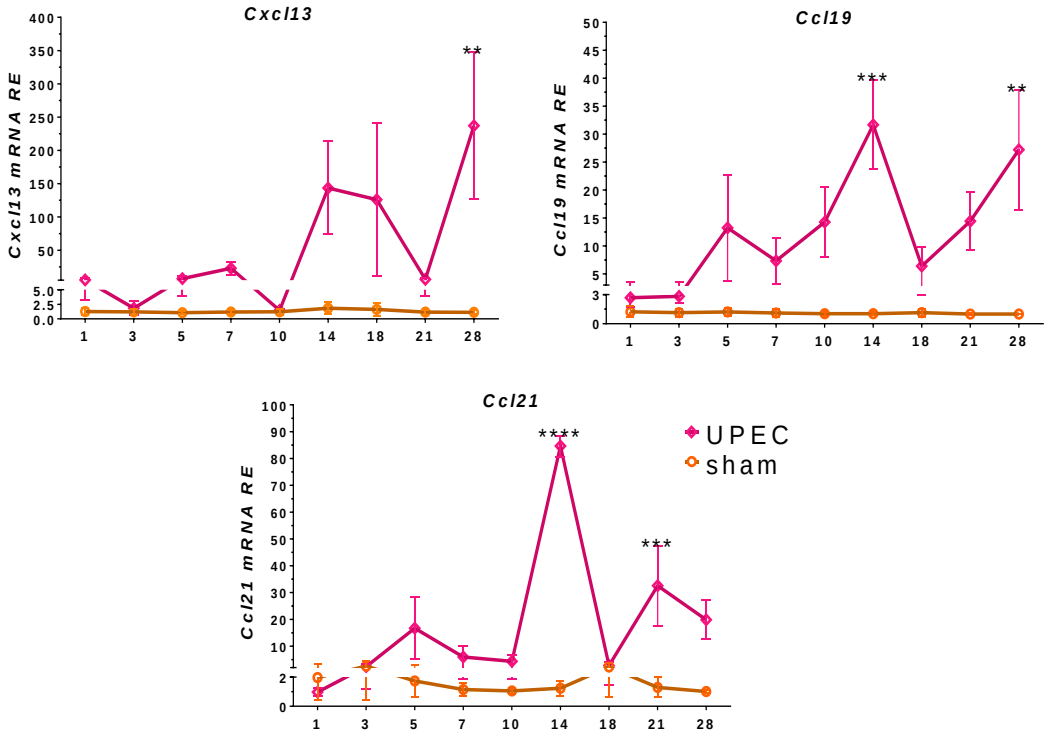

Figure 36. mRNA expression of TLO related genes was increased in UPEC-infected cauda epididymides. Relative expression (RE) of *Ccl19, Ccl21 and Cxcl13* mRNA was measured by qRT-PCR in sham and UPEC-infected cauda epididymides 1, 3, 5, 7, 10, 14, 18, 21 and 28 days post- UPEC infection and normalized to *Rplpo* (n = 3; mean ± SEM at each time-point). Statistical analysis used two-way ANOVA followed by Tukey's test (***P*<0.01, ****P*<0.001, *****P*<0.0001).

HEV formation and maturation-related genes, *Tnf, Lta, Ltβ, Tnfsf14,* displayed a peak of expression at 7 days post UPEC-infection and then declined by day 10

(Fig. 37). Another significant peak of *Ltβ* was observed at 28 days from the infection. These results suggest that, starting from 7 days post-UPEC infection, HEV begin to develop and mature, prior to the peak in TLO-related chemokines, presumably to facilitate movement of immune cells to the UPEC-infected cauda epididymidis.

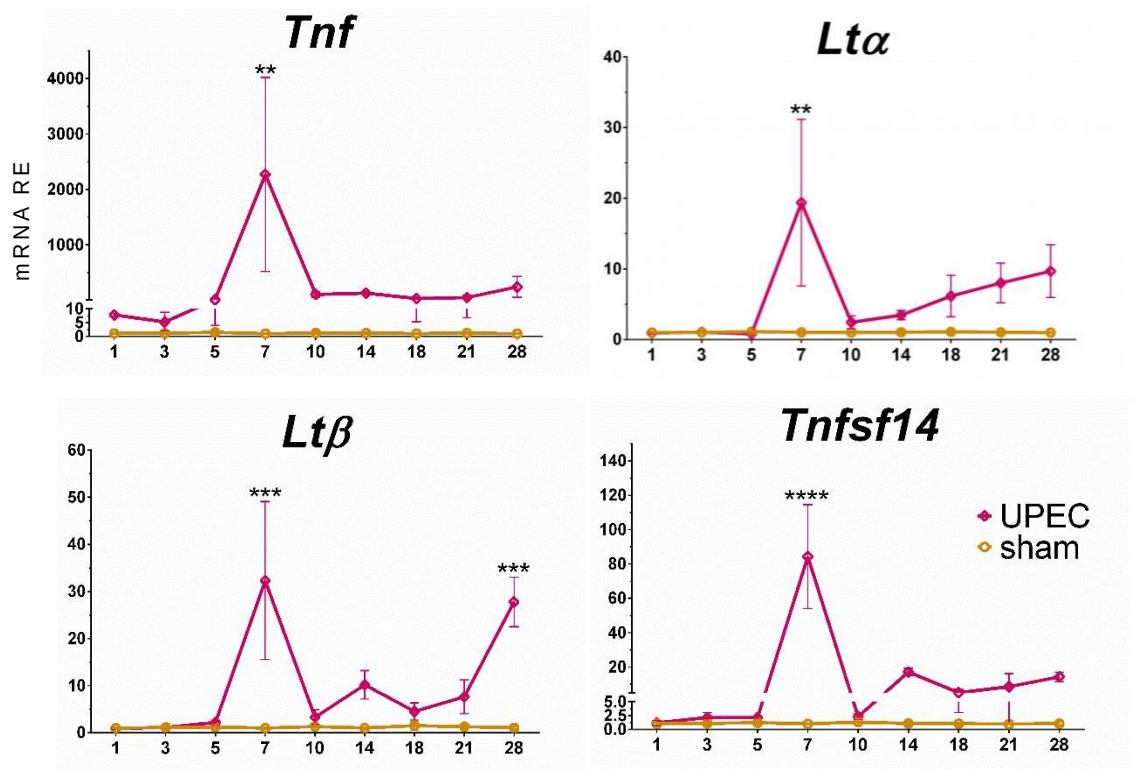

Figure 37. mRNA expression of HEV related genes was increased in UPEC-infected cauda epididymidis. Relative expression (RE) of *Tnf, Ltα, Ltβ* and *Tnfs14* mRNA was measured by qRT-PCR in sham and UPEC-infected cauda epididymides 1, 3, 5, 7, 10, 14, 18, 21 and 28 days post-UPEC infection and normalized to *Rplpo* (n = 3; mean ± SEM). Statistical test used two-way ANOVA followed by Tukey's test (***P*<0.01, ****P*<0.001, *****P*<0.0001).

3.14. UPEC-infected cauda epididymides showed the presence of abscesses as well as aggregates resembling lymphoid structures

Examining the histology of the cauda epididymidis revealed that immune cell infiltrates were seen peripherally by 5 days post-UPEC infection **(Fig. 38B)**. Fibrosis could be seen 5 days post-infection. Massive immune cell infiltrates (abscesses) were detected in the cauda starting from day 7 post-infection **(Fig. 38C)**. This was consistent with the mRNA expression data that all investigated

HEV related genes were significantly increased by 7 days post-UPEC infection, **(Fig. 37).** At 14 days post-UPEC infection, the number of cellular aggregates increased **(Fig. 38D).** At 28 days post-UPEC infection, infiltrates were still visible, but were smaller in size **(Fig. 38E)**.

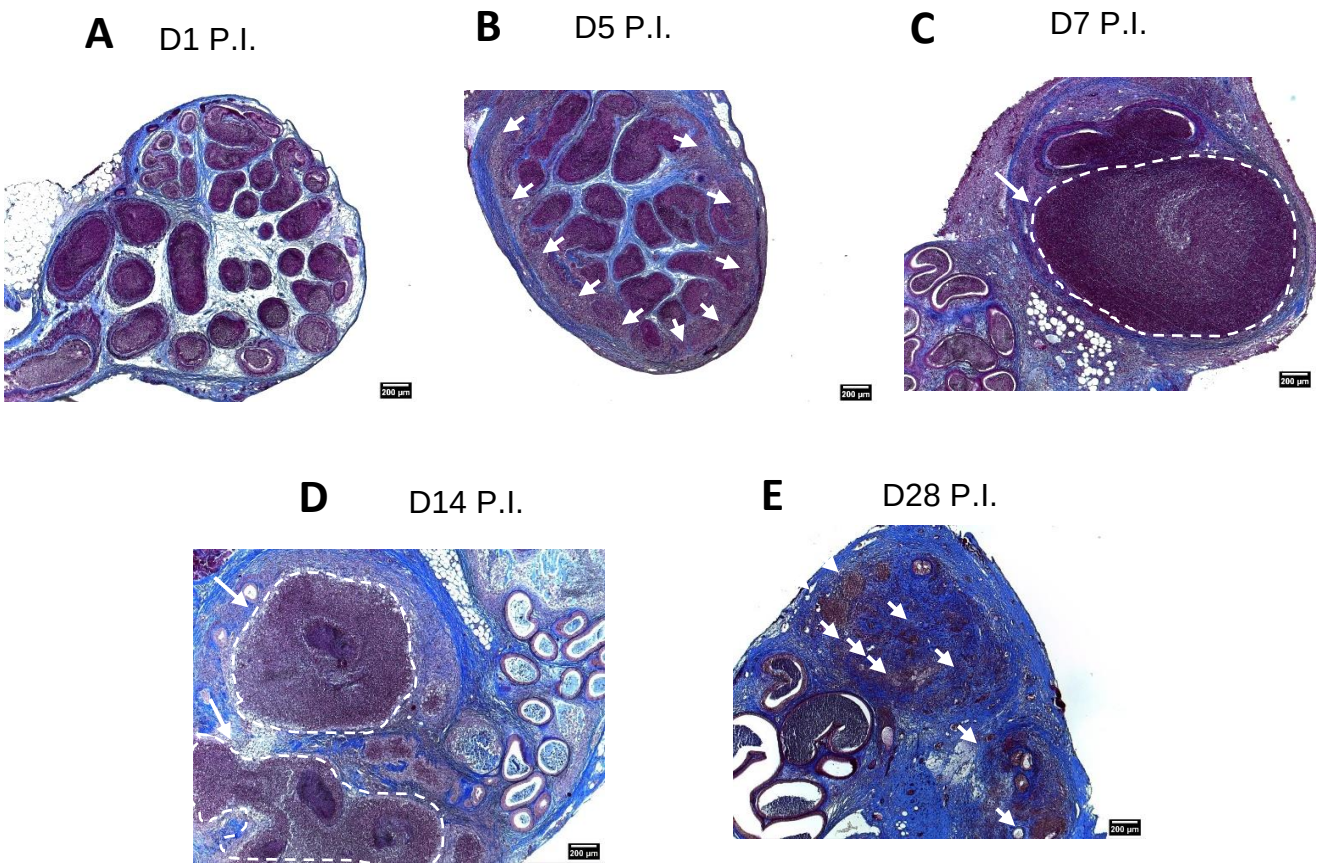

Figure 38. UPEC infection leads to the formation of abscesses and lymphoid aggregates resembling lymphoid structures in cauda epididymides. Representative photomicrographs of Azan staining in paraffin sections from cauda epididymides 1 day **(A)**, 5 **(B),** 7 **(C)**, 14 **(D)** and 28 days **(E)** post-UPEC infection (P.I.). Arrows point to the location of immune cell infiltrates.

3.15. At 5 days post-UPEC infection, the cauda epididymidis did not show the presence of TLO-related parameters

Based on the mRNA results and histological examination, three time points (5, 14 and 28 days post-UPEC infection) were examined for the presence of TLO-related parameters. Although the presence of first immune cell infiltrates at the periphery of the cauda was observed by 5 days post-UPEC infection, no HEV

were observed **(Fig. 39A).** Small B cell clusters were surrounded by macrophages, but no T cell clusters were visible **(Fig. 39B and C)**.

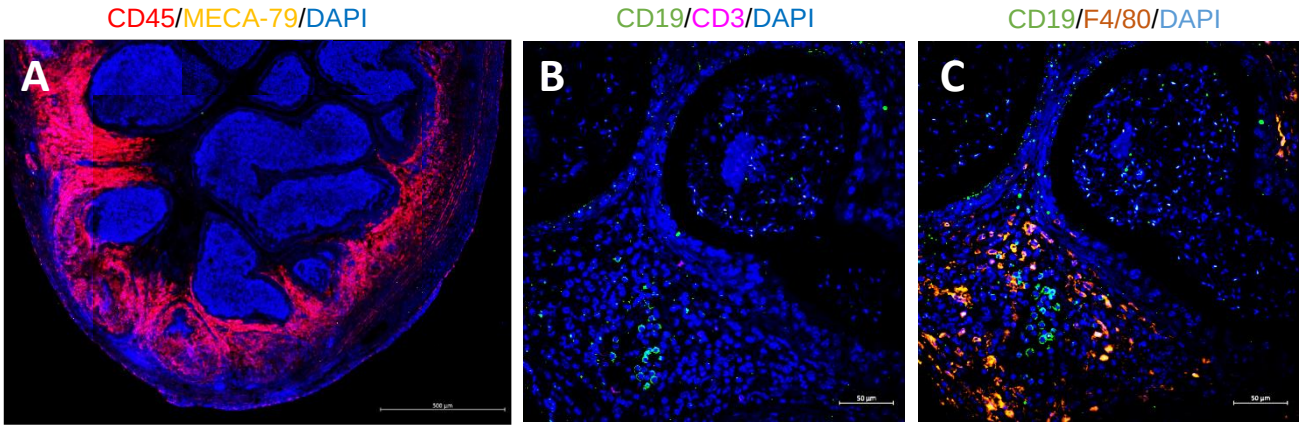

Figure 39. At 5 days post-UPEC infection the cauda epididymidis did not reveal the presence of TLO-related elements. Representative photomicrographs of immune cells (CD45, red), HEV (MECA-79, yellow) and DAPI (blue) **(A)**, B cells (CD19, green), T cells (CD3, pink) and DAPI (blue) **(B)**, B cells (CD19, green), macrophages (F4/80, orange) and DAPI (blue) **(C)** fluorescence staining in paraffin sections from cauda epididymidis 5 days post-UPEC infection.

3.16. At 14 days post-UPEC infection, the cauda epididymidis showed the presence of infiltrates, HEV and early stages of TLO formation

Based on the mRNA expression of TLO-related chemokines, the cauda epididymides were examined at 14 days post-UPEC infection for the presence of TLO-related elements. Immunostaining revealed that B and T cells were present in close proximity to the cellular aggregates **(Fig. 40A)**. The majority of the B and T cells present at this stage were mostly intermingled **(Fig. 40Ai),** with only a few separated small clusters **(Fig. 40Aii)**. The B cells were not proliferating, based on PCNA staining **(Fig. 40C)** and were surrounded by macrophages **(Fig. 40D)**. Staining for MECA-79 identified many HEV surrounding the cellular aggregates **(Fig. 40B)** that contained immune cells within their lumen **(Fig. 40Bi, Bii)**. It was clearly visible, using staining of consecutive section staining, that most of the $CD45^+$ stained immune cells were not B or T cells and that the abscesses did not contain any B or T cells at 14 days post-infection **(Fig. 39A, B).** The immunofluorescence staining combined with the mRNA results indicate that HEV

could be implicated in the formation of cellular aggregates and early stages of TLO present in the cauda at day 14 post-infection.

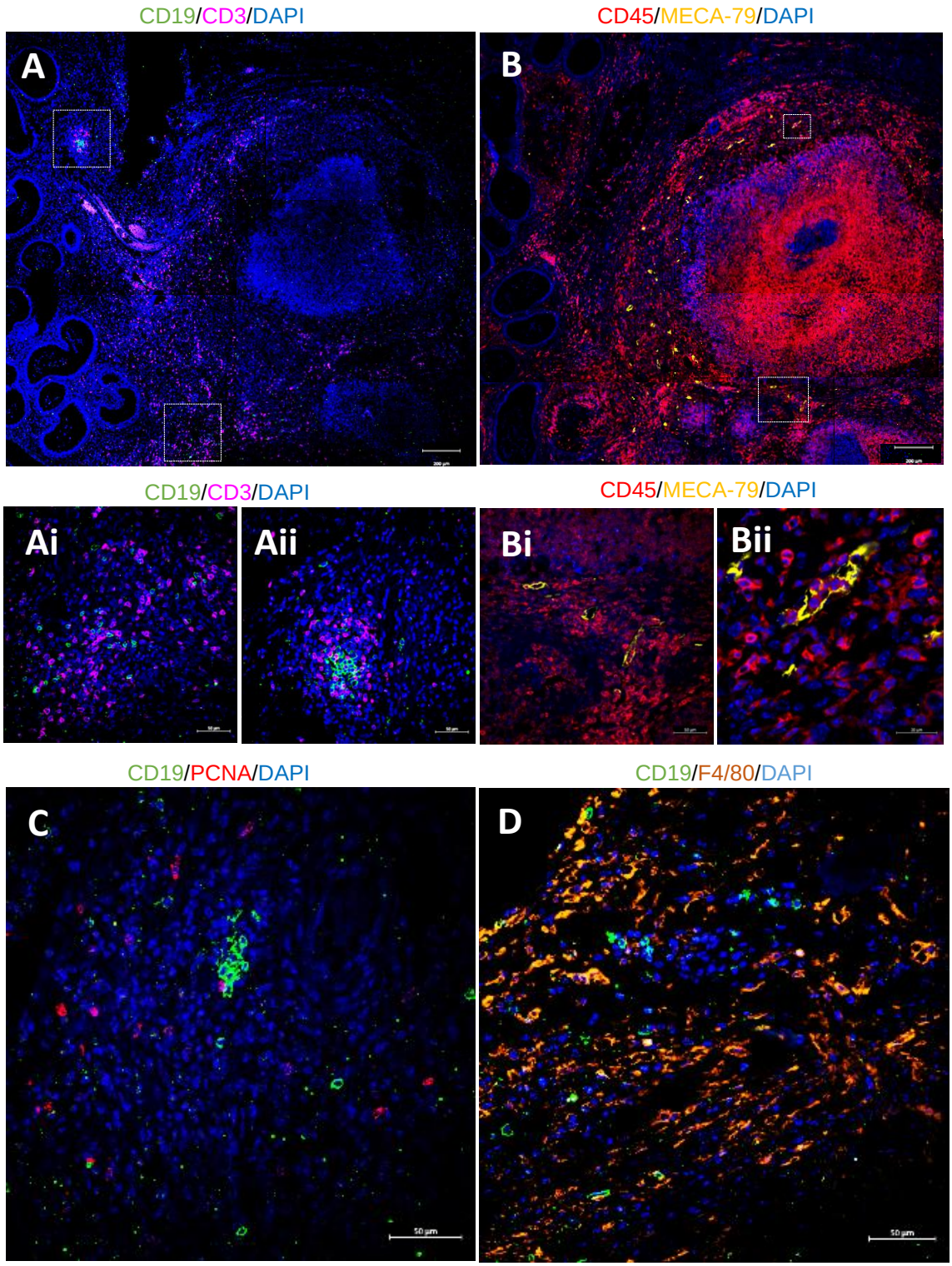

Figure 40. At 14 days post-UPEC infection, the cauda epididymidis revealed the presence of cellular aggregates, HEV and early TLO formation. Representative photomicrographs of B cells (CD19, green), T cells (CD3, pink) and DAPI (blue) **(A, Ai, Aii)**, immune cells (CD45, red), HEV (MECA-79, yellow) and DAPI (blue) **(B, Bi, Bii)**, B cells (CD19, green), proliferating cells (PCNA, red) and DAPI (blue) **(C)** B cells (CD19, green), macrophages (F4/80, orange) and DAPI (blue) **(D)** fluorescence staining in paraffin sections from cauda epididymidis 14 days post- UPEC infection. Images Ai, Aii, Bi and Bii show the magnified areas identified by the white boxes in part A and B, respectively.

3.17. At 28 days post-UPEC infection, the cauda epididymidis showed signs of advanced TLO

At 28 days post-UPEC infection, the cauda epididymides revealed the presence of more organized B and T cell clusters **(Fig. 41B)**. In comparison to 14 days post-UPEC infection, large cellular aggregates were absent, as confirmed by staining for immune cells, B cells and T cells in consecutive tissue sections. Almost all immune cell clusters detected 28 days post-UPEC infection were organized clusters of B and T cells **(Fig 41A, B)**. Importantly, HEV were localized within the T cell zones **(Fig. 41C, D)** and contained CXCL13 within their lumen **(Fig. 41E).** The B cells were proliferating, suggesting the presence of active germinal centers **(Fig. 41F).** In order to check whether the proliferating B cells were involved in germinal center reaction activities, the presence of isotype-switched B and plasma cells was analyzed. IgA isotype-switched B cells (IgA^+) and plasma cells ($CD138^+IgA^+$) were detected in the UPEC-infected cauda epididymides at day 21 post-UPEC infection **(Fig. 41G)**. Moreover, the immune cell clusters contained podoplanin, the marker for stromal lymphoid cells **(Fig. 41H)**. The B cell clusters were surrounded by F4/80+ macrophages **(Fig. 41I)**. Immune cell infiltrates composed of B and T cells could only be seen in the cauda epididymides post-UPEC infection and not in the caput or corpus of the epididymis **(Figure 42)**. These results demonstrate that the immune cell clusters are in fact organized lymphoid structures, which displayed advanced characteristics of a TLO.

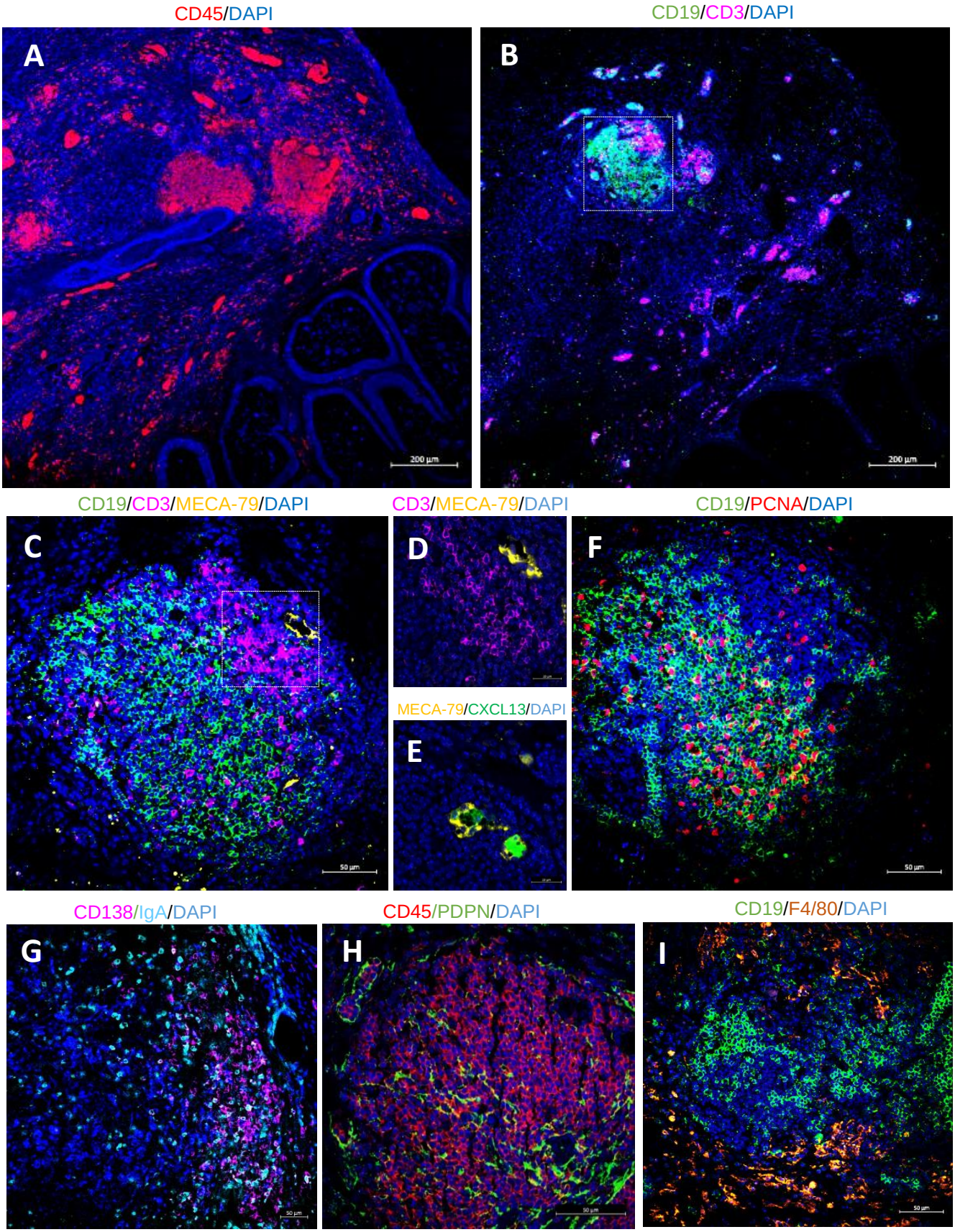
CD45/DAPI
CD19/CD3/DAPI
A
B
200 µm
200 µm
CD19/CD3/MECA-79/DAPI
CD3/MECA-79/DAPI
CD19/PCNA/DAPI
C
D
F
MECA-79/CXCL13/DAPI
E
50 µm
50 µm
CD138/IgA/DAPI
CD45/PDPN/DAPI
CD19/F4/80/DAPI
G
H
I
50 µm
50 µm
50 µm

Figure 41. At 28 days post-UPEC infection, the cauda epididymides contained organized TLO. Representative photomicrographs of immune cells (CD45, red) and DAPI (blue) **(A),** B cells (CD19, green), T cells (CD3, pink), HEV (MECA-79, yellow) and DAPI (blue**) (A, C, D)**, HEV (MECA-79, yellow), CXCL13 (green) and DAPI (blue) **(E)**, B cells (CD19, green), proliferating cells (PCNA, red) and DAPI (blue) **(F),** plasma cells (CD138,pink), IgA (turquoise) and DAPI (blue) **(G),** podoplanin (PDPN, green), immune cells (CD45, red) and DAPI (blue) **(H),** B cells (CD19, green), macrophages (F4/80, orange) and DAPI (blue) **(I)** fluorescence staining in paraffin sections from cauda epididymidis 28 days post-UPEC infection. **(H)** is a section from 21 days post-UPEC infection. All the remaining sections are from 28 days post-UPEC infection. Panel C shows the magnified area identified by the white box in part B. Panel D show the magnified area identified by the white box in panel C.

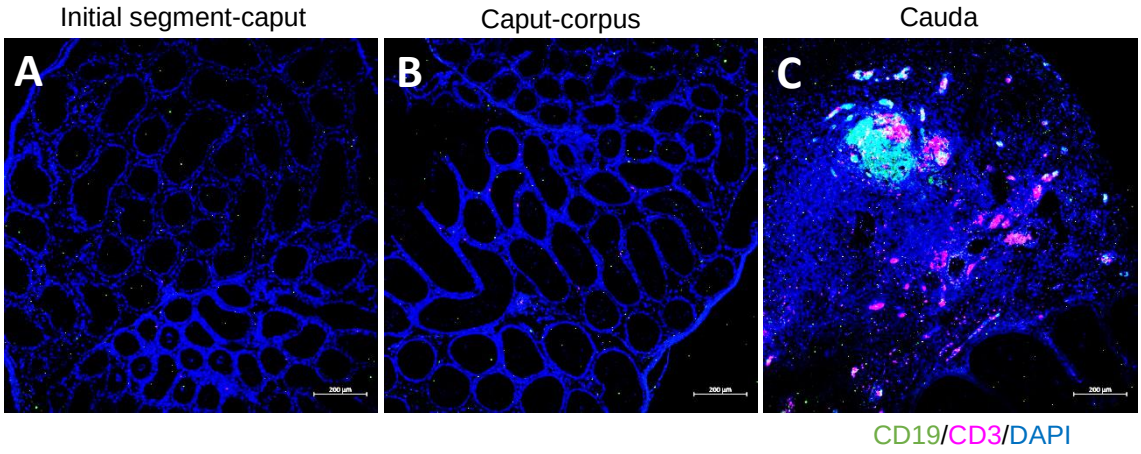

Figure 42. At 28 days post-UPEC infection, only the cauda epididymidis contained B and T cell clusters. Representative photomicrographs of B cells (CD19, green), T cells (CD3, pink) and DAPI (blue) in paraffin sections from initial segment-caput **(A)**, caput and corpus **(B)** and cauda **(C)** epididymidis 28 days post-UPEC infection.

3.18. B cells and plasma cells were increased in the UPEC-infected cauda epididymidis

Using flow cytometry, the percentage of immune cells, B cells and plasma cells at different time points post-UPEC infection was determined. The cauda epididymides exhibited a significant increase in immune cell numbers at day 10, 14 and 28 post-UPEC infection compared to sham control mice **(Fig. 43).** At 14 days post-infection, the cauda showed the highest increase in the immune cell percentage, consistent with the histopathological findings and the immunofluorescence staining, showing the presence of cellular aggregates **(Fig. 40B).** At all investigated time-points, an increase in B cell numbers was documented, showing statistical significance at day 10 and 28 post- UPEC

infection **(Fig. 43).** Furthermore, a significant increase in plasma cells ($CD138^{+}CD45R^{-}$) was detected at 28 days post-infection **(Fig. 43).**

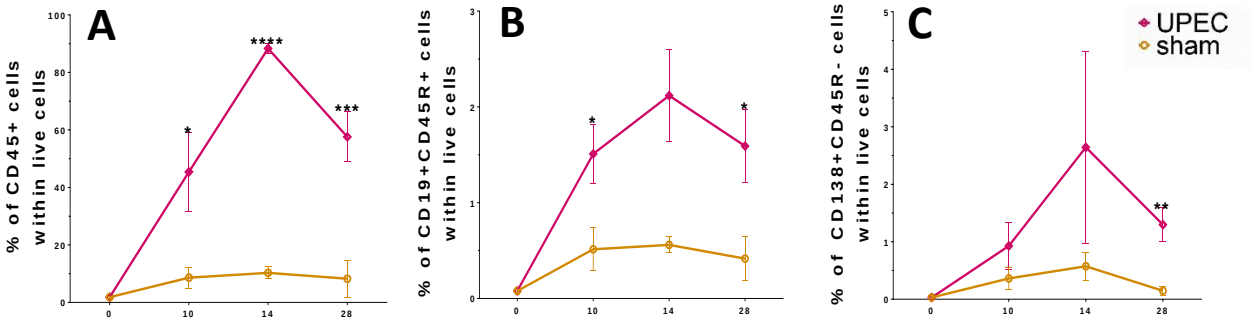

Figure 43. Immune cells, B cells and plasma cells were increased in UPEC-infected cauda epididymides. Percentages of immune ($CD45^{+}$) **(A)**, B ($CD19^{+}CD45R^{+}$) **(B)** and plasma ($CD138^{+}CD45R^{-}$) **(C)** cells were determined in sham and UPEC-infected cauda epididymides using flow cytometry after gating out doublets and nonviable cells. (n = 4 - 7; mean ± SEM). Statistical analyses used multiple unpaired *t*-test (**P*<0.05, ***P*<0.01, ****P*<0.001, *****P*<0.0001).

4. Discussion:

These studies indicate that key chemokines and their receptors, essential for T cell and macrophage trafficking were upregulated in EAEO testis, while in the absence of CCR2, these changes were attenuated. Consistently, an increase in macrophages expressing CCR2 in human testicular biopsies with impaired spermatogenesis and focal leukocytic infiltrates was demonstrated. Moreover, activin A was established as an essential regulator of expression of chemokines and their receptors in BMDM. Macrophages were identified as major cell population in inflamed testis expressing activin A, implicating macrophages and activin A both as potential therapeutical targets. Considering that chemokine ligands and receptors especially CCR2 have been proven to play a pathological role in exacerbating inflammation in many disease models (Baran et al., 2007; Guazzone et al., 2009; Stankovic et al., 2009; Dhaiban, 2020) as well as in testicular inflammation, in addition to the ability that activin A can increase the expression of CCR1, CCR2 and CCR5 – chemokines involved in macrophages recruitment- then targeting activin A could prove beneficial.

In addition, it was investigated if the alteration of chemokine networks in epididymo-orchitis can drive the formation of organized immune cell infiltrates, called tertiary lymphoid organs (TLO). Interestingly, the elements of TLO were not found in the inflamed testis, but they were detected in the inflamed epididymis, specifically the cauda. The cauda from mice with EAEO, and especially ones infected with UPEC, showed the presence of multiple elements and immune cells associated with TLO formation. Future studies investigating the impact of TLO development in the epididymis on male fertility are needed.

4.1. Chemokines associated with macrophage and T cell recruitment were altered in EAEO testies and in human testicular biopsies with leukocyte infiltration and CCR2 deficiency decreased such alterations.

EAEO serves as a model of chronic testicular inflammation, which is characterized by several key symptoms, also reported in men, including immune

cell infiltration, elevation of pro-inflammatory mediators (e.g. TNF, activin A), impairment of spermatogenesis, destruction of seminiferous tubules as well as steroidogenic disturbances and fibrotic remodeling (Fijak et al., 2018; Jacobo et al., 2015; Kauerhof et al., 2019; Nicolas et al., 2017a; Nicolas et al., 2017b; Peng et al., 2022; Schuppe et al., 2017; Schuppe & Bergmann, 2013). Macrophages, which are the most prominent immune cell population in the testis, are involved during EAEO in the secretion of pro-inflammatory cytokines, the most important of which are TNF and IL-6, as well as the chemokine CCL2 (Guazzone et al., 2003; Rival et al., 2006; Suescun et al., 2003). Previous reports demonstrated that testicular expression of the chemokines CCL2, CCL3, CCL4 and CXCL12 and the chemokine receptors CCR2, CCR5, CCR7 and CXCR4 was increased during EAEO (Guazzone et al., 2003, 2009, 2012; Rival et al., 2007; Peng et al., 2022;). Therefore, it was of interest to perform a more comprehensive examination of the chemokine networks and define the potential target cells and molecules affecting their expression during testicular inflammation. The results established that *Ccr1*, *Ccr2, Ccr3, Ccr5, Cxcr3* and *Cx3cr1* as well as most of their respective ligands (*Ccl6, Ccl7, Ccl8, Ccl9, Ccl12, Ccl22, Cxcl4, Cxcl9, Cxcl13, Cx3cl1*) were all significantly increased in EAEO testis in comparison to controls. Interestingly, testis from EAEO mice deficient for *Ccr2,* with reduced macrophage infiltration, exhibited significantly lower mRNA expression of the above mentioned chemokine receptors as well as some of their ligands (*Ccl8, Ccl12, Cxcl4, Cxcl13, Cx3cl1*). In line with this indication, *Ccr2*$^{-/-}$ EAEO mice demonstrated reduced testicular damage and were protected from fibrotic remodeling due to reduced number of immune cells expressing extracellular matrix proteins (Peng et al., 2022). This was also in accordance with reports demonstrating reduced inflammation in *Ccr2*-deficient mice (Boniakowski et al., 2018; Flegar et al., 2021; Tokuyama et al., 2005). Besides the very well investigated CCL2/CCR2 axis, other chemokines also are known to be implicated in the pathogenesis of several inflammatory and autoimmune diseases, including multiple sclerosis and rheumatoid arthritis (Flegar et al., 2021; Hao et al., 2020; Moore et al., 2001). White matter lesions from patients with multiple sclerosis, as well as from experimental models of this disease, exhibit high levels of CCL2, CCL3, CCL4, CCL5, CCL7, CCL8 and CXCL9 (Dhaiban, 2020). Moreover, CXCR3 is implicated in the recruitment of T cells to inflamed skin as well in the

progression of multiple sclerosis (Flier et al., 2001; Heng et al., 2022; Mahad et al., 2002; Sindern et al., 2002). During the course of experimental inflammatory arthritis, CCR1 and CXCR2 were involved in neutrophil recruitment into the joint (Chou et al., 2010). In a mouse model of multiple sclerosis demyelination, infiltration of immune cells and secretion of pro-inflammatory mediators were suppressed by deletion of the *Ccr5* gene (Gu et al., 2016). Moreover, CCL2, CX3CR1 and CCR5 have been reported to play roles in bone marrow monocytosis and their inhibition altered the incidence of atherosclerosis in mice (Combadière et al., 2008). CXCL13, a B cell chemoattractant, is regarded as a biomarker of multiple sclerosis severity and was shown to be involved in disease progression and in Th17-induced experimental autoimmune encephalomyelitis (Alvarez et al., 2013; Dhaiban, 2020; Khademi et al., 2011).

Most of the above-mentioned chemokines are considered as key regulators of macrophage trafficking to sites of inflammation and hence their depletion or inhibition could protect the testis from macrophage-induced damage. Testicular resident macrophages, a major cohort of testicular immune cells, display immunosuppressive characteristics and are regarded as sentinels in maintaining immune privilege (Fijak and Meinhardt, 2006; Han et al., 2016; Bhushan and Meinhardt, 2017; Meinhardt et al., 2022). Based on studies in rodent models, testicular resident macrophages are principally divided into (i) peritubular, surrounding the seminiferous tubules adjacent to the spermatogonial stem cell niche, and (ii) interstitial, which are in general in close contact with Leydig cells (DeFalco et al., 2015; Meinhardt et al., 2022). On the other hand, macrophages derived from peripheral circulating monocytes and frequently recruited to the sites of injury exhibit functional plasticity. They are capable of releasing proteolytic enzymes and can recruit other immune cells, such as B and T cells, to induce an immune response cascade and further tissue damage or recovery (Saradna et al., 2018).

In studies described in this thesis, it was revealed that $CD68^{+}$ macrophages express CCR2 in human testis with impaired spermatogenesis, but not in testis with intact spermatogenesis. In accordance with the analysis in EAEO testis, there was also a significant mRNA increase in *CCR1, CCR5, CCR2* and its ligand *CCL2* as well as *CXCL13* in biopsies of patients with impaired spermatogenesis

associated with focal leukocytic infiltration. The human testicular sections examined displayed different degrees of spermatogenesis impairment and immune cell infiltration. Both, peritubular and interstitial CCR2^{+} macrophages were seen in areas showing discrete inflammatory signs and tubular damage. In addition, almost all macrophages observed to be phagocytosing spermatozoa (‘spermiophages’) in the lumen of damaged seminiferous tubules were positive for CCR2, indicating their migratory properties. Regions with dense peritubular lymphocytic infiltrates, involving the lamina propria as well as adjacent blood vessels, contained a large proportion of macrophages positive for CCR2. In sections with extensive spermatogenic damage accompanied by prominent fibrosis, macrophages were present, but were negative for CCR2. Other chemokines, such as *CCL5* and *CXCL13,* as well as pro-inflammatory cytokines (IL-17A), were found to be increased in human biopsies with disturbed spermatogenesis and concomitant focal inflammatory infiltrates (Klein et al., 2016). The recruitment of CCR2^{+} macrophages to sites of inflammation mediates collateral tissue damage and this has been shown in multiple organs such as the gut, brain and liver in murine models (Abid et al., 2019; Francis et al., 2017; Kuroda et al., 2019; Miura et al., 2012; Moore et al., 2001). The recruitment of CCR2^{+} macrophages to the inflamed testis could also implicate these macrophages in the active destruction of germ cells as is seen in other disease models.

4.2. Activin A modulated chemokine expression *in-vitro* and was expressed by macrophages in cases of testicular inflammation.

In several earlier studies, activin A was found to be a key modulator of inflammation, immunity and fibrosis by regulating expression of chemokines (Hedger, 2011; Locci et al., 2016; Phillips, 2003; Salogni et al., 2009). A recent study from our laboratory identified activin A as an inducer of CCR2 and CXCR4 in macrophages and a critical regulator of testicular fibrosis (Peng et al., 2022). It became of interest to focus on the potential influence of activin A on other members of the chemokine network. It was revealed that, in BMDM, activin A increased the expression of *Ccr2* and *Ccr5,* chemokine receptors significantly

upregulated in inflamed mouse and human testis. Furthermore, blocking of activin A action in M1 polarized macrophages significantly reduced CCR2 expression in mice (Sierra-Filardi et al., 2011b). Altogether, the data indicate that activin A affects the recruitment of immune cells to the testis especially macrophages by modulating expression of chemokine receptors. Notably, in previous studies, activin βA subunit expression was increased in mouse and human testis with signs of inflammation, defined as leukocytic infiltration accompanying impaired spermatogenesis, and correlated with the severity of the disease (Kauerhof et al., 2019; Nicolas et al., 2017b; Peng et al., 2022). Antagonizing activin A action by exogenous FST showed positive therapeutical effects in rheumatoid arthritis, inflammatory bowel disease and allergy (de Kretser et al., 2012; Dohi et al., 2005; Hardy et al., 2006; Hedger & de Kretser, 2013; Yamada et al., 2014). These findings further corroborate the importance of activin A in the development and progression of testicular inflammation and the potential beneficial role of FST in suppressing its activity.

While stimulating the expression of the previously mentioned chemokine receptors, activin A downregulated the expression of their ligands (*Ccl2, Ccl3, Ccl4, Ccl6, Ccl7, Ccl8, Ccl12* and *Ccl22)* in BMDM*.* These opposite regulatory effects of activin A on the expression of chemokine receptors and their ligands demonstrate its dual role in inflammation, where it can increase the expression of the receptors to enhance the responsiveness of the cells to the ligands, while downregulating the ligands themselves (Peng et al., 2022; Sierra-Filardi et al., 2011b). Activin A triggers indirect effects on T cells as well. Culturing T cells with activin A-treated BMDM decreased TNF induction by the T cells. Conditioned media obtained from the co-culture of T cells with activin A-treated BMDM demonstrated a decrease in key pro-inflammatory chemokines, such as CCL2, 6, 8 and 12. Earlier studies demonstrated that macrophages can suppress T cells and even decrease their TNF production (Hilhorst et al., 2014; Huber et al., 2010). This was also revealed in the present study, where the basal levels of both measured cytokines were shown to be much lower in the co-culture of T cells with BMDM as compared to T cells alone. Addition of activin A-treated BMDM to the co-culture further attenuated the pro-inflammatory cytokine induction of T cells. It is worth mentioning that changes in the TNF or IFN-γ induction were not observed

during culture of T cells with activin A alone. Although previous reports have shown that activin A itself can reprogram the phenotype of T cells, it should be noted that the effects reported by activin A, as it is the case for many other immune cell modulators, are highly context- and time-dependent (Hedger & de Kretser, 2013). For example, activin A can suppress antigen-specific Th2 responses, which protect against allergic airway disease as well as inhibit Th17 cells in neuroinflammation (Morianos et al., 2020; Semitekolou et al., 2009).

Macrophages are identified as a source of cells expressing activin A. Given the potent effect of activin A on the expression of chemokines, this implicates macrophages in the development and progression of autoimmune orchitis by their ability to secrete activin A and subsequently attract more immune cells to the damaged testis. Macrophages expressing activin A have been shown to play a role in the progression of other autoimmune-based diseases (Kadiombo et al., 2017; Ota et al., 2003; Palacios et al., 2015).

This study raises the possibility that testicular macrophages are an important source of chemokines and chemokine receptors involved in the trafficking of immune cells to sites of injury and are implicated in the pathology of murine autoimmune orchitis as well as in human testicular inflammation. Macrophages can also express activin A, which can regulate chemokine expression and hence modulate the immune cell trafficking in testicular inflammation. This highlights macrophages expressing activin A and/or CCR2 as an attractive target for ameliorating testicular inflammation.

4.3. Tertiary lymphoid organs (TLO) and high endothelial venules (HEV) developed in the epididymis in response to local inflammatory stimuli.

Unresolved inflammation in response to pathological stimuli can disrupt the homeostasis established in a tissue. Under some circumstances, this process can allow the infiltrating immune cells along with local cells to organize into structures that resemble lymphoid tissues. These well-organized ectopic immune cell aggregates are termed TLO and can develop postnatally in non-lymphoid organs, usually driven by inflammation, which could be the consequence of

cancer, infection, autoimmunity, aging or allograft transplantation. TLO not only exhibit a similar composition to SLO, but also share their functionality. The structure and complexity of a TLO varies depending on the strength of the inflammatory stimuli as well as the type of tissues in which they develop (Neyt et al., 2012; Sato et al., 2023; Schumacher & Thommen, 2022). In comparison to lymph nodes, TLO exhibit higher plasticity and changeability. TLO could be simple in structure, where they are composed of intermingling B and T cell zones. These aggregates could also coalesce into clear separate zones of B and T cells as a result of CXCL13, CCL19 and CCL21 gradients. They could encompass a germinal center capable of producing high affinity antibodies by memory B cells and plasma cells, contain mature HEVs that accumulate chemokines in their lumen and would be supported by reticular conduits (Neyt et al., 2012; Ruddle, 2020; Sato et al., 2023; Schumacher & Thommen, 2022). In this study, the elements specific for TLO formation were detected in the inflamed cauda epididymidis, but not in the testis. This is the first study reporting TLO formation in the epididymis, which was driven by inflammatory signals from autoimmune reactions and infection, where the latter was able to lead to the development of more organized TLO.

In this study, neither HEV nor fully formed TLO were detected in EAEO testis by 50 days after the first immunization. However, elevated levels of *Cxcl13* and focal B cell clusters were found in EAEO testis. The absence of TLO in the inflamed testis could stem from the immune privileged status of testis, where an immunosuppressive environment predominates (Fijak & Meinhardt, 2006; Hedger & Meinhardt, 2003). However, the appearance of HEV expressing ICAM-1 has been reported before in the testis and they have been implicated in the recruitment of cytotoxic T lymphocytes in testicular seminoma (Sakai et al., 2014). In addition, the presence of follicular-like structures composed of separate zones of B cells and T cells and containing dendritic cells have been detected in testicular germ cell tumours (Fietz et al., 2022; Klein et al., 2016). Although inflammation is regarded as a hallmark precursor for TLO formation, it can be speculated that a threshold of inflammation needs to be exceeded to allow TLO to properly organize. Furthermore, some tissues are more susceptible to TLO formation, and the complexity of the TLO that form depends on the local

microenvironment as well as the strength of the inflammatory stimuli (Chen et al., 2002; Sato et al., 2023). Given these facts, it can be speculated that a stronger inflammatory stimulus might be needed for TLO to develop in the testis compared to the epididymis. Another possibility could be that TLO could have developed at earlier timepoints from the immunization, but have resolved by 50 days from the immunization.

In this study, two different models of inflammatory disease (sterile autoimmune and acute infection) were investigated for their capacity to induce TLO formation in the epididymis. Both models demonstrate inflammation as a central trigger of damage. Previous studies have shown that the cauda epididymidis is more susceptible to infection/inflammation-derived tissue damage compared to the proximal regions (Klein et al., 2020; Pleuger et al., 2022; Wijayarathna et al., 2020). Accordingly, in both models investigated in this study (EAEO and UPEC infection), elements and cells related to TLO formation were present in the cauda epididymidis only and not in other parts of the epididymis. The absence of TLO in the more proximal caput and corpus, could stem from the microenvironmental differences observed in the different regions of the epididymis. The cauda epididymidis is better equipped to mount an intense immune response compared to the proximal epididymis, which exhibits a more tolerogenic environment as is present in the testis. Unlike the cauda, the caput is enriched with immunomodulatory factors (Pleuger et al., 2022). While the proximal regions are heavily populated with resident macrophages, the distal parts especially the cauda is relatively rich with cells with innate-like characteristics (γδ T cells, dendritic cells and natural killer cells) as well as different subclasses of dendritic cells that could influence the initial induction, maturation and maintenance of TLO (Pleuger et al., 2022; Ruddle, 2020). Furthermore, the macrophages present in the cauda are more pro-inflammatory in function or display dendritic cell phenotypes that exhibit higher expression of phagosome-, antigen processing- and antigen presenting-related genes compared to other epididymal regions (Battistone et al., 2020; Mendelsohn et al., 2020). Compared to the proximal regions, the cauda contains less molecules with tolerogenic and immunosuppressive properties (Battistone et al., 2020; Jrad-Lamine et al., 2013). These differences that exist between the proximal and distal regions of the

epididymis could be explained by the fact that the distal parts are needed to combat ascending infections through a robust inflammatory response and possibly to limit the spread of the infection to other parts (Wijayarathna et al., 2020). To add, 10 days post-UPEC infection, increases in pro-inflammatory cytokines (e.g. Il-1α, Il-6, Il-17) and chemokines (e.g. Ccl2, Ccl3, Cxcl13) can only be seen in the cauda and not the caput. Moreover, it was observed that UPEC tends to persist in the cauda longer and in greater numbers compared to other parts of the epididymis. Considering the cauda harbors the immunogenic spermatozoa, a damage to the epithelial barrier could provide the needed fuel for the adaptive immune response (Pleuger et al., 2022). When combining all these factors together, this might explain why the cauda develops TLO as a consequence of inflammation, while other parts of the epididymis do not.

EAEO cauda epididymides showed the presence of clusters of B cells next to T cells along with HEV. The observed clusters were not clearly defined and were mostly intermingled. Although only very few of these B cells were proliferating, the increase in the TLO-related chemokines, especially *Cxcl13,* was apparently sufficient to allow the B cells to cluster in a specific location. The HEV that developed were not associated with huge immune cell aggregates, which were observed in the UPEC-infected cauda epididymidis. The TLO present in the EAEO cauda exhibited properties of a simple early stage TLO rather than a random immune cell infiltration. Distinguishing early TLO forms from lymphocyte infiltration is possible by determining the B cell: T cell ratio, which is higher in TLO. T cell infiltration is usually observed in multiple inflamed organs, but infiltrating B cells are almost exclusively associated with TLO in the tumor microenvironment (Sato et al., 2005). In addition, in early forms of TLO, very few immune cells were seen proliferating in contrast to a random immune cell infiltration in inflamed kidney models (Sato et al., 2020).

In comparison to the EAEO cauda, UPEC-infected cauda epididymides, displayed TLO that are complex and more closely resemble a lymph node in structure, especially at 28 days post- UPEC infection. The availability of tissues from multiple time points of the UPEC infection allowed for a detailed investigation of factors essential for TLO induction. In this model, an increase in the relative expression of TLO-related chemokines as well as TNF/lymphotoxin family

members preceded the gradual organization of TLO. TLO formation was not detected histologically at 5 days post- UPEC infection, while at day 14, a sharp increase in TLO-related chemokines was reported and very small clusters of B and T cell zones were observed, although the B cells were not proliferating. By 28 days post- infection, clear B and T cell zones as well as HEV were observed in the T cell region, containing CXCL13 within their lumen. Importantly, the B cells present were proliferating, which raises the possibility of a germinal center formation. The presence of a germinal center was indirectly investigated by examining the capacity of these TLO to activate the molecular machinery to sustain in situ differentiation of class-switched antibody-producing B cells. The presence of IgA isotype-switched B cells and plasma cells was detected in UPEC-infected epididymis. Furthermore, the present immune cells exhibited a reticular network, which could provide structural support and influence migration of immune cells and formation of antibodies (Astarita et al., 2012; Cinti & Denton, 2021). The separation into B and T cells zones was possible because of the high expression of genes essential for ectopic lymphoid organogenesis. TLO-related chemokines, *Ccl19, Ccl21* and *Cxcl13,* were upregulated at multiple time points following the infection. The expression levels of inflammatory cytokines like TNF, chemokines such as CCL19, CCL21 and CXCL13, as well as lymphotoxins LTβ and LTα, can influence TLO formation, its degree of complexity and further generation of germinal center (Bugatti et al., 2011; Krautler et al., 2012; Manzo et al., 2005; Thaunat et al., 2005; Weyand & Goronzy, 2003). This gradual increase in the complexity and structure demonstrates that TLO are highly plastic and interchangeable and their complexity and organization depends on the local microenvironment and the strength of the inflammatory stimuli (Sato et al., 2023). This plasticity and variability in TLO structure has also been reported in other studies. Kidneys from patients with mild pyelonephritis damage showed TLO with no distinct B and T cells zones, while in highly destroyed areas, TLO were clearly separated into B and T cells, a germinal center is active, and follicular dendritic cells were present (Sato et al., 2020). Furthermore, kidneys from aged mice display early stages of TLO, whereas kidneys from mice with polynephritis exhibited complex TLO composition (Sato et al., 2020). To add, aged mice develop spontaneous TLO in their bladders driven by age associated inflammation and these sites serve for B cell recruitment, activation, and

differentiation into plasma cells (Ligon et al., 2020) . Moreover, in a mouse model of spontaneous type 1 diabetes, the pancreas initially (8 weeks after induction of model) shows infiltrates that are not organized and lack HEV; however, after 20 weeks the infiltrates exhibit higher degree of organization, exhibit compartmentalization of B and T cells and show HEV. However, after the islet destruction, the TLO disappears in structure (Penaranda et al., 2010). These studies could also explain why varying complexities and morphology of TLO are detected in response to EAEO as opposed to UPEC infection. In the UPEC model examined, 28 days from the infection, advanced stages of TLO structures could still be seen in the cauda epididymidis. Based on the additional increase in the relative expression of TLO-related chemokines as well as some HEV-related mediators (28 days post-UPEC infection), one can speculate that further TLO may develop before they start to dissipate.

The presence of HEV in EAEO cauda epididymidis was associated with TLO elements. In UPEC-infected cauda, HEV were surrounding cellular aggregates that were detected starting from day 7 post-UPEC infection, before TLO have formed. The appearance of HEV has been reported in multiple sites under different inflammatory conditions, such as chronic *Helicobacter* gastritis, inflammatory bowel disease, pancreatitis, rheumatoid arthritis, multiple sclerosis as well as testicular seminoma (Blanchard & Girard, 2021; Kobayashi et al., 2004, 2009; Maruyama et al., 2013; Pablos et al., 2005; Sakai et al., 2014). Sometimes they are associated with unorganized immune cell infiltration, such as abscesses, but in general they are linked with TLO formation (Blanchard & Girard, 2021). It is speculated that the development of HEV is not organ- or disease-specific, but might be regarded as a consequence of chronic inflammation and they are involved in disease pathogenesis (Blanchard & Girard, 2021). In cases of chronic inflammatory diseases, experimentally inhibiting the formation or the functions of HEV is usually associated with amelioration of the disease (Rosen et al., 2005; Yang et al., 1993). HEV usually disappear once the inflammation subsides, for example when patients are in the remission phase of an autoimmune disease, after the administration of anti-TNF or anti-IL-17A treatment or when the causative pathogenic agent is eradicated (Cañete et al., 2009; Horjus Talabur Horje et al., 2017; Kaaij et al., 2020; Kobayashi et al., 2004, 2009; Suzawa et al.,

2007). HEV would revert to a normal phenotype after cessation of inflammation and can no longer sustain extensive lymphocyte recruitment (Blanchard & Girard, 2021).

This prolonged inflammation affecting the male reproductive tract can potentially in the long term affect male fertility. Inflammation can alter gene expression by inducing epigenetic changes. It is well established that sperms are subjected to epigenetic modifications such as DNA methylation, histone modifications, and chromatin remodeling to become fully mature (Lismer et al., 2023). However, the presence the inflammatory microenvironment can alter the epigenetic modifications that the sperms undergo potentially affecting fertility. Patients with low sperm counts have been shown to have altered DNA methylation where there was an increase in methylation of genes involved in spermatogenesis and a decrease in methylation of genes involved in inflammation and immune response (Schütte et al., 2013). To add, oxidative stress in infertile patients was shown to alter DNA methylation patterns (Tunc et al., 2009). The inflammatory microenvironment created by the presence of TLO in the epididymis could possibly impact fertility by altering the epigenetics of the residing sperms in the cauda.

Research focusing on TLO mechanisms and precise functions are currently growing. Yet, much still remains unknown. Therapeutic approaches are currently focusing on manipulation of TLO. However, to be able to determine which factors would allow for their fine-tuning, deeper molecular and phenotypic understanding of TLO is desired. Deciphering the signals that regulate different pathways pertaining to the migration and differentiation of immune cells and the formation and regulation of a germinal center is essential. Considering SLO and TLO perform similar functions, it remains to be determined, why the body mounts this redundant immune response. To add, the reason why some cancer patients develop TLO and others do not remains elusive (Neyt et al., 2012; Ruddle, 2020; Schumacher & Thommen, 2022). The occurrence of TLO in epididymis is for the first time reported here in this study. So far, it is elusive whether TLO formation is beneficial or deleterious for this male reproductive organ, which is responsible for sperm maturation and storage. It could be speculated that the damage observed in the cauda epididymides which could arise from the formation of TLO

might lead to future cases of infertility. Further investigations on fertility associated implications and consequences of TLO formation in the cauda epididymidis are needed.

4.4. Limitations of the study

It is worthwhile mentioning that utilizing BMDM as surrogates for testicular macrophages does not fully capture the in *vivo* situation in the testis or epididymis. Studying testicular macrophages *in-vitro* would require a substantial number of animals be sacrificed and in line with 3R principles this is not recommended. BMDM exhibit more plasticity in comparison to TM. Although they exhibit similar gene profiles at steady state the two cell types behave differently when stimulated. BMDM have the capacity to be classically and alternatively activated whereas TM favor alternative over classical activated phenotype.

Critically, it should be noted that the relative expression analysis in mouse and human testis was performed in total testicular RNA, not in single cells. Therefore, we cannot conclude that immune cells are the only source of these chemokines. Besides immune cells, also other testicular cells (Sertoli, Leydig, peritubular and germ cells) are considered as producers of a number of chemokines (Guazzone et al., 2009). Future studies are needed to better determine, which testicular cell subtypes also contribute as a source of the investigated chemokines.

The used *Ccr2* knockout out model was not a conditional knockout out model. Macrophages here in this study were speculated to play the major role in the destruction in the testis. Considering, cells other than macrophages (B, T cells and dendritic cells) could also express CCR2, it should be noted that a conditional deletion of CCR2 in macrophages would be needed to strengthen the findings from this study.

This study was the first one to discuss the formation of TLO in the male reproductive tract; hence, comparisons with previous findings was not possible. In depth analysis of TLO formation, induction and maintenance in the male reproductive tract was not investigated yet. The factors responsible for the formation of TLO formation specifically in the cauda epididymidis were not

delineated. A thorough investigation of genes involved in lymphoid organ formation, high endothelial venule maturation and B cells proliferation and activation in the cauda epididymidis post-UPEC infection is well needed. The occurrence of TLO in clinical samples was not checked. Moreover, the influence of TLO formation on fertility in the mice was not tackled. Future studies thoroughly investigating the impact of TLO on the male reproductive tract are urgently needed.

5. Appendix

5.1 Materials

Table 8. Chemicals

2-Propanol	Sigma-Aldrich, Steinheim, Germany
β-mercaptoethanol	Sigma-Aldrich, Steinheim, Germany
Acetic acid	Merck, Darmstadt, Germany
Agarose	Invitrogen, Carlsbad, USA
Aniline alcohol	Merck, Darmstadt, Germany
Azo-carmine G solution	Chroma-Gesellschaft, Stuttgart, Germany
4′,6-Diamidino-2-phenyl-indol -dihydrochlorid, 2-(4-Amidinophenyl)-6-indolcarbamidin -dihydrochlorid, DAPI -dihydrochlorid	Sigma-Aldrich, Steinheim, Germany
Bordetella pertussis toxin	Calbiochem, Darmstadt, Germany
Bovine serum albumin (BSA)	Sigma-Aldrich, Steinheim, Germany
Bromophenol blue sodium salt	Sigma-Aldrich, Steinheim, Germany
Bouin's fixative	Carl Roth, Karlsruhe, Germany
Complete Freund's adjuvant	Sigma-Aldrich, Saint Louis, USA
Collagenase A	Roche Diagnostic, Mannheim, Germany
Ethanol	Sigma-Aldrich, Steinheim, Germany
Ethidium bromide	Carl Roth, Karlsruhe, Germany

Ethylenediaminetetraacetic acid (EDTA)	Merck, Darmstadt, Germany
Eukitt Quick hardening mounting medium	Sigma-Aldrich, Saint Louis, USA
FcR Blocking Reagent	Miltenyi Biotec, Bergisch Gladbach, Germany
Glycerol	Carl Roth, Karlsruhe, Germany
Goat serum	BioLegend, San Diego, CA, USA
Hydrochloric acid, concentrated	Merck, Munich, Germany
Hydrochloric acid 37%	Carl Roth, Karlsruhe, Germany
MACS BSA stock solution	Miltenyi Biotec, Bergisch Gladbach, Germany
Methanol	Sigma-Aldrich, Steinheim, Germany
Isoflurane	Baxter, Unterschleißheim, Germany
Paraformaldehyde	Merck, Darmstadt, Germany
ProLong Gold Antifade Mountant with DAPI	Life Technologies, Carlsbad, CA, USA
ProLong Gold Antifade Mountant	Life Technologies, Carlsbad, CA, USA
Proteinase K (30 units/mg)	Sigma-Aldrich, Steinheim, Germany
Sodium chloride (NaCl)	Roth, Karlsruhe, Germany
Sodium hydroxide (NaOH)	Roth, Karlsruhe, Germany
Sudan Black B	Sigma-Aldrich, Steinheim, Germany

Tramadol	STADApharm GmbH, Bad Vilbel, Germany
Tris	Carl Roth, Karlsruhe, Germany
Tris-hydrochloride	Carl Roth, Karlsruhe, Germany
Triton X-100	Sigma-Aldrich, Steinheim, Germany
Tween 20	Sigma-Aldrich, Steinheim, Germany
Xylene	Carl Roth, Karlsruhe, Germany

Table 9. PCR and reverse transcription reagents

6 x Blue/orange DNA loading dye	Promega, Mannheim, Germany
Desoxyribonucleosidtriphosphate (dNTP) 10mM	Promega, Mannheim, Germany
DNA ladder 100bp	Promega, Mannheim, Germany
Go Taq G2 Flexi DNA polymerase	Promega, Mannheim, Germany
iTaq Universal SYBR Green Supermix	Bio-Rad Laboratories, Munich, Germany
Moloney Murine Leukemia Virus Reverse Transcriptase (M-MLV RT)	Promega, Mannheim, Germany
Oligo-dT15 primer	Promega, Mannheim, Germany
RNasin ribonuclease inhibitor	Promega, Mannheim, Germany

Table 10. Cell culture reagents

4-(2-hydroxyethyl)-1-piperazineethanesulfonic acid (HEPES)	Gibco, Grand Island, NY, USA
β-mercaptoethanol	Gibco, Grand Island, NY, USA
Bovine serum albumin (BSA)	Sigma-Aldrich, Steinheim, Germany
Brefeldin A solution (1,000X)	BioLegend, San Diego, CA, USA
Cell Stimulation Cocktail (500X)	Thermo Fisher Scientific, Waltham, MA, USA
Dulbecco´s PBS	Gibco, Grand Island, NY, USA
Fetal bovine serum (FBS)	Gibco, Grand Island, NY, USA
Follistatin 288 (FST288)	Purified from HEK-293 cells transfected with human follistatin 288; Monash University, Melbourne, Australia
LS columns	Miltenyi Biotec, Bergisch Gladbach, Germany
Macrophage colony-stimulating factor (M-CSF)	Miltenyi Biotec, Bergisch Gladbach, Germany
MACS MultiStand	Miltenyi Biotec, Bergisch Gladbach, Germany
MEM non-essential amino acids	Sigma-Aldrich, Steinheim, Germany
MidiMACS™ separator	Miltenyi Biotec, Bergisch Gladbach, Germany
Penicillin/Streptomycin	Gibco, Grand Island, NY, USA

Pre-separation filter, 30µm	Miltenyi Biotec, Bergisch Gladbach, Germany
RBC lysis buffer	Qiagen, Hilden, Germany
Recombinant human activin A	Miltenyi Biotec, Bergisch Gladbach, Germany
RPMI-1640 medium	Gibco, Grand Island, NY, USA
Sodium pyruvate	Gibco, Grand Island, NY, USA
Trypan blue solution 0.4%	Gibco, Grand Island, NY, USA
Ultra-LEAF purified anti-mouse CD3ε antibody	BioLegend, San Diego, CA, USA
Ultra-LEAF purified anti-mouse CD28 antibody	BioLegend, San Diego, CA, USA

Table 11. Kits

MACS Comp Bead Kit, anti-REA	Miltenyi Biotec, Bergisch Gladbach, Germany
Mouse Chemokines & Receptors RT² Profiler PCR Array	Qiagen, Hilden, Germany
MaxFluorTM Mouse on Mouse Fluorescence Detection Kit MaxFluor 488	MaxVision Biosciences Inc. Washington, USA
Pan T Cell Isolation Kit II, mouse	Miltenyi Biotec, Bergisch Gladbach, Germany
Proteome Profiler Mouse Chemokine Array Kit	R&D Systems, Minneapolis, Minnesota, USA
RNeasy Fibrous Tissue Mini Kit	Qiagen, Hilden, Germany

RNase-Free DNase Set	Qiagen, Hilden, Germany
RNeasy Mini Kit	Qiagen, Hilden, Germany
RT^2 First Strand Kit	Qiagen, Hilden, Germany
RT^2 SYBR Green Mastermix	Qiagen, Hilden, Germany
Ultracomp eBeads™ compensation-beads	Thermo Fisher Scientific, Waltham, MA, USA

Table 12. Consumables

Cell culture plate, 6/ 96 well	Sarstedt, Nümbrecht, Germany
Cell filter, 70µm/ 100µm	Greiner Bio-One, Frickenhausen, Germany
Cell scraper	Sarstedt, Nümbrecht, Germany
Cell filter, 0.20µm	BD Bioscience, Heidelberg, Germany
Falcon tube, 15/ 50ml	Greiner Bio-One, Frickenhausen, Germany
Filter tips	nerbe plus, Winsen/Luhe, Germany
Flow cytometry tubes	Sarstedt, Nümbrecht, Germany
Hard-shell 96-well PCR plates	Bio-Rad Laboratories, Munich, Germany
Microseal B adhesive seals (PCR plates)	Bio-Rad Laboratories, Munich, Germany
Needles, 24G/ 30G	BD, Franklin Lakes, NJ, USA
Screw cap tubes, graduated and sterile	Greiner Bio-One, Frickenhausen, Germany

Stainless steel beads, 5mm	Qiagen, Hilden, Germany
SuperFrost Plus microscope slides	R.Langenbrinck, Emmendingen, Germany
Syringes	BD Bioscience, Heidelberg, Germany
Tips and tubes	Sarstedt, Nümbrecht, Germany

Table 13. Software

Bio-Rad CFX Manager 3.1	Bio-Rad Laboratories, Munich, Germany
BioRender	Toronto, Canada
FlowJo V10	FlowJo LLC, Oregon, USA
GraphPad Prism 6	GraphPad Software, San Diego, CA, USA
ImageJ	National Institutes of Health, Bethesda, Maryland, USA
Zeiss ZEN lite 3.3	Carl Zeiss, Göttingen, Germany

Table 14. Equipment

Cell culture CO_2 incubator	Binder, Tuttlingen, Germany
Centrifuge Labofuge 400R	Heraeus, Hanau, Germany
CFX96 Touch real-time PCR detection system	Bio-Rad Laboratories, Munich, Germany

Confocal laser scanning microscope 710	Carl Zeiss, Göttingen, Germany
Cryostat CM30509	Leica, Wetzlar, Germany
Electronic balance SPB50	Ohaus, Giessen, Germany
Gel Jet Imager 2000 documentation system	Intas, Göttingen, Germany
Heat block DB-2A	Techne Inc., Cambridge, UK
Horizontal mini electrophoresis system	PEQLAB, Erlangen, Germany
Microtome RM2255	Leica, Wetzlar, Germany
Microwave oven	Samsung, Schwalbach, Germany
Mixer Mill MM 400	Retsch, Haan, Germany
NanoDrop ND 2000	Thermo Fisher Scientific, Waltham, USA
Bürker Counting Chamber	Fisher Scientific, Waltham, MA, USA
PCR thermocycler	Biozyme Scientific, Hessisch Oldendor, Germany
Potter S homogenizer	B. Braun, Melsungen, Germany
pH-meter 766	Knick, Berlin, Germany
Power supply units	PEQLAB, Erlangen, Germany
Shaker 3005 orbital	GFL, Burgwedel, Germany
Vertical microscope Leica DM750	Leica, Wetzlar, Germany

Table 15. Primary and secondary antibodies used in immunofluorescence staining.

Antibody	Company	Catalog No.	Final Dilution
Primary antibodies			
Mouse monoclonal anti-activin βA	Oxford-Brooks University, Oxford, UK	-	1:50
Rabbit anti-mouse CCR2	Novus Biologicals, Littleton, Colorado, USA	NBP2-67700	1:50
Rat monoclonal anti-mouse CD138	BioLegend, San Diego, CA, USA	142501	1:100
Rabbit anti-mouse CD19	Abcam, Cambridge, UK	ab245235	1:50
Rat monclonal anti-mouse CD3ε	Cell Signaling Technology, Danvers, Massachusetts, USA	4443	1:50
Rabbit anti-mouse CD45	Cell Signaling Technology, Danvers, Massachusetts, USA	D3F8Q	1:50
Rat monoclonal anti-human CD68	BioLegend, San Diego, CA, USA	375602	1:20
Goat anti-mouse CXCL13	Invitrogen, Oregon, USA	PA5-47018	1:20
Rat monoclonal anti-mouse F4/80	Cell Signaling Technology, Danvers, MA, USA	71299	1:100

Rat monoclonal anti-mouse IgA FITC-conjugated	SouthernBiotech, Birmingham, Alabama, USA	1165-02	1:50
Rat monoclonal anti-mouse MECA-79	BioLegend, San Diego, CA, USA	120801	1:100
Rat monoclonal anti-mouse MECA-79 Alexa Fluor 647-conjugated	BioLegend, San Diego, CA, USA	120807	1:100
Mouse monoclonal anti-mouse,PCNA	BioLegend, San Diego, CA, USA	307901	1:50
Goat anti- mouse podoplanin	R&D Systems, Minneapolis, Minnesota, USA	AF3244	1:20
Secondary Antibodies			
Goat anti-rat IgG (H+L) Alexa Fluor 546 conjugated	Invitrogen, Oregon, USA	A-11081	1:2000
Goat anti-rabbit IgG (H+L) Alexa Fluor 488 conjugated	Invitrogen, Oregon, USA	A-11034	1:2000
Donkey anti-goat IgG (H+L) Alexa Fluor 488 conjugated	Abcam, Cambridge, UK	ab150129	1:2000
Goat anti-mouse IgG F(ab)2 Alexa Fluor 488 conjugated	Jackson ImmunoResearch Labs, West Grove, PA, USA	115-546-072	1:800

Table 16. Antibodies and isotype control antibodies used for flow cytometry analysis.

Antibodies	Companies	Catalog No.	Clones	Dilution
Recombinant monoclonal anti-mouse CD19 PE-Vio770 REAfinity conjugated	Miltenyi Biotec, Bergisch Gladbach, Germany	130-112-037	REA749	1:50
Recombinant monoclonal anti-mouse CD138 APC REAfinity conjugated	Miltenyi Biotec, Bergisch Gladbach, Germany	130-122-945	REA104	1:25
Rat monclonal anti-CD3ε APC	BioLegend, San Diego, CA, USA	155605	KT3.1.1	1:40
Recombinant monoclonal anti-mouse CD3 PE REAfinity™ conjugated	Miltenyi Biotec, Bergisch Gladbach, Germany	130-121-133	REA641	1:50
Recombinant monoclonal anti-mouse CD45 VioGreen REAfinity™ conjugated	Miltenyi Biotec, Bergisch Gladbach, Germany	130-110-665	REA737	1:50
Recombinant monoclonal anti-mouse CD45R PE-Vio615 REAfinity™ conjugated	Miltenyi Biotec, Bergisch Gladbach, Germany	130-110-853	REA755	1:25
Recombinant monoclonal anti-mouse IFN-γ PE REAfinity™ conjugated	Miltenyi Biotec, Bergisch Gladbach, Germany	130-117-502	REA638	1:50
Recombinant monoclonal anti-mouse IgD FITC	Miltenyi Biotec, Bergisch	130-111-495	REA772	1:50

REAfinity™ conjugated	Gladbach, Germany			
Recombinant monoclonal anti-mouse IgM APC-Vio770 REAfinity conjugated	Miltenyi Biotec, Bergisch Gladbach, Germany	130-116-315	REA979	1:50
Rat monoclonal anti-mouse TNF PerCP/Cyanine5.5 conjugated	BioLegend, San Diego, CA, USA	506321	MP6-XT22	1:80
Isotype control antibodies				
Rat IgG2b, κ APC isotype control antibody	BioLegend, San Diego, CA, USA	400611	RTK4530	1:40
Rat IgG1, κ PerCP/Cyanine5.5 isotype control antibody	BioLegend, San Diego, CA, USA	400425	RTK2071	1:80
Recombinant monoclonal REA control VioGreen	Miltenyi Biotec, Bergisch Gladbach, Germany	130-104-624	REA293	1:50
Recombinant monoclonal REA control FITC	Miltenyi Biotec, Bergisch Gladbach, Germany	130-113-437	REA293	1:50
Recombinant monoclonal REA control PE	Miltenyi Biotec, Bergisch Gladbach, Germany	130-104-628	REA293	1:50
Recombinant monoclonal REA control PE-Vio615	Miltenyi Biotec, Bergisch Gladbach, Germany	130-113-439	REA293	1:25

Recombinant monoclonal REA control PE-Vio770	Miltenyi Biotec, Bergisch Gladbach, Germany	130-104-632	REA293	1:50
Recombinant monoclonal REA control APC	Miltenyi Biotec, Bergisch Gladbach, Germany	130-104-630	REA293	1:25
Recombinant monoclonal REA control APC-Vio770	Miltenyi Biotec, Bergisch Gladbach, Germany	130-104-634	REA293	1:50

Table 17. Primers used in qRT-PCR.

Gene	**Forward 5' – 3'**	**Reverse 5' – 3'**	**Product size (bp)**
Mouse			
Actb **(β-actin)**	TGACAGGATGCAGAAGGAGAT	TACTCCTGCTTGCTGATCCAC	156
Ccl3	TTCTCTGTACCATGACACTCTGC	CGTGGAATCTTCCGGCTGTAG	100
Ccl4	TTCCTGCTGTTTCTCTTACACCT	CTGTCTGCCTCTTTTGGTCAG	121
Ccl5	AGATCTCTGCAGCTGCCCTCA	GGAGCACTTGCTGCTGGTGTAG	170
Ccl6	AGCTTTGTGGGTTCCCAGTT	CCTGTGGCTACATGGAGTGG	83
Ccl7	GCTGCTTTCAGCATCCAAGTG	CCAGGGACACCGACTACTG	135
Ccl8	TCTACGCAGTGCTTCTTTGCC	AAGGGGGATCTTCAGCTTTAGTA	122

Ccl12	ATTTCCACACTTCTATGCCTCCT	ATCCAGTATGGTCCTGAAGATCA	204
Ccl19	ATGTGAATCACTCTGGCCCAGGAA	AAGCGGCTTTATTGGAAGCTCTGC	188
Ccl21	TGAGCTATGTGCAAACCCTGAGGA	TGAGGGCTGTGTCTGTTCAGTTCT	178
Ccr2	GGTCATGATCCCTATGTGG	CTGGGCACCTGATTTAAAGG	253
Ccr5	TTTTCAAGGGTCAGTTCCGA	GGAAGACCATCATGTTACCCAC	158
Cxcl1	GCGCCTATCGCCAATGAG	GCAACACCTTCAAGCTCTGGAT	88
Cxcl2	GAGCTTGAGTGTGACGCCCCCAGG	GTTAGCCTTGCCTTTGTTCAGTATC	148
Cxcl9	TGTGGAGTTCGAGGAACCCT	TGCCTTGGCTGGTGCTG	67
Cxcl13	GGCCACGGTATTCTGGAAGC	ACCGACAACAGTTGAAATCACTC	75
Cxcl14	TGGTTATCGTCACCACCAAG	TCTCTCAACTGGCCTGGAGT	180
Cxcl16	TGAACTAGTGGACTGCTTTGAGC	GCAAATGTTTTTGGTGGTGA	77
Hprt	CTGGTAAAAGGACCTC	CTGAAGTACTCATTATAGTCAAG	110
Ltα	AGCCGTCAGATGACAACTAGG	CAAGCAGTGGCTGGCTTTTA	148
Ltβ	AAAGACTGGATGACAGCAAA	GCTAGATTCCTGGAAGCATT	112
Rplpo	CTGCACTCTCGCTTTCTGGA	ACGCGCTTGTAGCCATTGAT	113
Tnf	CCCTCCTGGCCAACGGCATG	TCGGGGCAGCCTTGTCCCTT	109

Tnfs14	ATCAGGACCATGTTGGCAGG	GTGGCTGGAAACCAATGCAG	90
Human			
CCL2	GCTCATAGCAGCCACCTTCATTC	TGCAGATTCTTGGGTTGTGGAG	297
CCR1	ACCTGCAGCCTTCACTTTCCTCA	GGCGATCACCTCCGTCACTTG	327
CCR2	CCAACTCCTGCCTCCGCTCTA	CCGCCAAAATAACCGATGTGATAC	255
CCR5	TGCTACTCGGGAATCCTAAAAACT	TTCTGAACTTCTCCCCGACAAA	280
CXCL13	TCTCTGCTTCTCATGCTGCT	TCAAGCTTGTGTAATAGACCTCCA	76
GAPDH	CATGTTCGTCATGGGTGTGAACCA	AGTGATGGCATGGACTGTGGTCAT	160

6. Abbreviation

ActB	β-actin
ANOVA	Analysis of variance
BMDM	Bone marrow-derived macrophages
BSA	Bovine serum albumin
CD	Cluster of differentiation
cDNA	Complementary deoxyribonucleic acid
CFA	Complete Freund’s adjuvant
CFU	Colony forming unit
CLSM	Confocal laser scanning microscope
CM	Conditioned medium
Cq	Cycle threshold
CSC	Cell stimulation cocktail
DC	Dendritic cell
DEG	Differentially expressed genes
DMEM	Dulbecco’s modified Eagle’s medium
DNase	Deoxyribonuclease
dNTP	Deoxynucleoside triphosphate
EAEO	Experimental autoimmune-epididymo orchitis
EDTA	Ethylene diamine tetraacetic acid
FBS	Fetal bovine serum
FDC	Follicular dendritic cell
FSH	Follicle-stimulating hormone

FST	Follistatin
GAPDH	Glyceraldehyde 3-phosphate dehydrogenase
GC	Germinal center
gDNA	Genomic DNA
GPCR	G-protein-coupled receptor
HEPES	4-(2-hydroxyethyl)-1-piperazineethanesulfonic acid
HEV	High endothelial venule
HPRT	Hypoxanthine guanine phosphoribosyl transferase
IDO	Indolamin-2,3-Dioxygenase
IF	Immunofluorescence
IFN-γ	Interferon gamma
IL	Interleukin
LH	Luteinizing hormone
LPS	Lipopolysaccharide
LT	Lymphotoxin
LTβR	Lymphotoxin beta receptor
MACS	Magnetic-activated cell sorting
M-CSF	Macrophage-colony stimulating factor
MHCII	Major histocompatibility complex class II
mRNA	Messenger ribonucleic acid
NaCl	Sodium chloride
NaOH	Sodium hydroxide
NGS	Normal goat serum

PBS	Phosphate buffered saline
PCR	Polymerase chain reaction
PMA	Phorbol 12-myristate 13-acetate
PTC	Peritubular cell
q-PCR	Quantitative - PCR
RBC	Red blood cell
RE	Relative expression
RPMI	Roswell park memorial institute
RT	Room temperature
SEM	Standard error of the mean
SLO	Secondary lymphoid organ
SPF	Specific pathogen free
TAE	Tris-acetate-EDTA
TBS	Tris-buffered saline
TE	Tris-EDTA buffer
TH	Testicular homogenate
TLO	Tertiary lymphoid organ
TM	Testicular macrophage
TNF	Tumor necrosis factor
TNFSF14	TNF Superfamily Member 14
UPEC	Uropathogenic *Escherchia coli*
WT	Wild type

7. References

Abid, S., Marcos, E., Parpaleix, A., Amsellem, V., Breau, M., Houssaini, A., Vienney, N., Lefevre, M., Derumeaux, G., Evans, S., Hubeau, C., Delcroix, M., Quarck, R., Adnot, S., & Lipskaia, L. (2019). CCR2/CCR5-mediated macrophage-smooth muscle cell crosstalk in pulmonary hypertension. European Respiratory Journal, 54(4). https://doi.org/10.1183/13993003.02308-2018

Alberts, B., Johnson, A., Lewis, J., Raff, M., Roberts, K., & Walter, P. (2008). T Cells and MHC Proteins. In Molecular Biology of the Cell.

Alvarez, E., Piccio, L., Mikesell, R. J., Klawiter, E. C., Parks, B. J., Naismith, R. T., & Cross, A. H. (2013). CXCL13 is a biomarker of inflammation in multiple sclerosis, neuromyelitis optica, and other neurological conditions. Multiple Sclerosis Journal, 19(9). https://doi.org/10.1177/1352458512473362

Astarita, J. L., Acton, S. E., & Turley, S. J. (2012). Podoplanin: Emerging functions in development, the immune system, and cancer. In Frontiers in Immunology (Vol. 3, Issue SEP). https://doi.org/10.3389/fimmu.2012.00283

Aubry, F., Habasque, C., Satie, A.-P., Jégou, B., & Samson, M. (2000). Expression and Regulation of the CC-Chemokine Monocyte Chemoattractant Protein-1 in Rat Testicular Cells in Primary Culture1. Biology of Reproduction. https://doi.org/10.1095/biolreprod62.5.1427

Bachelerie, F., Ben-Baruch, A., Burkhardt, A. M., Combadiere, C., Farber, J. M., Graham, G. J., Horuk, R., Sparre-Ulrich, A. H., Locati, M., Luster, A. D., Mantovani, A., Matsushima, K., Murphy, P. M., Nibbs, R., Nomiyama, H., Power, C. A., Proudfoot, A. E. I., Rosenkilde, M. M., Rot, A., … Zlotnik, A. (2014). International union of pharmacology. LXXXIX. Update on the extended family of chemokine receptors and introducing a new nomenclature for atypical chemokine receptors. In Pharmacological Reviews. https://doi.org/10.1124/pr.113.007724

Barakat, B., O'Connor, A. E., Gold, E., de Kretser, D. M., & Loveland, K. L. (2008). Inhibin, activin, follistatin and FSH serum levels and testicular production are highly modulated during the first spermatogenic wave in mice. Reproduction, 136(3), 345–359. https://doi.org/10.1530/REP-08-0140

Barker, C. F., & Billingham, R. E. (1978). Immunologically privileged sites. Advances in Immunology. https://doi.org/10.1016/S0065-2776(08)60930-X

Battistone, M. A., Mendelsohn, A. C., Spallanzani, R. G., Brown, D., Nair, A. V., & Breton, S. (2020). Region-specific transcriptomic and functional signatures of mononuclear phagocytes in the epididymis. Molecular Human Reproduction, 26(1). https://doi.org/10.1093/molehr/gaz059

Battistone M. A., Elizagaray M. L., Barrachina F., Ottino K., Mendelsohn A. C., Breton S., Immunoregulatory mechanisms between epithelial clear cells and mononuclear phagocytes in the epididymis. Andrology. 2023; 1-15. https://doi.org/10.1111/andr.13509

Bazan, J. F., Bacon, K. B., Hardiman, G., Wang, W., Soo, K., Rossi, D., Greaves, D. R., Zlotnik, A., & Schall, T. J. (1997). A new class of membrane-bound chemokine with a CX3C motif. Nature, 385(6617). https://doi.org/10.1038/385640a0

Bery, A. I., Shepherd, H. M., Li, W., Krupnick, A. S., Gelman, A. E., & Kreisel, D. (2022). Role of tertiary lymphoid organs in the regulation of immune responses in the periphery. In Cellular and Molecular Life Sciences (Vol. 79, Issue 7). https://doi.org/10.1007/s00018-022-04388-x

Bhushan, S., & Meinhardt, A. (2017). The macrophages in testis function. In Journal of Reproductive Immunology (Vol. 119, pp. 107–112). Elsevier Ireland Ltd. https://doi.org/10.1016/j.jri.2016.06.008

Bhushan, S., Tchatalbachev, S., Klug, J., Fijak, M., Pineau, C., Chakraborty, T., & Meinhardt, A. (2008). Uropathogenic Escherichia coli block MyD88-dependent and activate MyD88-independent signaling pathways in rat testicular cells. The Journal of Immunology, 180(8), 5537. https://doi.org/10.4049/jimmunol.180.8.5537

Bhushan, S., Theas, M. S., Guazzone, V. A., Jacobo, P., Wang, M., Fijak, M., Meinhardt, A., & Lustig, L. (2020). Immune Cell Subtypes and Their Function in the Testis. Frontiers in Immunology, 11(September), 1–7. https://doi.org/10.3389/fimmu.2020.583304

Blanchard, L., & Girard, J. P. (2021). High endothelial venules (HEVs) in immunity, inflammation and cancer. In Angiogenesis (Issue 0123456789). Springer Netherlands. https://doi.org/10.1007/s10456-021-09792-8

Boniakowski, A. E., Kimball, A. S., Joshi, A., Schaller, M., Davis, F. M., denDekker, A., Obi, A. T., Moore, B. B., Kunkel, S. L., & Gallagher, K. A. (2018). Murine macrophage chemokine receptor CCR2 plays a crucial role in macrophage recruitment and regulated inflammation in wound healing. European Journal of Immunology, 48(9), 1445–1455. https://doi.org/10.1002/eji.201747400

Borregaard, N. (2010). Neutrophils, from Marrow to Microbes. In Immunity (Vol. 33, Issue 5). https://doi.org/10.1016/j.immuni.2010.11.011

Bruno, T. C. (2020). B cells to the forefront of immunotherapy. Nature, 577(7791).

Bugatti, S., Manzo, A., Bombardieri, M., Vitolo, B., Humby, F., Kelly, S., Montecucco, C., & Pitzalis, C. (2011). Synovial tissue heterogeneity and peripheral blood biomarkers. Current Rheumatology Reports, 13(5). https://doi.org/10.1007/s11926-011-0201-y

Cabrita, R., Lauss, M., Sanna, A., Donia, M., Skaarup Larsen, M., Mitra, S., Johansson, I., Phung, B., Harbst, K., Vallon-Christersson, J., van Schoiack, A., Lövgren, K., Warren, S., Jirström, K., Olsson, H., Pietras, K., Ingvar, C., Isaksson, K., Schadendorf, D., … Jönsson, G. (2020). Tertiary lymphoid structures improve immunotherapy and survival in melanoma. Nature, 577(7791). https://doi.org/10.1038/s41586-019-1914-8

Cañete, J. D., Celis, R., Moll, C., Izquierdo, E., Marsal, S., Sanmartí, R., Palacín, A., Lora, D., De La Cruz, J., & Pablos, J. L. (2009). Clinical significance of synovial lymphoid neogenesis and its reversal after anti-tumour necrosis factor α therapy in rheumatoid arthritis. Annals of the Rheumatic Diseases, 68(5). https://doi.org/10.1136/ard.2008.089284

Chakradhar, S. (2018). Puzzling over privilege: How the immune system protects - And fails - The testes. Nature Medicine. https://doi.org/10.1038/nm0118-2

Chang, A., Henderson, S. G., Brandt, D., Liu, N., Guttikonda, R., Hsieh, C., Kaverina, N., Utset, T. O., Meehan, S. M., Quigg, R. J., Meffre, E., & Clark, M. R. (2011). In Situ B Cell-Mediated Immune Responses and Tubulointerstitial Inflammation in Human Lupus Nephritis. The Journal of Immunology, 186(3). https://doi.org/10.4049/jimmunol.1001983

Cheng, X., Dai, H., Wan, N., Moore, Y., Vankayalapati, R., & Dai, Z. (2009). Interaction of programmed death-1 and programmed death-1 ligand-1 contributes to testicular immune privilege. Transplantation, 87(12). https://doi.org/10.1097/TP.0b013e3181a75633

Chen, S.-C., Vassileva, G., Kinsley, D., Holzmann, S., Manfra, D., Wiekowski, M. T., Romani, N., & Lira, S. A. (2002). Ectopic Expression of the Murine Chemokines CCL21a and CCL21b Induces the Formation of Lymph Node-Like Structures in Pancreas, But Not Skin, of Transgenic Mice. The Journal of Immunology, 168(3). https://doi.org/10.4049/jimmunol.168.3.1001

Chou, R. C., Kim, N. D., Sadik, C. D., Seung, E., Lan, Y., Byrne, M. H., Haribabu, B., Iwakura, Y., & Luster, A. D. (2010). Lipid-Cytokine-Chemokine Cascade Drives Neutrophil Recruitment in a Murine Model of Inflammatory Arthritis. Immunity, 33(2). https://doi.org/10.1016/j.immuni.2010.07.018

Cinti, I., & Denton, A. E. (2021). Lymphoid stromal cells—more than just a highway to humoral immunity. Oxford Open Immunology, 2(1). https://doi.org/10.1093/oxfimm/iqab011

Combadière, C., Potteaux, S., Rodero, M., Simon, T., Pezard, A., Esposito, B., Merval, R., Proudfoot, A., Tedgui, A., & Mallat, Z. (2008). Combined inhibition of CCL2, CX3CR1, and CCR5 abrogates Ly6Chi and Ly6Clo monocytosis and almost abolishes atherosclerosis in hypercholesterolemic mice. Circulation. https://doi.org/10.1161/CIRCULATIONAHA.107.745091

Cornwall, G. A. (2009). New insights into epididymal biology and function. Human Reproduction Update, 15(2). https://doi.org/10.1093/humupd/dmn055

Countries, D. (2004). Infecundity, Infertility, and Childlessness in Developing Countries. In World Health.

Cutolo, M. (2009). Androgens in rheumatoid arthritis: When are they effectors? In Arthritis Research and Therapy. https://doi.org/10.1186/ar2804

DeFalco, T., Potter, S. J., Williams, A. V., Waller, B., Kan, M. J., & Capel, B. (2015). Macrophages Contribute to the Spermatogonial Niche in the Adult Testis. Cell Reports, 12(7). https://doi.org/10.1016/j.celrep.2015.07.015

De Grava Kempinas, W., & Klinefelter, G. R. (2014). Interpreting histopathology in the epididymis. Spermatogenesis, 4(2). https://doi.org/10.4161/21565562.2014.979114

de Kretser, D. M., O'Hehir, R. E., Hardy, C. L., & Hedger, M. P. (2012). The roles of activin A and its binding protein, follistatin, in inflammation and tissue repair. In Molecular and Cellular Endocrinology. https://doi.org/10.1016/j.mce.2011.10.009

Deshmane, S. L., Kremlev, S., Amini, S., & Sawaya, B. E. (2009). Monocyte chemoattractant protein-1 (MCP-1): An overview. In Journal of Interferon and Cytokine Research. https://doi.org/10.1089/jir.2008.0027

De Togni, P., Goellner, J., Ruddle, N. H., Streeter, P. R., Fick, A., Mariathasan, S., Smith, S. C., Carlson, R., Shornick, L. P., Strauss-Schoenberger, J., Russell, J. H., Karr, R., & Chaplin, D. D. (1994). Abnormal Development of Peripheral Lymphoid Organs in Mice Deficient in Lymphotoxin. Science, 264(5159), 703–707. https://doi.org/10.1126/science.8171322

Dhaiban, S. (2020). Targeting Chemokines and Chemokine Receptors in Multiple Sclerosis and Experimental Autoimmune Encephalomyelitis.

Diao, R., Cai, X., Liu, L., Yang, L., Duan, Y. G., Cai, Z., Gui, Y., & Mou, L. (2018). In vitro chemokine (C-C motif) receptor 6-dependent non-inflammatory chemotaxis during spermatogenesis. Biological Research. https://doi.org/10.1186/s40659-018-0161-z

Dohi, T., Ejima, C., Kato, R., Kawamura, Y. I., Kawashima, R., Mizutani, N., Tabuchi, Y., & Kojima, I. (2005). Therapeutic potential of follistatin for colonic inflammation in mice. Gastroenterology, 128(2). https://doi.org/10.1053/j.gastro.2004.11.063

Drayton, D. L., Liao, S., Mounzer, R. H., & Ruddle, N. H. (2006). Lymphoid organ development: From ontogeny to neogenesis. In Nature Immunology (Vol. 7, Issue 4). https://doi.org/10.1038/ni1330

Drayton, D. L., Ying, X., Lee, J., Lesslauer, W., & Ruddle, N. H. (2003). Ectopic LTαβ directs lymphoid organ neogenesis with concomitant expression of peripheral node addressin and a HEV-restricted sulfotransferase. Journal of Experimental Medicine, 197(9). https://doi.org/10.1084/jem.20021761

Eddens, T., Elsegeiny, W., Garcia-Hernadez, M. de la L., Castillo, P., Trevejo-Nunez, G., Serody, K., Campfield, B. T., Khader, S. A., Chen, K., Rangel-Moreno, J., & Kolls, J. K. (2017). Pneumocystis-Driven Inducible Bronchus-Associated Lymphoid Tissue Formation Requires Th2 and Th17 Immunity. Cell Reports, 18(13). https://doi.org/10.1016/j.celrep.2017.03.016

Eickhoff, J. H., Frimodt-Møller, N., Walter, S., & Frimodt-Møller, C. (1999). A double-blind, randomized, controlled multicentre study to compare the efficacy of ciprofloxacin with pivampicillin as oral therapy for epididymitis in men over 40 years of age. BJU International, 84(7). https://doi.org/10.1046/j.1464-410x.1999.00252.x

Fietz, D., Schuppe, H. C., & Loveland, K. L. (2022). Immunobiology of Testicular Cancer. https://doi.org/10.1007/16833_2022_7

Fijak, M., & Meinhardt, A. (2006). The testis in immune privilege. Immunological Reviews, 213(1), 66–81. https://doi.org/https://doi.org/10.1111/j.1600-065X.2006.00438.x

Fijak, M., Pilatz, A., Hedger, M. P., Nicolas, N., Bhushan, S., Michel, V., Tung, K. S. K., Schuppe, H. C., & Meinhardt, A. (2018). Infectious, inflammatory and “autoimmune” male factor infertility: How do rodent models inform clinical practice? Human Reproduction Update, 24(4), 416–441. https://doi.org/10.1093/humupd/dmy009

Fijak, M., Schneider, E., Klug, J., Bhushan, S., Hackstein, H., Schuler, G., Wygrecka, M., Gromoll, J., & Meinhardt, A. (2011). Testosterone Replacement Effectively Inhibits the Development of Experimental Autoimmune Orchitis in Rats: Evidence for a Direct Role of Testosterone on Regulatory T Cell Expansion. The Journal of Immunology, 186(9), 5162–5172. https://doi.org/10.4049/jimmunol.1001958

Fisher, J., & Hammarberg, K. (2017). Endocrinology of the Testis and Male Reproduction. 1–31. https://doi.org/10.1007/978-3-319-29456-8

Flegar, D., Filipović, M., Šućur, A., Markotić, A., Lukač, N., Šisl, D., Ikić Matijašević, M., Jajić, Z., Kelava, T., Katavić, V., Kovačić, N., & Grčević, D. (2021). Preventive CCL2/CCR2 Axis Blockade Suppresses Osteoclast Activity in a Mouse Model of Rheumatoid Arthritis by Reducing Homing of CCR2hi Osteoclast Progenitors to the Affected Bone. Frontiers in Immunology, 12. https://doi.org/10.3389/fimmu.2021.767231

Fleig, S., Kapanadze, T., Bernier-Latmani, J., Lill, J. K., Wyss, T., Gamrekelashvili, J., Kijas, D., Liu, B., Hüsing, A. M., Bovay, E., Jirmo, A. C., Halle, S., Ricke-Hoch, M., Adams, R. H., Engel, D. R., von Vietinghoff, S., Förster, R., Hilfiker-Kleiner, D., Haller, H., … Limbourg, F. P. (2022). Loss of vascular endothelial notch signaling promotes spontaneous formation of tertiary lymphoid structures. Nature Communications, 13(1). https://doi.org/10.1038/s41467-022-29701-x

Flier, J., Boorsma, D. M., Van Beek, P. J., Nieboer, C., Stoof, T. J., Willemze, R., & Tensen, C. P. (2001). Differential expression of CXCR3 targeting chemokines CXCL10, CXCL9, and CXCL11 in different types of skin inflammation. Journal of Pathology, 194(4). https://doi.org/10.1002/1096-9896(200108)194:4<397::AID-PATH899>3.0.CO;2-S

Förster, R., Mattis, A. E., Kremmer, E., Wolf, E., Brem, G., & Lipp, M. (1996). A putative chemokine receptor, BLR1, directs B cell migration to defined lymphoid organs and specific anatomic compartments of the spleen. Cell, 87(6). https://doi.org/10.1016/S0092-8674(00)81798-5

Francis, M., Groves, A. M., Sun, R., Cervelli, J. A., Choi, H., Laskin, J. D., & Laskin, D. L. (2017). CCR2 regulates inflammatory cell accumulation in the lung and tissue injury following ozone exposure. Toxicological Sciences, 155(2). https://doi.org/10.1093/toxsci/kfw226

Freemont, A. J., Jones, C. J. P., Bromley, M., & Andrews, P. (1983). Changes in vascular endothelium related to lymphocyte collections in diseased synovia. Arthritis & Rheumatism, 26(12). https://doi.org/10.1002/art.1780261203

Friend, D. S., & Gilula, N. B. (1972). Variations in tight and gap junctions in mammalian tissues. Journal of Cell Biology, 53(3). https://doi.org/10.1083/jcb.53.3.758

Gerdprasert, O. (2002). Expression of monocyte chemoattractant protein-1 and macrophage colony-stimulating factor in normal and inflamed rat testis. Molecular Human Reproduction. https://doi.org/10.1093/molehr/8.6.518

Getz, G. S. (2005). Bridging the innate and adaptive immune systems. In Journal of Lipid Research (Vol. 46, Issue 4). https://doi.org/10.1194/jlr.E500002-JLR200

Ghafouri-fard, S., Honarmand, K., & Taheri, M. (2021). A comprehensive review on the role of chemokines in the pathogenesis of multiple sclerosis.

Gilbert, SF. Developmental Biology. 6th edition. Sunderland (MA): Sinauer Associates; 2000. Spermatogenesis.

Girard, J. P., & Springer, T. A. (1995). High endothelial venules (HEVs): specialized endothelium for lymphocyte migration. Immunology Today, 16(9). https://doi.org/10.1016/0167-5699(95)80023-9

Girbl, T., Lenn, T., Perez, L., Rolas, L., Barkaway, A., Thiriot, A., del Fresno, C., Lynam, E., Hub, E., Thelen, M., Graham, G., Alon, R., Sancho, D., von Andrian, U. H., Voisin, M. B., Rot, A., & Nourshargh, S. (2018). Distinct Compartmentalization of the Chemokines CXCL1 and CXCL2 and the Atypical Receptor ACKR1 Determine Discrete Stages of Neutrophil Diapedesis. Immunity. https://doi.org/10.1016/j.immuni.2018.09.018

Gray, P. C., Bilezikjian, L. M., Harrison, C. A., Wiater, E., & Vale, W. (2005). Activins and inhibins: Physiological roles, signaling mechanisms and regulation. In Hormones and the Brain. https://doi.org/10.1007/3-540-26940-1_1

Groom, J. R., & Luster, A. D. (2011). CXCR3 in T cell function. In Experimental Cell Research (Vol. 317, Issue 5, pp. 620–631). Academic Press Inc. https://doi.org/10.1016/j.yexcr.2010.12.017

Gualdoni, G. S., Jacobo, P. V., Sobarzo, C. M., Pérez, C. V., Matzkin, M. E., Höcht, C., Frungieri, M. B., Hill, M., Anegon, I., Lustig, L., & Guazzone, V. A. (2019). Role of indoleamine 2,3-dioxygenase in testicular immune-privilege. Scientific Reports, 9(1), 1–14. https://doi.org/10.1038/s41598-019-52192-8

Guazzone, V. A., Hollwegs, S., Mardirosian, M., Jacobo, P., Hackstein, H., Wygrecka, M., Schneider, E., Meinhardt, A., Lustig, L., & Fijak, M. (2011). Characterization of dendritic cells in testicular draining lymph nodes in a rat model of experimental autoimmune orchitis. International Journal of Andrology, 34(3), 276–289. https://doi.org/10.1111/j.1365-2605.2010.01082.x

Guazzone, V. A., Jacobo, P., Denduchis, B., & Lustig, L. (2012). Expression of cell adhesion molecules, chemokines and chemokine receptors involved in leukocyte traffic in rats undergoing autoimmune orchitis. Reproduction. https://doi.org/10.1530/REP-11-0079

Guazzone, V. A., Jacobo, P., Theas, M. S., & Lustig, L. (2009). Cytokines and chemokines in testicular inflammation: A brief review. In Microscopy Research and Technique. https://doi.org/10.1002/jemt.20704

Guazzone, V. A., Rival, C., Denduchis, B., & Lustig, L. (2003). Monocyte chemoattractant protein-1 (MCP-1/CCL2) in experimental autoimmune orchitis. Journal of Reproductive Immunology. https://doi.org/10.1016/j.jri.2003.08.001

Gu, S. M., Park, M. H., Yun, H. M., Han, S. B., Oh, K. W., Son, D. J., Yun, J. S., & Hong, J. T. (2016). CCR5 knockout suppresses experimental autoimmune encephalomyelitis in C57BL/6 mice. Oncotarget, 7(13). https://doi.org/10.18632/oncotarget.8097

Gu, X., Li, S. Y., Matsuyama, S., & DeFalco, T. (2022). Immune Cells as Critical Regulators of Steroidogenesis in the Testis and Beyond. In Frontiers in Endocrinology (Vol. 13). Frontiers Media S.A. https://doi.org/10.3389/fendo.2022.894437

Habasque, C. (2003). Expression of fractalkine in the rat testis: molecular cloning of a novel alternative transcript of its gene that is differentially regulated by pro-inflammatory cytokines. Molecular Human Reproduction. https://doi.org/10.1093/molehr/gag059

Haidl, G., Allam, J. P., & Schuppe, H. C. (2008). Chronic epididymitis: Impact on semen parameters and therapeutic options. Andrologia. https://doi.org/10.1111/j.1439-0272.2007.00819.x

Hakovirta, H., Vierula, M., Wolpe, S. D., & Parvinen, M. (1994). MIP-1α is a regulator of mitotic and meiotic DNA synthesis during spermatogenesis. Molecular and Cellular Endocrinology. https://doi.org/10.1016/0303-7207(94)90154-6

Hales, D. B. (2002). Testicular macrophage modulation of Leydig cell steroidogenesis. Journal of Reproductive Immunology, 57(1), 3–18. https://doi.org/https://doi.org/10.1016/S0165-0378(02)00020-7

Han, D., Liu, Z., & Yan, K. (2016). Immunology of the Testis and Privileged Sites. In Encyclopedia of Immunobiology (Vol. 5, pp. 46–53). Elsevier Inc. https://doi.org/10.1016/B978-0-12-374279-7.19009-5

Hao, Q., Vadgama, J. v., & Wang, P. (2020). CCL2/CCR2 signaling in cancer pathogenesis. In Cell Communication and Signaling (Vol. 18, Issue 1). https://doi.org/10.1186/s12964-020-00589-8

Hardy, C. L., King, S. J., Mifsud, N. A., Hedger, M. P., Phillips, D. J., Mackay, F., De Kretser, D. M., Wilson, J. W., Rolland, J. M., & O'Hehir, R. E. (2015). The activin A antagonist follistatin inhibits cystic fibrosis-like lung inflammation and pathology. Immunology and Cell Biology, 93(6), 567–574. https://doi.org/10.1038/icb.2015.7

Hardy, C. L., O'Connor, A. E., Yao, J., Sebire, K., De Kretser, D. M., Rolland, J. M., Anderson, G. P., Phillips, D. J., & O'Hehir, R. E. (2006). Follistatin is a candidate endogenous negative regulator

of activin A in experimental allergic asthma. Clinical and Experimental Allergy, 36(7). https://doi.org/10.1111/j.1365-2222.2006.02523.x

Harrer, C., Otto, F., Radlberger, R. F., Moser, T., Pilz, G., Wipfler, P., & Harrer, A. (2022). The CXCL13/CXCR5 Immune Axis in Health and Disease—Implications for Intrathecal B Cell Activities in Neuroinflammation. In Cells (Vol. 11, Issue 17). MDPI. https://doi.org/10.3390/cells11172649

Haschek, W. M., Rousseaux, C. G., & Wallig, M. A. (2010). Chapter 18 - Male Reproductive System. In W. M. Haschek, C. G. Rousseaux, & M. A. Wallig (Eds.), Fundamentals of Toxicologic Pathology (Second Edition) (pp. 553–597). Academic Press. https://doi.org/https://doi.org/10.1016/B978-0-12-370469-6.00018-0

Hayasaka, H., Taniguchi, K., Fukai, S., & Miyasaka, M. (2010). Neogenesis and development of the high endothelial venules that mediate lymphocyte trafficking. Cancer Science, 101(11), nov cover-nov cover. https://doi.org/10.1111/j.1349-7006.2010.01773.x

Head, J. R., & Billingham, R. E. (1985). Immune privilege in the testis: II. Evaluation of potential local factors. Transplantation. https://doi.org/10.1097/00007890-198509000-00010

Head, J. R., Neaves, W. B., & Billingham, R. E. (1983). Immune privilege in the testis: I. basic parameters of allograft survival. Transplantation. https://doi.org/10.1097/00007890-198310000-00014

Hedger, M. P. (2011). Immunophysiology and pathology of inflammation in the testis and epididymis. Journal of Andrology, 32(6), 625–640. https://doi.org/10.2164/jandrol.111.012989

Hedger, M. P., & de Kretser, D. M. (2013). The activins and their binding protein, follistatin—Diagnostic and therapeutic targets in inflammatory disease and fibrosis. Cytokine & Growth Factor Reviews, 24(3), 285–295. https://doi.org/https://doi.org/10.1016/j.cytogfr.2013.03.003

Hedger, M. P., Drummond, A. E., Robertson, D. M., Risbridger, G. P., & de Kretse, D. M. (1989). Inhibin and activin regulate [3H]thymidine uptake by rat thymocytes and 3T3 cells in vitro. Molecular and Cellular Endocrinology. https://doi.org/10.1016/0303-7207(89)90198-6

Hedger, M. P., & Meinhardt, A. (2003). Cytokines and the immune-testicular axis. Journal of Reproductive Immunology, 58(1), 1–26. https://doi.org/10.1016/S0165-0378(02)00060-8

Hedger, M. P., & Winnall, W. R. (2012). Regulation of activin and inhibin in the adult testis and the evidence for functional roles in spermatogenesis and immunoregulation. In Molecular and Cellular Endocrinology. https://doi.org/10.1016/j.mce.2011.09.031

Hedger, M. P., Winnall, W. R., Phillips, D. J., & de Kretser, D. M. (2011). The Regulation and Functions of Activin and Follistatin in Inflammation and Immunity. In Vitamins and Hormones (1st ed., Vol. 85). Elsevier Inc. https://doi.org/10.1016/B978-0-12-385961-7.00013-5

Heng, A. H. S., Han, C. W., Abbott, C., McColl, S. R., & Comerford, I. (2022). Chemokine-Driven Migration of Pro-Inflammatory CD4+ T Cells in CNS Autoimmune Disease. In Frontiers in Immunology (Vol. 13). https://doi.org/10.3389/fimmu.2022.817473

Hilhorst, M., Shirai, T., Berry, G., Goronzy, J. J., & Weyand, C. M. (2014). T cell-macrophage interactions and granuloma formation in vasculitis. In Frontiers in Immunology (Vol. 5, Issue SEP). Frontiers Media S.A. https://doi.org/10.3389/fimmu.2014.00432

Horjus Talabur Horje, C. S., Smids, C., Meijer, J. W. R., Groenen, M. J., Rijnder, M. K., van Lochem, E. G., & Wahab, P. J. (2017). High endothelial venules associated with T cell subsets in

the inflamed gut of newly diagnosed inflammatory bowel disease patients. Clinical and Experimental Immunology, 188(1). https://doi.org/10.1111/cei.12918

Huber, S., Hoffmann, R., Muskens, F., & Voehringer, D. (2010). Alternatively activated macrophages inhibit T-cell proliferation by Stat6-dependent expression of PD-L2. Blood, 116(17), 3311–3320. https://doi.org/10.1182/blood-2010-02-271981

Hughes, C. E., & Nibbs, R. J. B. (2018). A guide to chemokines and their receptors. FEBS Journal, 285(16), 2944–2971. https://doi.org/10.1111/febs.14466

Hu, J., You, S., Li, W., Wang, D., Nagpal, M. L., Mi, Y., Liang, P., & Lin, T. (1998). Expression and Regulation of Interferon-γ-Inducible Protein 10 Gene in Rat Leydig Cells*. Endocrinology, 139(8), 3637–3645. https://doi.org/10.1210/endo.139.8.6143

Humby, F., Bombardieri, M., Manzo, A., Kelly, S., Blades, M. C., Kirkham, B., Spencer, J., & Pitzalis, C. (2009). Ectopic lymphoid structures support ongoing production of class-switched autoantibodies in rheumatoid synovium. PLoS Medicine, 6(1). https://doi.org/10.1371/journal.pmed.0060001

Hutson, J. C. (2006). Physiologic interactions between macrophages and Leydig cells. In Experimental Biology and Medicine (Vol. 231, Issue 1). https://doi.org/10.1177/153537020623100101

Itoh, M., Xie, Q., Miyamoto, K., & Takeuchi, Y. (1999). Major differences between the testis and epididymis in the induction of granulomas in response to extravasated germ cells. I. A light microscopical study in mice. International Journal of Andrology, 22(5). https://doi.org/10.1046/j.1365-2605.1999.00186.x

Jacobo, P., Guazzone, V. A., Pérez, C. V., & Lustig, L. (2015). CD4+ Foxp3+ regulatory T cells in autoimmune orchitis: Phenotypic and functional characterization. American Journal of Reproductive Immunology. https://doi.org/10.1111/aji.12312

Jequier, A. M. (2000). WHO manual for standardized investigation and diagnosis of the infertile male. The Obstetrician & Gynaecologist. https://doi.org/10.1576/toag.2000.2.4.55

Johnston, D. S., Jelinsky, S. A., Bang, H. J., Dicandeloro, P., Wilson, E., Kopf, G. S., & Turner, T. T. (2005). The mouse epididymal transcriptome: Transcriptional profiling of segmental gene expression in the epididymis. Biology of Reproduction, 73(3). https://doi.org/10.1095/biolreprod.105.039719

Jones, E., Gallimore, A., & Ager, A. (2018). Defining High Endothelial Venules and Tertiary Lymphoid Structures in Cancer. Methods in Molecular Biology, 1845, 99–118. https://doi.org/10.1007/978-1-4939-8709-2_7

Jones, G. W., Hill, D. G., & Jones, S. A. (2016). Understanding immune cells in tertiary lymphoid organ development: It is all starting to come together. In Frontiers in Immunology (Vol. 7). https://doi.org/10.3389/fimmu.2016.00401

Jones, K. L., Kretser, D. M. D., Patella, S., & Phillips, D. J. (2004). Activin A and follistatin in systemic inflammation. Molecular and Cellular Endocrinology. https://doi.org/10.1016/j.mce.2004.07.010

Jones, K. L., Mansell, A., Patella, S., Scott, B. J., Hedger, M. P., De Kretser, D. M., & Phillips, D. J. (2007). Activin A is a critical component of the inflammatory response, and its binding protein, follistatin, reduces mortality in endotoxemia. Proceedings of the National Academy of Sciences

of the United States of America, 104(41), 16239–16244. https://doi.org/10.1073/pnas.0705971104

Jrad-Lamine, A., Henry-Berger, J., Damon-Soubeyrand, C., Saez, F., Kocer, A., Janny, L., Pons-Rejraji, H., Munn, D. H., Mellor, A. L., Gharbi, N., Cadet, R., Guiton, R., Aitken, R. J., & Drevet, J. R. (2013). Indoleamine 2,3-Dioxygenase 1 (Ido1) Is Involved in the Control of Mouse Caput Epididymis Immune Environment. PLoS ONE, 8(6). https://doi.org/10.1371/journal.pone.0066494

Kaaij, M. H., Helder, B., van Mens, L. J. J., van de Sande, M. G. H., Baeten, D. L. P., & Tas, S. W. (2020). Anti-IL-17A treatment reduces serum inflammatory, angiogenic and tissue remodeling biomarkers accompanied by less synovial high endothelial venules in peripheral spondyloarthritis. Scientific Reports, 10(1). https://doi.org/10.1038/s41598-020-78204-6

Kadiombo, A. T., Maeshima, A., Kayakabe, K., Ikeuchi, H., Sakairi, T., Kaneko, Y., Hiromura, K., & Nojima, Y. (2017). Involvement of infiltrating macrophage-derived activin A in the progression of renal damage in MRL-lpr mice. Am J Physiol Renal Physiol, 312, 297–304. https://doi.org/10.1152/ajprenal.00191.2016.-Lupus

Kahnert, A., Höpken, U. E., Stein, M., Bandermann, S., Lipp, M., & Kaufmann, S. H. E. (2007). Mycobacterium tuberculosis Triggers Formation of Lymphoid Structure in Murine Lungs. The Journal of Infectious Diseases, 195(1), 46–54. https://doi.org/10.1086/508894

Kauerhof, A. C., Nicolas, N., Bhushan, S., Wahle, E., Loveland, K. A., Fietz, D., Bergmann, M., Groome, N. P., Kliesch, S., Schuppe, H. C., Pilatz, A., Meinhardt, A., Hedger, M. P., & Fijak, M. (2019). Investigation of activin A in inflammatory responses of the testis and its role in the development of testicular fibrosis. Human Reproduction (Oxford, England), 34(8), 1536–1550. https://doi.org/10.1093/humrep/dez109

Kaur G, Thompson LA, Dufour JM. 2014 Sertoli cells: Immunological sentinels of spermatogenesis. Seminars in Cell and Developmental Biology 30:36-44. https://doi.org/10.1016/j.semcdb.2014.02.011

Kazutaka, S., Winnall, W. R., Muir, J. A., & Hedger, M. P. (2011). Regulation of Sertoli cell activin A and inhibin B by tumour necrosis factor α and interleukin 1α: Interaction with follicle-stimulating hormone/adenosine 3',5'-cyclic phosphate signalling. Molecular and Cellular Endocrinology, 335(2), 195–203. https://doi.org/10.1016/j.mce.2011.01.014

Kern, S., Robertson, S. A., Mau, V. J., & Maddocks, S. (1995). Cytokine Secretion by Macrophages in the Rat Testis1. Biology of Reproduction. https://doi.org/10.1095/biolreprod53.6.1407

Khademi, M., Kockum, I., Andersson, M. L., Iacobaeus, E., Brundin, L., Sellebjerg, F., Hillert, J., Piehl, F., & Olsson, T. (2011). Cerebrospinal fluid CXCL13 in multiple sclerosis: A suggestive prognostic marker for the disease course. Multiple Sclerosis Journal, 17(3). https://doi.org/10.1177/1352458510389102

Kikui, Y., & Miki, A. (1995). A differential staining method for adenohypophyseal cells. Archives of Histology and Cytology, 58(3). https://doi.org/10.1679/aohc.58.375

Klein, B., Bhushan, S., Günther, S., Middendorff, R., Loveland, K. L., Hedger, M. P., & Meinhardt, A. (2020). Differential tissue-specific damage caused by bacterial epididymo-orchitis in the mouse. Molecular Human Reproduction, 26(4). https://doi.org/10.1093/molehr/gaaa011

Klein, B., Haggeney, T., Fietz, D., Indumathy, S., Loveland, K. L., Hedger, M., Kliesch, S., Weidner, W., Bergmann, M., & Schuppe, H. C. (2016). Specific immune cell and cytokine

characteristics of human testicular germ cell neoplasia. Human Reproduction, 31(10), 2192–2202. https://doi.org/10.1093/humrep/dew211

Kobayashi, M., Hoshino, H., Masumoto, J., Fukushima, M., Suzawa, K., Kageyama, S., Suzuki, M., Ohtani, H., Fukuda, M., & Nakayama, J. (2009). GlcNAc6ST-1-mediated decoration of MAdCAM-1 protein with L-selectin ligand carbohydrates directs disease activity of ulcerative colitis. Inflammatory Bowel Diseases, 15(5). https://doi.org/10.1002/ibd.20827

Kobayashi, M., Mitoma, J., Nakamura, N., Katsuyama, T., Nakayama, J., & Fukuda, M. (2004). Induction of peripheral lymph node addressin in human gastric mucosa infected by Helicobacter pylori. Proceedings of the National Academy of Sciences of the United States of America, 101(51). https://doi.org/10.1073/pnas.0407503101

Kohno, S., Munoz, J. A., Williams, T. M., Teuscher, C., Bernard, C. C., & Tung, K. S. (1983). Immunopathology of murine experimental allergic orchitis. Journal of Immunology (Baltimore, Md. : 1950).

Korbutt, G. S., Suarez-Pinzon, W. L., Power, R. F., Rajotte, R. V., & Rabinovitch, A. (2000). Testicular Sertoli cells exert both protective and destructive effects on syngeneic islet grafts in non-obese diabetic mice. Diabetologia. https://doi.org/10.1007/s001250051331

Kratz, A., Campos-Neto, A., Hanson, M. S., & Ruddle, N. H. (1996). Chronic inflammation caused by lymphotoxin is lymphoid neogenesis. Journal of Experimental Medicine, 183(4). https://doi.org/10.1084/jem.183.4.1461

Krautler, N. J., Kana, V., Kranich, J., Tian, Y., Perera, D., Lemm, D., Schwarz, P., Armulik, A., Browning, J. L., Tallquist, M., Buch, T., Oliveira-Martins, J. B., Zhu, C., Hermann, M., Wagner, U., Brink, R., Heikenwalder, M., & Aguzzi, A. (2012). Follicular dendritic cells emerge from ubiquitous perivascular precursors. Cell, 150(1). https://doi.org/10.1016/j.cell.2012.05.032

Kumar, S. N., & Boss, J. M. (2000). Site A of the MCP-1 distal regulatory region functions as a transcriptional modulator through the transcription factor NF1. Molecular Immunology. https://doi.org/10.1016/S0161-5890(00)00097-3

Kuranobu, T., Mokuda, S., Oi, K., Tokunaga, T., Yukawa, K., Kohno, H., Yoshida, Y., Hirata, S., & Sugiyama, E. (2020). Activin A Expressed in Rheumatoid Synovial Cells Downregulates TNFα-Induced CXCL10 Expression and Osteoclastogenesis. Pathobiology, 87(3), 198–207. https://doi.org/10.1159/000506260

Kuroda, N., Masuya, M., Tawara, I., Tsuboi, J., Yoneda, M., Nishikawa, K., Kageyama, Y., Hachiya, K., Ohishi, K., Miwa, H., Yamada, R., Hamada, Y., Tanaka, K., Kato, T., Takei, Y., & Katayama, N. (2019). Infiltrating CCR2+ monocytes and their progenies, fibrocytes, contribute to colon fibrosis by inhibiting collagen degradation through the production of TIMP-1. Scientific Reports, 9(1). https://doi.org/10.1038/s41598-019-45012-6

Lalor, S. J., & Segal, B. M. (2010). Lymphoid chemokines in the CNS. Journal of Neuroimmunology, 224(1–2), 56–61. https://doi.org/10.1016/j.jneuroim.2010.05.017

Ley, K. (2001). History of Inflammation Research. In Physiology of Inflammation. https://doi.org/10.1007/978-1-4614-7512-5_1

Li, F., Xu, X., Geng, J., Wan, X., & Dai, H. (2020). The autocrine CXCR4/CXCL12 axis contributes to lung fibrosis through modulation of lung fibroblast activity. Experimental and Therapeutic Medicine. https://doi.org/10.3892/etm.2020.8433

Li, N., Wang, T., & Han, D. (2012). Structural, cellular and molecular aspects of immune privilege in the testis. Frontiers in Immunology, 3(JUN), 1–12. https://doi.org/10.3389/fimmu.2012.00152

Ligon, M.M., Wang, C., DeJong, E.N. et al. Single cell and tissue-transcriptomic analysis of murine bladders reveals age- and TNFα-dependent but microbiota-independent tertiary lymphoid tissue formation. Mucosal Immunol 13, 908–918 (2020). https://doi.org/10.1038/s41385-020-0290-x

Livak, K. J., & Schmittgen, T. D. (2001). Analysis of relative gene expression data using real-time quantitative PCR and the 2-ΔΔCT method. Methods, 25(4), 402–408. https://doi.org/10.1006/meth.2001.1262

Lin, T., Calkins, J. H., Morris, P. L., Vale, W., & Bardin, C. W. (1989). Regulation of leydig cell function in primary culture by inhibin and activin. Endocrinology. https://doi.org/10.1210/endo-125-4-2134

Lismer, A., Kimmins, S. Emerging evidence that the mammalian sperm epigenome serves as a template for embryo development. Nat Commun 14, 2142 (2023). https://doi.org/10.1038/s41467-023-37820-2

Locci, M., Wu, J. E., Arumemi, F., Mikulski, Z., Dahlberg, C., Miller, A. T., & Crotty, S. (2016). Activin A programs the differentiation of human T FH cells. Nature Immunology, 17(8), 976–984. https://doi.org/10.1038/ni.3494

Loveland, K. L., Klein, B., Pueschl, D., Indumathy, S., Bergmann, M., Loveland, B. E., Hedger, M. P., & Schuppe, H. C. (2017). Cytokines in male fertility and reproductive pathologies: Immunoregulation and beyond. Frontiers in Endocrinology, 8(NOV), 1–16. https://doi.org/10.3389/fendo.2017.00307

Lustig, L., Guazzone, V. A., Theas, M. S., Pleuger, C., Jacobo, P., Pérez, C. V., Meinhardt, A., & Fijak, M. (2020). Pathomechanisms of Autoimmune Based Testicular Inflammation. Frontiers in Immunology, 11(September), 1–8. https://doi.org/10.3389/fimmu.2020.583135

Luther, S. A., Bidgol, A., Hargreaves, D. C., Schmidt, A., Xu, Y., Paniyadi, J., Matloubian, M., & Cyster, J. G. (2002). Differing Activities of Homeostatic Chemokines CCL19, CCL21, and CXCL12 in Lymphocyte and Dendritic Cell Recruitment and Lymphoid Neogenesis. The Journal of Immunology, 169(1). https://doi.org/10.4049/jimmunol.169.1.424

Mahad, D. J., Howell, S. J. L., & Woodroofe, M. N. (2002). Expression of chemokines in the CSF and correlation with clinical disease activity in patients with multiple sclerosis. Journal of Neurology Neurosurgery and Psychiatry, 72(4). https://doi.org/10.1136/jnnp.72.4.498

Manzo, A., Paoletti, S., Carulli, M., Blades, M. C., Barone, F., Yanni, G., FitzGerald, O., Bresnihan, B., Caporali, R., Montecucco, C., Uguccioni, M., & Pitzalis, C. (2005). Systematic microanatomical analysis of CXCL13 and CCL21 in situ production and progressive lymphoid organization in rheumatoid synovitis. European Journal of Immunology, 35(5). https://doi.org/10.1002/eji.200425830

Marinkovic, T., Garin, A., Yokota, Y., Fu, Y. X., Ruddle, N. H., Furtado, G. C., & Lira, S. A. (2006). Interaction of mature CD3+CD4+ T cells with dendritic cells triggers the development of tertiary lymphoid structures in the thyroid. Journal of Clinical Investigation, 116(10). https://doi.org/10.1172/JCI28993

Maruyama, M., Kobayashi, M., Sakai, Y., Hiraoka, N., Ohya, A., Kageyama, S., Tanaka, E., Nakayama, J., & Morohoshi, T. (2013). Periductal induction of high endothelial venule-like vessels

in type 1 autoimmune pancreatitis. Pancreas, 42(1). https://doi.org/10.1097/MPA.0b013e318258ce4c

Marshall, J. S., Warrington, R., Watson, W., & Kim, H. L. (2018). An introduction to immunology and immunopathology. In Allergy, Asthma and Clinical Immunology (Vol. 14). https://doi.org/10.1186/s13223-018-0278-1

Mauduit, C., Chauvin, M. A., de Peretti, E., Morera, A. M., & Benai-Imed, M. (1991). Effect of Activin A on Dehydroepiandrosterone and Testosterone Secretion by Primary Immature Porcine Leydig Cells1. Biology of Reproduction. https://doi.org/10.1095/biolreprod45.1.101

Mayerhofer, A. (2013). Human testicular peritubular cells: More than meets the eye. In Reproduction. https://doi.org/10.1530/REP-12-0497

McDonald, K. G., McDonough, J. S., & Newberry, R. D. (2005). Adaptive Immune Responses Are Dispensable for Isolated Lymphoid Follicle Formation: Antigen-Naive, Lymphotoxin-Sufficient B Lymphocytes Drive the Formation of Mature Isolated Lymphoid Follicles. The Journal of Immunology, 174(9). https://doi.org/10.4049/jimmunol.174.9.5720

McLachlan, R. I. (2002). Basis, diagnosis and treatment of immunological infertility in men. Journal of Reproductive Immunology. https://doi.org/10.1016/S0165-0378(02)00014-1

Mealy, K., Robinson, B., Millette, C. F., Majzoub, J., & Wilmore, D. W. (1990). The testicular effects of tumor necrosis factor. Annals of Surgery. https://doi.org/10.1097/00000658-199004000-00014

Meinhardt, A., Dejucq-Rainsford, N., & Bhushan, S. (2022). Testicular macrophages: development and function in health and disease. Trends in Immunology, 43(1), 51–62. https://doi.org/https://doi.org/10.1016/j.it.2021.11.003

Meinhardt, A., & Hedger, M. P. (2011). Immunological, paracrine and endocrine aspects of testicular immune privilege. Molecular and Cellular Endocrinology, 335(1), 60–68. https://doi.org/10.1016/j.mce.2010.03.022

Mendelsohn, A. C., Sanmarco, L. M., Spallanzani, R. G., Brown, D., Quintana, F. J., Breton, S., & Battistone, M. A. (2020). From initial segment to cauda: A regional characterization of mouse epididymal CD11c+ mononuclear phagocytes based on immune phenotype and function. American Journal of Physiology - Cell Physiology, 319(6). https://doi.org/10.1152/ajpcell.00392.2020

Michel, V., Duan, Y., Stoschek, E., Bhushan, S., Middendorff, R., Young, J. M., Loveland, K. L., Kretser, D. M. D., Hedger, M. P., & Meinhardt, A. (2016). Uropathogenic Escherichia coli causes fibrotic remodelling of the epididymis. Journal of Pathology, 240(1), 15–24. https://doi.org/10.1002/path.4748

Mita, P., Hinton, B. T., & Dufour, J. M. (2011). The blood-testis and blood-epididymis barriers are more than just their tight junctions. In Biology of Reproduction (Vol. 84, Issue 5). https://doi.org/10.1095/biolreprod.110.087452

Mittal, S., Revell, M., Barone, F., Hardie, D. L., Matharu, G. S., Davenport, A. J., Martin, R. A., Grant, M., Mosselmans, F., Pynsent, P., Sumathi, V. P., Addison, O., Revell, P. A., & Buckley, C. D. (2013). Lymphoid Aggregates That Resemble Tertiary Lymphoid Organs Define a Specific Pathological Subset in Metal-on-Metal Hip Replacements. PLoS ONE, 8(5). https://doi.org/10.1371/journal.pone.0063470

Miura, K., Yang, L., van Rooijen, N., Ohnishi, H., & Seki, E. (2012). Hepatic recruitment of macrophages promotes nonalcoholic steatohepatitis through CCR2. American Journal of Physiology - Gastrointestinal and Liver Physiology, 302(11). https://doi.org/10.1152/ajpgi.00365.2011

Moore, B. B., Paine, R., Christensen, P. J., Moore, T. A., Sitterding, S., Ngan, R., Wilke, C. A., Kuziel, W. A., & Toews, G. B. (2001). Protection from Pulmonary Fibrosis in the Absence of CCR2 Signaling. The Journal of Immunology, 167(8). https://doi.org/10.4049/jimmunol.167.8.4368

Morianos, I., Papadopoulou, G., Semitekolou, M., & Xanthou, G. (2019). Activin-A in the regulation of immunity in health and disease. In Journal of Autoimmunity (Vol. 104). Academic Press. https://doi.org/10.1016/j.jaut.2019.102314

Morianos, I., Trochoutsou, A. I., Papadopoulou, G., Semitekolou, M., Banos, A., Konstantopoulos, D., Manousopoulou, A., Kapasa, M., Wei, P., Lomenick, B., Belaidi, E., Kalamatas, T., Karageorgiou, K., Doskas, T., Sallusto, F., Pan, F., Garbis, S. D., Quintanan, F. J., & Xanthou, G. (2020). Activin-A limits Th17 pathogenicity and autoimmune neuroinflammation via CD39 and CD73 ectonucleotidases and Hif1-α-dependent pathways. Proceedings of the National Academy of Sciences of the United States of America, 117(22). https://doi.org/10.1073/pnas.1918196117

Mossadegh-Keller, N., Gentek, R., Gimenez, G., Bigot, S., Mailfert, S., & Sieweke, M. H. (2017). Developmental origin and maintenance of distinct testicular macrophage populations. Journal of Experimental Medicine, 214(10). https://doi.org/10.1084/jem.20170829

Moyron-quiroz, J. E., Rangel-moreno, J., Kusser, K., Hartson, L., Sprague, F., Goodrich, S., Woodland, D. L., Lund, F. E., & Randall, T. D. (2004). Role of inducible bronchus associated lymphoid tissue (iBALT) in respiratory immunity. 10(9), 927–934. https://doi.org/10.1038/nm1091

Naz, R. K. (2004). Modalities for Treatment of Antisperm Antibody Mediated Infertility: Novel Perspectives. American Journal of Reproductive Immunology. https://doi.org/10.1111/j.1600-0897.2004.00174.x

Nes, W. D., Lukyanenko, Y. O., Jia, Z. H., Quideau, S., Howald, W. N., Pratum, T. K., West, R. R., & Hutson, J. C. (2000). Identification of the lipophilic factor produced by macrophages that stimulates steroidogenesis. Endocrinology, 141(3). https://doi.org/10.1210/endo.141.3.7350

Neyt, K., Perros, F., GeurtsvanKessel, C. H., Hammad, H., & Lambrecht, B. N. (2012). Tertiary lymphoid organs in infection and autoimmunity. Trends in Immunology, 33(6), 297–305. https://doi.org/10.1016/j.it.2012.04.006

Nicolas, N., Michel, V., Bhushan, S., Wahle, E., Hayward, S., Ludlow, H., de Kretser, D. M., Loveland, K. L., Schuppe, H. C., Meinhardt, A., Hedger, M. P., & Fijak, M. (2017a). Testicular activin and follistatin levels are elevated during the course of experimental autoimmune epididymo-orchitis in mice. Scientific Reports, 7(February), 1–15. https://doi.org/10.1038/srep42391

Nicolas, N., Muir, J. A., Hayward, S., Chen, J. L., Stanton, P. G., Gregorevic, P., De Kretser, D. M., Loveland, K. L., Bhushan, S., Meinhardt, A., Fijak, M., & Hedger, M. P. (2017b). Induction of experimental autoimmune orchitis in mice: responses to elevated circulating levels of the activin-binding protein, follistatin. Reproduction, 154(3), 293–305. https://doi.org/10.1530/REP-17-0010

Nieschlag, E., Simoni, M., Gromoll, J., & Weinbauer, G. F. (1999). Role of FSH in the regulation of spermatogenesis: Clinical aspects. In Clinical Endocrinology. https://doi.org/10.1046/j.1365-2265.1999.00846.x

Nistal, M., & Paniagua, R. (2008). Non-neoplastic diseases of the testis. In Urologic Surgical Pathology. https://doi.org/10.1016/b978-0-323-01970-5.50014-2

Okuma, Y., Saito, K., O'Connor, A. E., Phillips, D. J., de Kretser, D. M., & Hedger, M. P. (2005). Reciprocal regulation of activin A and inhibin B by interleukin-1 (IL-1) and follicle-stimulating hormone (FSH) in rat Sertoli cells in vitro. Journal of Endocrinology, 185(1), 99–110. https://doi.org/10.1677/joe.1.06053

Oppenheim, J. J. (2013). Cytokines, their Receptors and Signals. The Autoimmune Diseases: Fifth Edition, 229–241. https://doi.org/10.1016/B978-0-12-384929-8.00016-2

Oritani, K., Tomiyama, Y., Kincade, P. W., Aoyama, K., Yokota, T., Matsumura, I., Kanakura, Y., Nakajima, K., Hirano, T., & Matsuzawa, Y. (1999). Both Stat3-activation and Stat3-independent BCL2 downregulation are important for interleukin-6-induced apoptosis of 1A9-M cells. Blood. https://doi.org/10.1182/blood.v93.4.1346.404k15_1346_1354

Osegbe, D. N. (1991). Testicular function affter unilateral bacterial epididymo-orchitis. European Urology, 19(3). https://doi.org/10.1159/000473620

Ota, F., Maeshima, A., Yamashita, S., Ikeuchi, H., Kaneko, Y., Kuroiwa, T., Hiromura, K., Ueki, K., Kojima, I., & Nojima, Y. (2003). Activin A induces cell proliferation of fibroblast-like synoviocytes in rheumatoid arthritis. Arthritis and Rheumatism, 48(9), 2442–2449. https://doi.org/10.1002/art.11249

Pablos, J. L., Santiago, B., Tsay, D., Singer, M. S., Palao, G., Galindo, M., & Rosen, S. D. (2005). A HEV-restricted sulfotransferase is expressed in rheumatoid arthritis synovium and is induced by lymphotoxin-α/β and TNF-α in cultured endothelial cells. BMC Immunology, 6. https://doi.org/10.1186/1471-2172-6-6

Palacios, B. S., Estrada-Capetillo, L., Izquierdo, E., Criado, G., Nieto, C., Municio, C., González-Alvaro, I., Sánchez-Mateos, P., Pablos, J. L., Corbí, A. L., & Puig-Kröger, A. (2015). Macrophages from the synovium of active rheumatoid arthritis exhibit an activin a-dependent pro-inflammatory profile. Journal of Pathology, 235(3), 515–526. https://doi.org/10.1002/path.4466

Penaranda, C., Tang, Q., Ruddle, N. H., & Bluestone, J. A. (2010). Prevention of diabetes by FTY720-mediated stabilization of peri-islet tertiary lymphoid organs. Diabetes, 59(6). https://doi.org/10.2337/db09-1129

Peng, W., Kepsch, A., Kracht, T. O., Hasan, H., Wijayarathna, R., Wahle, E., Pleuger, C., Bhushan, S., Günther, S., Kauerhof, A. C., Planinić, A., Fietz, D., Schuppe, H. C., Wygrecka, M., Loveland, K. L., Ježek, D., Meinhardt, A., Hedger, M. P., & Fijak, M. (2022). Activin A and CCR2 regulate macrophage function in testicular fibrosis caused by experimental autoimmune orchitis. Cellular and Molecular Life Sciences, 79(12), 602. https://doi.org/10.1007/s00018-022-04632-4

Pérez, C. V., Sobarzo, C. M., Jacobo, P. V., Pellizzari, E. H., Cigorraga, S. B., Denduchis, B., & Lustig, L. (2012). Loss of occludin expression and impairment of blood-testis barrier permeability in rats with autoimmune orchitis: effect of interleukin 6 on Sertoli cell tight junctions. Biology of Reproduction, 87(5), 122. https://doi.org/10.1095/biolreprod.112.101709

Petersen, C., & Söder, O. (2006). The Sertoli cell - A hormonal target and "super" nurse for germ cells that determines testicular size. In Hormone Research (Vol. 66, Issue 4). https://doi.org/10.1159/000094142

Phillips, D. J. (2003). The activin/inhibin family. In The Cytokine Handbook. https://doi.org/10.1016/B978-012689663-3/50054-5

Phillips, D. J., de Kretser, D. M., & Hedger, M. P. (2009). Activin and related proteins in inflammation: Not just interested bystanders. Cytokine and Growth Factor Reviews, 20(2), 153–164. https://doi.org/10.1016/j.cytogfr.2009.02.007

Picker, L. J., & Butcher, E. C. (1992). Physiological and molecular mechanisms of lymphocyte homing. In Annual Review of Immunology (Vol. 10). https://doi.org/10.1146/annurev.iy.10.040192.003021

Pilatz, A., Hossain, H., Kaiser, R., Mankertz, A., Schüttler, C. G., Domann, E., Schuppe, H. C., Chakraborty, T., Weidner, W., & Wagenlehner, F. (2015). Acute Epididymitis Revisited: Impact of Molecular Diagnostics on Etiology and Contemporary Guideline Recommendations. European Urology, 68(3), 428–435. https://doi.org/https://doi.org/10.1016/j.eururo.2014.12.005

Pilatz, A., Wagenlehner, F., Bschleipfer, T., Schuppe, H. C., Diemer, T., Linn, T., Weidner, W., & Altinkilic, B. (2013). Acute epididymitis in ultrasound: Results of a prospective study withbaseline and follow-up investigations in 134 patients. European Journal of Radiology, 82(12). https://doi.org/10.1016/j.ejrad.2013.08.050

Pinjusic, K., Dubey, O. A., Egorova, O., Nassiri, S., Meylan, E., Faget, J., & Constam, D. B. (2022). Activin-A impairs CD8 T cell-mediated immunity and immune checkpoint therapy response in melanoma. Journal for ImmunoTherapy of Cancer, 10(5). https://doi.org/10.1136/jitc-2022-004533

Pipi, E., Nayar, S., Gardner, D. H., Colafrancesco, S., Smith, C., & Barone, F. (2018). Tertiary Lymphoid Structures : Autoimmunity Goes Local. 9(September), 1–21. https://doi.org/10.3389/fimmu.2018.01952

Pleuger, C., Ai, D., Hoppe, M. L., Winter, L. T., Bohnert, D., Karl, D., Guenther, S., Epelman, S., Kantores, C., Fijak, M., Ravens, S., Middendorff, R., Mayer, J. U., Loveland, K. L., Hedger, M., Bhushan, S., & Meinhardt, A. (2022). The regional distribution of resident immune cells shapes distinct immunological environments along the murine epididymis. ELife, 11. https://doi.org/10.7554/ELIFE.82193

Pleuger, C., Silva, E. J. R., Pilatz, A., Bhushan, S., & Meinhardt, A. (2020). Differential Immune Response to Infection and Acute Inflammation Along the Epididymis. Frontiers in Immunology, 11(November), 1–8. https://doi.org/10.3389/fimmu.2020.599594

Riccioli, A., Starace, D., Galli, R., Fuso, A., Scarpa, S., Palombi, F., De Cesaris, P., Ziparo, E., & Filippini, A. (2006). Sertoli Cells Initiate Testicular Innate Immune Responses through TLR Activation. The Journal of Immunology, 177(10). https://doi.org/10.4049/jimmunol.177.10.7122

Rival, C., Guazzone, V. A., von Wulffen, W., Hackstein, H., Schneider, E., Lustig, L., Meinhardt, A., & Fijak, M. (2007). Expression of co-stimulatory molecules, chemokine receptors and proinflammatory cytokines in dendritic cells from normal and chronically inflamed rat testis. Molecular Human Reproduction. https://doi.org/10.1093/molehr/gam067

Rival, C., Theas, M. S., Guazzone, V. A., & Lustig, L. (2006). Interleukin-6 and IL-6 receptor cell expression in testis of rats with autoimmune orchitis. Journal of Reproductive Immunology, 70(1–2), 43–58. https://doi.org/10.1016/j.jri.2005.10.006

Robson, N. C., Phillips, D. J., McAlpine, T., Shin, A., Svobodova, S., Toy, T., Pillay, V., Kirkpatrick, N., Zanker, D., Wilson, K., Helling, I., Wei, H., Chen, W., Cebon, J., & Maraskovsky, E. (2008). Activin-A: A novel dendritic cell derived cytokine that potently attenuates CD40 ligand specific cytokine and chemokine production. Blood. https://doi.org/10.1182/blood-2007-03-080994

Rosen, S. D., Tsay, D., Singer, M. S., Hemmerich, S., & Abraham, W. M. (2005). Therapeutic targeting of endothelial ligands for L-selectin (PNAd) in a sheep model of asthma. American Journal of Pathology, 166(3). https://doi.org/10.1016/S0002-9440(10)62313-9

Ruddle, N. H. (2016). High endothelial venules and lymphatic vessels in tertiary lymphoid organs: Characteristics, functions, and regulation. In Frontiers in Immunology (Vol. 7, Issue NOV). Frontiers Media S.A. https://doi.org/10.3389/fimmu.2016.00491

Ruddle, N. H. (2020). Basics of Inducible Lymphoid Organs. In Current Topics in Microbiology and Immunology (Vol. 426). https://doi.org/10.1007/82_2020_218

Rusz, A., Pilatz, A., Wagenlehner, F., Linn, T., Diemer, Th., Schuppe, H. C., Lohmeyer, J., Hossain, H., & Weidner, W. (2012). Influence of urogenital infections and inflammation on semen quality and male fertility. World Journal of Urology, 30(1), 23–30. https://doi.org/10.1007/s00345-011-0726-8

Sacca, R., Cuff, C. A., Lesslauer, W., & Ruddle, N. H. (1998). Differential Activities of Secreted Lymphotoxin-α3 and Membrane Lymphotoxin-α1β2 in Lymphotoxin-Induced Inflammation: Critical Role of TNF Receptor 1 Signaling. The Journal of Immunology, 160(1). https://doi.org/10.4049/jimmunol.160.1.485

Sainio-Pöllänen, S., Saari, T., Simell, O., & Pöllänen, P. (1996). CD28-CD80/CD86 interactions in testicular immunoregulation. Journal of Reproductive Immunology. https://doi.org/10.1016/0165-0378(96)00983-7

Sakai, Y., Hoshino, H., Kitazawa, R., & Kobayashi, M. (2014). High endothelial venule-like vessels and lymphocyte recruitment in testicular seminoma. Andrology, 2(2). https://doi.org/10.1111/j.2047-2927.2014.00192.x

Salogni, L., Musso, T., Bosisio, D., Mirolo, M., Jala, V. R., Haribabu, B., Locati, M., & Sozzani, S. (2009). Activin A induces dendritic cell migration through the polarized release of CXC chemokine ligands 12 and 14. Blood. https://doi.org/10.1182/blood-2008-12-194597

Salomonsson, S., & Wahren-Herlenius, M. (2003). Local production of Ro/SSA and La/SSB autoantibodies in the target organ coincides with high levels of circulating antibodies in sera of patients with Sjögren's syndrome. Scandinavian Journal of Rheumatology, 32(2). https://doi.org/10.1080/03009740310000076

Saradna, A., Do, D. C., Kumar, S., Fu, Q. L., & Gao, P. (2018). Macrophage polarization and allergic asthma. In Translational Research (Vol. 191, pp. 1–14). Mosby Inc. https://doi.org/10.1016/j.trsl.2017.09.002

Sato, E., Olson, S. H., Ahn, J., Bundy, B., Nishikawa, H., Qian, F., Jungbluth, A. A., Frosina, D., Gnjatic, S., Ambrosone, C., Kepner, J., Odunsi, T., Ritter, G., Lele, S., Chen, Y. T., Ohtani, H., Old, L. J., & Odunsi, K. (2005). Intraepithelial CD8+ tumor-infiltrating lymphocytes and a high CD8+/regulatory T cell ratio are associated with favorable prognosis in ovarian cancer. Proceedings of the National Academy of Sciences of the United States of America, 102(51). https://doi.org/10.1073/pnas.0509182102

Sato, Y., Boor, P., Fukuma, S., Klinkhammer, B. M., Haga, H., Ogawa, O., Floege, J., & Yanagita, M. (2020). Developmental stages of tertiary lymphoid tissue reflect local injury and inflammation in mouse and human kidneys. Kidney International, 98(2), 448–463. https://doi.org/10.1016/j.kint.2020.02.023

Sato, Y., Silina, K., van den Broek, M., Hirahara, K., & Yanagita, M. (2023). The roles of tertiary lymphoid structures in chronic diseases. Nature Reviews Nephrology. https://doi.org/10.1038/s41581-023-00706-z

Sautès-Fridman, C., Petitprez, F., Calderaro, J., & Fridman, W. H. (2019). Tertiary lymphoid structures in the era of cancer immunotherapy. In Nature Reviews Cancer (Vol. 19, Issue 6). https://doi.org/10.1038/s41568-019-0144-6

Schell, C., Albrecht, M., Mayer, C., Schwarzer, J. U., Frungieri, M. B., & Mayerhofer, A. (2008). Exploring human testicular peritubular cells: Identification of secretory products and regulation by tumor necrosis factor-α. Endocrinology. https://doi.org/10.1210/en.2007-1064

Schrum, S., Probst, P., Fleischer, B., & Zipfel, P. F. (1996). Synthesis of the CC-Chemokines MIP-1α, MIP-1β, and RANTES Is Associated with a Type 1 Immune Response. Journal of Immunology.

Schumacher, T. N., & Thommen, D. S. (2022). Tertiary lymphoid structures in cancer. In Science (Vol. 375, Issue 6576). https://doi.org/10.1126/science.abf9419

Schuppe, H. C., & Bergmann, M. (2013). Inflammatory Conditions of the Testis. In Atlas on the Human Testis. https://doi.org/10.1007/978-1-4471-2763-5_9

Schuppe, H. C., Meinhardt, A., Allam, J. P., Bergmann, M., Weidner, W., & Haidl, G. (2008). Chronic orchitis: A neglected cause of male infertility? Andrologia. https://doi.org/10.1111/j.1439-0272.2008.00837.x

Schuppe, H. C., Pilatz, A., Hossain, H., Diemer, T., Wagenlehner, F., & Weidner, W. (2017). Urogenital Infection as a Risk Factor for Male Infertility. Deutsches Arzteblatt International, 114(19), 339–346. https://doi.org/10.3238/arztebl.2017.0339

Schütte B, El Hajj N, Kuhtz J, Nanda I, Gromoll J, Hahn T, Dittrich M, Schorsch M, Müller T, Haaf T. Broad DNA methylation changes of spermatogenesis, inflammation and immune response-related genes in a subgroup of sperm samples for assisted reproduction. Andrology. 2013 Nov;1(6):822-9. doi: 10.1111/j.2047-2927.2013.00122.x.

Semitekolou, M., Alissafi, T., Aggelakopoulou, M., Kourepini, E., Kariyawasam, H. H., Kay, A. B., Robinson, D. S., Lloyd, C. M., Panoutsakopoulou, V., & Xanthou, G. (2009). Activin-A induces regulatory T cells that suppress T helper cell immune responses and protect from allergic airway disease. Journal of Experimental Medicine, 206(8), 1769–1785. https://doi.org/10.1084/jem.20082603

Shabgah, A. G., Shariati-Sarabi, Z., Tavakkol-Afshari, J., & Mohammadi, M. (2019). The role of BAFF and APRIL in rheumatoid arthritis. In Journal of Cellular Physiology (Vol. 234, Issue 10). https://doi.org/10.1002/jcp.28445

Shomer, N. H., Fox, J. G., Juedes, A. E., & Ruddle, N. H. (2003). Helicobacter-induced chronic active lymphoid aggregates have characteristics of tertiary lymphoid tissue. Infection and Immunity, 71(6). https://doi.org/10.1128/IAI.71.6.3572-3577.2003

Shum, W. W. C., Ruan, Y. C., Da Silva, N., & Breton, S. (2011). Establishment of cell-cell cross review talk in the epididymis: Control of luminal acidification. In Journal of Andrology (Vol. 32, Issue 6). https://doi.org/10.2164/jandrol.111.012971

Sierra-Filardi, E., Nieto, C., Domínguez-Soto, Á., Barroso, R., Sánchez-Mateos, P., Puig-Kroger, A., López-Bravo, M., Joven, J., Ardavín, C., Rodríguez-Fernández, J. L., Sánchez-Torres, C., Mellado, M., & Corbí, Á. L. (2014). CCL2 Shapes Macrophage Polarization by GM-CSF and M-

CSF: Identification of CCL2/CCR2-Dependent Gene Expression Profile. The Journal of Immunology, 192(8), 3858–3867. https://doi.org/10.4049/jimmunol.1302821

Sierra-Filardi, E., Puig-Kröger, A., Blanco, F. J., Nieto, C., Bragado, R., Palomero, M. I., Bernabéu, C., Vega, M. A., & Corbí, A. L. (2011a). Activin A skews macrophage polarization by promoting a proinflammatory phenotype and inhibiting the acquisition of anti-inflammatory macrophage markers. Blood, 117(19), 5092–5101. https://doi.org/10.1182/blood-2010-09-306993

Sierra-Filardi, E., Puig-Kröger, A., Blanco, F. J., Nieto, C., Bragado, R., Palomero, M. I., Bernabéu, C., Vega, M. A., & Corbí, A. L. (2011b). Activin A skews macrophage polarization by promoting a proinflammatory phenotype and inhibiting the acquisition of anti-inflammatory macrophage markers. Blood, 117(19), 5092–5101. https://doi.org/10.1182/blood-2010-09-306993

Sindern, E., Patzold, T., Ossege, L. M., Gisevius, A., & Malin, J. P. (2002). Expression of chemokine receptor CXCR3 on cerebrospinal fluid T-cells is related to active MRI lesion appearance in patients with relapsing-remitting multiple sclerosis. Journal of Neuroimmunology, 131(1–2). https://doi.org/10.1016/S0165-5728(02)00263-1

Smith, L. B., & Walker, W. H. (2014). The regulation of spermatogenesis by androgens. In Seminars in Cell and Developmental Biology (Vol. 30). https://doi.org/10.1016/j.semcdb.2014.02.012

Springer, T. A. (1994). Traffic signals for lymphocyte recirculation and leukocyte emigration: The multistep paradigm. In Cell. https://doi.org/10.1016/0092-8674(94)90337-9

Stone, M. J., Hayward, J. A., Huang, C., Huma, Z. E., & Sanchez, J. (2017). Mechanisms of regulation of the chemokine-receptor network. In International Journal of Molecular Sciences (Vol. 18, Issue 2). https://doi.org/10.3390/ijms18020342

Suescun, M. O., Rival, C., Theas, M. S., Calandra, R. S., & Lustig, L. (2003). Involvement of tumor necrosis factor-alpha in the pathogenesis of autoimmune orchitis in rats. Biology of Reproduction, 68(6), 2114–2121. https://doi.org/10.1095/biolreprod.102.011189

Sullivan, R., & Mieusset, R. (2016). The human epididymis: Its function in sperm maturation. Human Reproduction Update, 22(5). https://doi.org/10.1093/humupd/dmw015

Suzawa, K., Kobayashi, M., Sakai, Y., Hoshino, H., Watanabe, M., Harada, O., Ohtani, H., Fukuda, M., & Nakayama, J. (2007). Preferential induction of peripheral lymph node addressin on high endothelial venule-like vessels in the active phase of ulcerative colitis. American Journal of Gastroenterology, 102(7). https://doi.org/10.1111/j.1572-0241.2007.01189.x

Taylor, S., Wakem, M., Dijkman, G., Alsarraj, M., & Nguyen, M. (2010). A practical approach to RT-qPCR-Publishing data that conform to the MIQE guidelines. In Methods (Vol. 50, Issue 4). https://doi.org/10.1016/j.ymeth.2010.01.005

Thaunat, O., Field, A. C., Dai, J., Louedec, L., Patey, N., Bloch, M. F., Mandet, C., Belair, M. F., Bruneval, P., Meilhac, O., Bellon, B., Joly, E., Michel, J. B., & Nicoletti, A. (2005). Lymphoid neogenesis in chronic rejection: Evidence for a local humoral alloimmune response. Proceedings of the National Academy of Sciences of the United States of America, 102(41). https://doi.org/10.1073/pnas.0507223102

Tokuyama, H., Ueha, S., Kurachi, M., Matsushima, K., Moriyasu, F., Blumberg, R. S., & Kakimi, K. (2005). The simultaneous blockade of chemokine receptors CCR2, CCR5 and CXCR3 by a

non-peptide chemokine receptor antagonist protects mice from dextran sodium sulfate-mediated colitis. International Immunology. https://doi.org/10.1093/intimm/dxh284

Tompkins, A. B., Hutchinson, P., de Kretser, D. M., & Hedger, M. P. (1998). Characterization of Lymphocytes in the Adult Rat Testis by Flow Cytometry: Effects Of Activin and Transforming Growth Factor β on Lymphocyte Subsets in Vitro1. Biology of Reproduction, 58(4), 943–951. https://doi.org/10.1095/biolreprod58.4.943

Tunc O, Tremellen K. Oxidative DNA damage impairs global sperm DNA methylation in infertile men. J Assist Reprod Genet. 2009 Sep-Oct;26(9-10):537-44. doi: 10.1007/s10815-009-9346-2.

Tung, K. S. K., Harakal, J., Qiao, H., Rival, C., Li, J. C. H., Paul, A. G. A., Wheeler, K., Pramoonjago, P., Grafer, C. M., Sun, W., Sampson, R. D., Wong, E. W. P., Reddi, P. P., Deshmukh, U. S., Hardy, D. M., Tang, H., Cheng, C. Y., & Goldberg, E. (2017). Egress of sperm autoantigen from seminiferous tubules maintains systemic tolerance. Journal of Clinical Investigation. https://doi.org/10.1172/JCI89927

Turley, S. J., Fletcher, A. L., & Elpek, K. G. (2010). The stromal and haematopoietic antigen-presenting cells that reside in secondary lymphoid organs. In Nature Reviews Immunology (Vol. 10, Issue 12). https://doi.org/10.1038/nri2886

Ulrichs, T., Kosmiadi, G. A., Jörg, S., Pradl, L., Titukhina, M., Mishenko, V., Gushina, N., & Kaufmann, S. H. E. (2005). Differential organization of the local immune response in patients with active cavitary tuberculosis or with nonprogressive tuberculoma. Journal of Infectious Diseases, 192(1). https://doi.org/10.1086/430621

Van De Pavert, S. A., Olivier, B. J., Goverse, G., Vondenhoff, M. F., Greuter, M., Beke, P., Kusser, K., Höpken, U. E., Lipp, M., Niederreither, K., Blomhoff, R., Sitnik, K., Agace, W. W., Randall, T. D., de Jonge, W. J., & Mebius, R. E. (2009). Chemokine cxcl13 is essential for lymph node initiation and is induced by retinoic acid and neuronal stimulation. Nature Immunology, 10(11). https://doi.org/10.1038/ni.1789

Vanhersecke, L., Brunet, M., Guégan, J. P., Rey, C., Bougouin, A., Cousin, S., Le Moulec, S., Besse, B., Loriot, Y., Larroquette, M., Soubeyran, I., Toulmonde, M., Roubaud, G., Pernot, S., Cabart, M., Chomy, F., Lefevre, C., Bourcier, K., Kind, M., … Italiano, A. (2021). Mature tertiary lymphoid structures predict immune checkpoint inhibitor efficacy in solid tumors independently of PD-L1 expression. Nature Cancer, 2(8). https://doi.org/10.1038/s43018-021-00232-6

Vondenhoff, M. F., Greuter, M., Goverse, G., Elewaut, D., Dewint, P., Ware, C. F., Hoorweg, K., Kraal, G., & Mebius, R. E. (2009). LTβR Signaling Induces Cytokine Expression and Up-Regulates Lymphangiogenic Factors in Lymph Node Anlagen. The Journal of Immunology, 182(9). https://doi.org/10.4049/jimmunol.0801165

Wang, P., & Duan, Y. G. (2016). The role of dendritic cells in male reproductive tract. In American Journal of Reproductive Immunology. https://doi.org/10.1111/aji.12536

Weidner, W., Garbe, C., Weissbach, L., Harbrecht, J., Kleinschmidt, K., Schiefer, H. G., & Friedrich, H. J. (1990). [Initial therapy of acute unilateral epididymitis using ofloxacin. I. Clinical and microbiological findings]. Der Urologe. Ausg. A, 29(5).

Weidner, W., Pilatz, A., Diemer, T., Schuppe, H. C., Rusz, A., & Wagenlehner, F. (2013). Male urogenital infections: Impact of infection and inflammation on ejaculate parameters. World Journal of Urology, 31(4). https://doi.org/10.1007/s00345-013-1082-7

Welch, R. A., Burland, V., Plunkett, G., Redford, P., Roesch, P., Rasko, D., Buckles, E. L., Liou, S. R., Boutin, A., Hackett, J., Stroud, D., Mayhew, G. F., Rose, D. J., Zhou, S., Schwartz, D. C., Perna, N. T., Mobley, H. L. T., Donnenberg, M. S., & Blattner, F. R. (2002). Extensive mosaic structure revealed by the complete genome sequence of uropathogenic Escherichia coli. Proceedings of the National Academy of Sciences of the United States of America, 99(26). https://doi.org/10.1073/pnas.252529799

Werner, S., & Grose, R. (2003). Regulation of wound healing by growth factors and cytokines. In Physiological Reviews. https://doi.org/10.1152/physrev.2003.83.3.835

Weyand, C. M., & Goronzy, J. J. (2003). Ectopic germinal center formation in rheumatoid synovitis. Annals of the New York Academy of Sciences, 987. https://doi.org/10.1111/j.1749-6632.2003.tb06042.x

Wheeler, K., Tardif, S., Rival, C., Luu, B., Bui, E., Del Rio, R., Teuscher, C., Sparwasser, T., Hardy, D., & Tung, K. S. K. (2011). Regulatory T cells control tolerogenic versus autoimmune response to sperm in vasectomy. Proceedings of the National Academy of Sciences of the United States of America. https://doi.org/10.1073/pnas.1017615108

WHO. (2023). *Infertility prevalence estimates, 1990–2021*. http://digitallibrary.un.org/record/4008382

Wijayarathna, R., & de Kretser, D. M. (2016). Activins in reproductive biology and beyond. Human Reproduction Update, 22(3), 342–357. https://doi.org/10.1093/humupd/dmv058

Wijayarathna, R., & Hedger, M. P. (2019). Activins, follistatin and immunoregulation in the epididymis. Andrology, 7(5), 703–711. https://doi.org/10.1111/andr.12682

Wijayarathna, R., Pasalic, A., Nicolas, N., Biniwale, S., Ravinthiran, R., Genovese, R., Muir, J. A., Loveland, K. L., Meinhardt, A., Fijak, M., & Hedger, M. P. (2020). Region-specific immune responses to autoimmune epididymitis in the murine reproductive tract. Cell and Tissue Research, 381(2). https://doi.org/10.1007/s00441-020-03215-8

Wijayarathna, R., Sarraj, M. A., Genovese, R., Girling, J. E., Michel, V., Ludlow, H., Loveland, K. L., Meinhardt, A., de Kretser, D. M., & Hedger, M. P. (2017). Activin and follistatin interactions in the male reproductive tract: activin expression and morphological abnormalities in mice lacking follistatin 288. Andrology, 5(3), 578–588. https://doi.org/10.1111/andr.12337

Winnall, W. R., Muir, J. A., & Hedger, M. P. (2011). Rat resident testicular macrophages have an alternatively activated phenotype and constitutively produce interleukin-10 in vitro. Journal of Leukocyte Biology. https://doi.org/10.1189/jlb.1010557

Xavier, R., De Carvalho, R. C., & Fraietta, R. (2021). Semen quality from patients affected by seminomatous and non-seminomatous testicular tumor. International Braz J Urol, 47(3). https://doi.org/10.1590/S1677-5538.IBJU.2021.99.01

Yamada, J., Tsuji, K., Miyatake, K., Matsukura, Y., Abula, K., Inoue, M., Sekiya, I., & Muneta, T. (2014). Follistatin alleviates synovitis and articular cartilage degeneration induced by carrageenan. International Journal of Inflammation, 2014. https://doi.org/10.1155/2014/959271

Yang, X. D., Karin, N., Tisch, R., Steinman, L., & Mcdevitt, H. O. (1993). Inhibition of insulitis and prevention of diabetes in nonobese diabetic mice by blocking L-selectin and very late antigen 4 adhesion receptors. Proceedings of the National Academy of Sciences of the United States of America, 90(22). https://doi.org/10.1073/pnas.90.22.10494

Yule, T. D., Montoya, G. D., Russell, L. D., Williams, T. M., & Tung, K. S. (1988). Autoantigenic germ cells exist outside the blood testis barrier. Journal of Immunology (Baltimore, Md. : 1950).

Zhao, S., Zhu, W., Xue, S., & Han, D. (2014). Testicular defense systems: Immune privilege and innate immunity. Cellular and Molecular Immunology, 11(5), 428–437. https://doi.org/10.1038/cmi.2014.38

Zheng, J., Yang, M., Shao, J., Miao, Y., Han, J., & Du, J. (2013). Chemokine receptor CX3CR1 contributes to macrophage survival in tumor metastasis. Molecular Cancer. https://doi.org/10.1186/1476-4598-12-141

Zou, X., Zhang, Y., Wang, X., Zhang, R., & Yang, W. (2021). The Role of AIRE Deficiency in Infertility and Its Potential Pathogenesis. In Frontiers in Immunology (Vol. 12). https://doi.org/10.3389/fimmu.2021.641164

8. Zusammenfassung

Unfruchtbarkeit gilt als weltweites Problem, wobei etwa 50 % der Fälle auf männliche Faktoren zurückzuführen sind. Infektionen und Entzündungen des Genitaltrakts gehören zu den identifizierbaren und potenziell heilbaren Ursachen der männlichen Infertilität.

Die experimentelle Autoimmun-Epididymo-Orchitis (EAEO) ist ein Mausmodell einer chronische Hodenentzündung, die durch mehrere Symptome gekennzeichnet ist, die auch bei infertilen Männern auftreten. Dazu gehören die Immunzellinfiltration, die Erhöhung von pro-inflammatorischen und pro-fibrotischen Mediatoren (z. B. TNF, CCL2, Aktivin A), die Beeinträchtigung der Spermatogenese, die Zerstörung der Architektur der Samenkanälchen sowie die Steroidogenesestörungen und das fibrotische *Remodeling*. CCL2 und sein Rezeptor CCR2 gilt als ein wichtiger Chemokin-Signalweg, der an der Rekrutierung von Monozyten und Makrophagen zu den Entzündungsherden und nachfolgenden Gewebeschäden beteiligt ist. Activin A, ein pleiotroper Faktor, dessen Produktion mit dem Schweregrad der EAEO korreliert, ist in der Lage, die Expression von Chemokinen, insbesondere CCR2, zu modulieren.

Daher sollte in dieser Studie untersucht werden, wie sich das Chemokinnetzwerk während einer EAEO bei C57BL/6J (WT) und CCR2-defizienten (Ccr2-/-) Mäusen verändert und wie Aktivin A die Expression von Chemokinen und deren Rezeptoren beeinflussen kann. EAEO wurde in WT- und Ccr2-/- Mäusen induziert und die Hoden wurden 50 Tage nach der ersten Immunisierung entnommen. Die Ergebnisse der mRNA-Expression zeigen, dass die wichtigsten Chemokine und ihre Rezeptoren, die in der Makrophagen-Migration essenziell sind, in den EAEO-Hoden erhöht sind, während die Ablation von CCR2 diese Veränderungen abmildert. Darüber hinaus wurde die Expression von Chemokin/Chemokinrezeptor-kodierenden Genen in menschlichen Hodenbiopsien untersucht. Die Hodenbiopsien von Patienten mit beeinträchtigter Spermatogenese und fokalen leukozytären Infiltraten zeigten eine Zunahme von Makrophagen, die CCR2 exprimieren. Nennenswert ist, dass die Biopsien mit gestörter Spermatogenese und fokaler leukozytärer Infiltration eine höhere Expression von CCL2 und CCR2 aufwiesen als Kontrollbiopsien ohne

Entzündungszeichen und mit intakter Spermatogenese. Darüber hinaus wurde in einem *in-vitro* Versuch, bei dem die Makrophagen aus dem Knochenmark als Ersatz für testikuläre Makrophagen verwendet wurden, nachgewiesen, dass Aktivin A als wichtiger Regulator der Expression des Chemokinnetzwerks in diesen Zellen dient. Die spezifische Effekte der Aktivin-A wurden durch den Inhibitor Follistatin bestätigt. Zusätzlich wurden die Makrophagen als die Hauptzellpopulation im EAEO-Hoden identifiziert, die Aktivin A exprimieren. Dies impliziert sowohl CCR2 als auch Aktivin A als potenzielle therapeutische Targets.

Veränderungen in der Chemokinexpression können das betroffene Gewebe für die Infiltration durch Immunzellen prädisponieren, die sich in einigen Fällen zu Immunzellaggregaten zusammenschließen können und in ihrer Struktur, Zusammensetzung, Chemokinexpression sowie ihrer Funktionalität Lymphknoten ähneln. Tertiäre lymphoide Organe (TLO) entwickeln sich als Folge einer Entzündung, die durch eine Vielzahl von Ursachen wie Infektionen und Autoimmunität ausgelöst werden kann. Daher wurde im zweiten Teil der Studie die vermeintliche Entwicklung von TLO in Hoden und Nebenhoden unter entzündlichen Bedingungen anhand von zwei Mausmodellen untersucht, d. h. sterile EAEO und akute UPEC-Infektion. Die akute Epididymitis wird häufig durch Bakterien verursacht, wobei UPEC ein vorherrschender Erreger ist. Im UPEC-Infektionsmodell reagieren verschiedene Teile des Nebenhodens differenziert auf die Infektion, so dass die Cauda epididymidis selektiv stark geschädigt ist und eine interstitielle Fibrose, einen Verlust der epithelialen Integrität, eine Zunahme des Luminaldurchmessers, eine Immunzellinfiltration und eine Abszess Bildung aufweist.

Die Ergebnisse zeigten, dass die Elemente der TLO nicht in den EAEO-Hoden, sondern in der entzündeten Cauda epididymidis zu finden waren. Die Cauda von EAEO-Mäusen und insbesondere von Tieren, die mit UPEC infiziert waren, wies mehrere Elemente und Immunzellen auf, die mit der TLO-Bildung in Verbindung stehen. UPEC-infizierte Cauda epididymidis zeigte unterschiedliche B- und T-Zell-Zonen auf, wobei die hochendothelialen Venolen (HEV) in der T-Zell-Region CXCL13 in ihrem Lumen enthielten. Die B-Zellen proliferierten, was auf ihre Rolle bei der Durchführung von Keimzentrumsreaktionen hinweist. Darüber hinaus demonstrierten die Clusters von Immunzellen ein netzartiges Netzwerk, das

strukturelle Unterstützung bietet und die Migration von Immunzellen und die Bildung von Antikörpern beeinflussen könnte. Die B- und T-Zellen bildeten getrennten Zonen, was mit der hohen Expression von TLO-relevanten Chemokinen (Cxcl13, Ccl19 und Ccl21) übereinstimmte. Außerdem waren die ausschlaggebenden Gene für die HEV-Bildung (Tnf, Ltα) und -Reifung (Ltβ, Tnfsf14) erhöht. Die Cauda von EAEO-Mäusen entwickelte ebenfalls TLO und HEV, jedoch in einer weniger organisierten Weise. Auf der Grundlage dieser Ergebnisse wird spekuliert, dass der Nebenhoden unter entzündlichen Bedingungen für die Bildung von TLO anfällig ist. Zukünftige Studien sind erforderlich, um die die Auswirkungen der TLO-Entwicklung im Nebenhoden auf die männliche Fertilität zu untersuchen.

9. Publications:

Publications from this thesis

1. Hasan, H., Peng, W., Wijayarathna, R., Wahle, E., Fietz, D., Bhushan, S., Pleuger, C., Planinić, A., Günther, S., Loveland, K.L., Pilatz, A., Ježek, D., Schuppe, H.C., Meinhardt, A., Hedger, M.P., Fijak, M. (2024) Monocytes expressing activin A and CCR2 exacerbate chronic testicular inflammation by promoting immune cell infiltration. Human Reproduction. deae107, https://doi.org/10.1093/humrep/deae107

Other Publications

1. Hasan H., Bhushan S., Fijak M. and Meinhardt A. (2022) Mechanism of Inflammatory Associated Impairment of Sperm Function, Spermatogenesis and Steroidogenesis. Front. Endocrinol. 13:897029. doi: 10.3389/fendo.2022.897029
2. Peng, W., Kepsch, A., Kracht, T. O., Hasan, H., Wijayarathna, R., Wahle, E., Pleuger, C., Bhushan, S., Günther, S., Kauerhof, A. C., Planinić, A., Fietz, D., Schuppe, H. C., Wygrecka, M., Loveland, K. L., Ježek, D., Meinhardt, A., Hedger, M. P., & Fijak, M. (2022). Activin A and CCR2 regulate macrophage function in testicular fibrosis caused by experimental autoimmune orchitis. Cellular and Molecular Life Sciences, 79(12), 602. https://doi.org/10.1007/s00018-022-04632-4

Conference abstracts

18-22 June 2023	22nd European Testis Worskhsop	Caux, Switzerland	Presentation: Macrophages expressing activin A and CCR2 are implicated in testicular inflammation

10 Oct 2022	Autumn School Academy for Immunology	Merseburg Germany	Poster: Uropathogenis Escherichia coli infection leads to the formation of tertiary lymphoid organs in the epididymis
15 Sep 2022	15th GGL Annual Conference	Giessen Germany	Presentation: Uropathogenic Escherichia coli infection leads to the formation of tertiary lymphoid organs in the epididymis
08-10 Sep 2022	34th DGA Annual Meeting	Giessen Germany	Presentation: Specialized immune cell portals and tertiary lymphoid organ layers during inflammations in the epididymis.
04-07 Sep 2022	vBR-Symposium 2022 "The Epididymis"	Giessen Germany	Presentation and poster: Uropathogenic Escherichia coli infection leads to the formation of tertiary lymphoid organs in the epididymis
29-30 Sep 2021	14th GGL Annual Conference (digital)	Giessen Germany	Presentation: The role of chemokines in the development of inflammatory responses in the testis and epididymis: implications for tertiary lymphoid structure formation
30 May-03 Jun 2021	21st European Testis Worskhsop (digital)	Girona, Spain	Poster: Chemokines and Activin A play a role in inflammatory responses during chronic testicular imflammation in mice
29-30 May 2021	13th NYRA Meeting (digital)	Girona, Spain	Presentation: Chemokines and Activin A play a role in inflammatory responses during chronic testicular imflammation in mice
20 Sep 2020	13th GGL Annual	Giessen Germany	Presentation: The role of activins and chemokines in the development of

	Conference (digital)		inflammatory responses during chronic testicular inflammation in mice

10. Acknowledgments

The experimental work for this dissertation was performed at the Institute of Anatomy and Cell Biology at the Justus Liebig University Giessen, Germany, under the direction of Prof. Dr. Andreas Meinhardt to whom I am deeply indebted and hold the utmost respect for establishing and fostering an environment conducive for running a successful lab.

Words cannot express my gratitude to Dr. Monika Fijak, for her superior guidance and mentorship. Working on this thesis while having her as a supervisor made the journey pleasant and invoked seeds for accomplishing independence. She shared with me her enormous expertise and exceptional scientific knowledge and offered me support and encouragement when needed. I truly enjoyed working on this thesis, and this was made possible because of her.

I would like to thank my supervisor Prof. Dr. Mark Hedger for his invaluable advice, opinion, guidance and support.

Part of this thesis would do not have been possible without the collaboration with P9 from the IRTG. For this, I would like to offer my deepest gratitude and appreciation to Dr. Christiane Pleuger and DingDing Ai.

I would like to extend my sincere thanks to all our dear lab members for their support and help, and I dedicate special thanks to: Wei Peng, Dr. Sudhanshu Bhushan, Dr. Aileen Harrer, Eva Wahle, Suada Fröhlich, Dr. Jörg Klug and Vishnu Kumar.

I want to thank our collaborators, Dr. Daniela Fietz, Prof. Dr. med. Hans-Christian Schuppe and Priv.-Doz. Dr. med. Adrian Pilatz for their willingness to provide both human samples and clinical expertise.

I am also extremely grateful to Pia Jürgens for her support and willingness to help substantially with administrative work and the endless paperwork trial. I extend my appreciation as well to Eva Wewel.

I would like to dedicate this thesis to my mother Mimo. You set an example for what true strong independent women truly are and for that you set the bar very

high and I would do my best to follow in that path. I dedicate my whole journey in life to you.

Last but not least, to my brother Hisham, I would say thank you for being there and for being my best friend in life. I would like to thank my second family here in Germany, especially Reem and Marwa, without whom life in Germany would not have been the same. Thank you for being there when I needed you. Thank you for making life here beautiful and joyful.

11. Ehrenwörtliche Erklärung

Ich erkläre: Ich habe die vorgelegte Dissertation selbständig und ohne unerlaubte fremde Hilfe und nur mit den Hilfen angefertigt, die ich in der Dissertation angegeben habe. Alle Textstellen, die wörtlich oder sinngemäß aus veröffentlichten oder nicht veröffentlichten Schriften entnommen sind, und alle Angaben, die auf mündlichen Auskünften beruhen, sind als solche kenntlich gemacht. Bei den von mir durchgeführten und in der Dissertation erwähnten Untersuchungen habe ich die Grundsätze guter wissenschaftlicher Praxis, wie sie in der „Satzung der Justus-Liebig-Universität Gießen zur Sicherung guter wissenschaftlicher Praxis“ niedergelegt sind, eingehalten.

I declare that I have completed this dissertation single-handedly without the unauthorized help of a second party and only with the assistance acknowledged therein. I have appropriately acknowledged and referenced all text passages that are derived from or are based on the content of published or unpublished work of others, and all information that relates to verbal communication. I have abided by the principles of good scientific conduct laid down in the charter of the Justus Liebig University of Giessen in carrying out the investigations described in the dissertation.

Giessen, den

Hiba Hasan